12-2009

HYDRODYNAMICS OF FRESHWATER TURTLES: MANEUVERABILITY, STABILITY, AND EFFECTS OF SHELL SHAPE

Gabriel Rivera
Clemson University, grivera@clemson.edu

HYDRODYNAMICS OF FRESHWATER TURTLES: MANEUVERABILITY, STABILITY, AND EFFECTS OF SHELL SHAPE

A Dissertation
Presented to
the Graduate School of
Clemson University

In Partial Fulfillment
of the Requirements for the Degree
Doctor of Philosophy
Biological Sciences

---

by
Gabriel Rivera
December 2009

Accepted by:
Dr. Richard W. Blob, Committee Chair
Dr. Margaret B. Ptacek
Dr. Michael J. Childress
Dr. Ian K. Bartol

ABSTRACT

Aquatic organisms exhibit tremendous diversity in body design and modes of propulsion that can strongly influence locomotor performance. Understanding how such differences affect locomotor performance is a major focus of research in integrative organismal biology and can provide insight into the evolutionary origins of such variation. Turtles are unique among extant tetrapods (i.e., amphibians, reptiles, birds, and mammals) in that they possess rigid bodies. In turtles, the vertebrae are fused dorsally with a bony carapace, precluding movement of the axial skeleton between the base of the neck and the tail. As a result of their immobilized axial skeleton and reduced tail, thrust in swimming turtles is generated exclusively by the movements of fore- and hind-limbs. Despite the potential constraints of a rigid body on locomotion in turtles, over 100 extant species inhabit aquatic environments. Moreover, these turtles display considerable variation in shell and propulsor morphology and have evolved two different modes of propulsion (four-limbed rowing vs. forelimb flapping).

My dissertation is a collection of three studies that examined the interaction between morphology and hydrodynamic performance (maneuverability, stability, and drag) in freshwater turtles. First, I described the patterns of limb movements used to produce turns and quantified turning performance, comparing results to that of other rigid- and flexible-bodied animals. Second, I assessed kinematics and hydrodynamic stability during straight-line swimming. I also compared data I collected from freshwater turtles to previous

data collected from two species of sea turtles to assess how the different modes of propulsion used by the two groups affect stability. Finally, I examined the relationship between habitat (environmental flow regime), morphology (shell shape), and performance (hydrodynamic drag) among intraspecific populations of the large riverine turtle *Pseudemys concinna*. Specially, I tested for three-dimensional differences in shell shape between turtles from slow- and fast-flowing habitats, while concomitantly testing whether the carapace and plastron demonstrate the same propensity for environmentally correlated differences. I also used physical models to test whether morphological differences of the shell confer reductions in drag, and provide preliminary data regarding the potential role of phenotypic plasticity in generating the morphological variation observed in turtles between the two flow regimes. Data from these studies provides insight into the evolutionary origins of intra- and inter-specific variation in shell shape.

DEDICATION

For always loving me, for inspiring me and bringing unbelievable joy to my life, for always supporting me. This dissertation is dedicated to my wife Angela, my boys Bosco and Russell, and my family.

ACKNOWLEDGMENTS

I am sincerely grateful to the people and organizations that assisted me in completing my dissertation research. I am particularly thankful to my dissertation committee: chair Dr. R. W. Blob, and members Dr. M. B. Ptacek, Dr. M. J. Childress and Dr. I. K. Bartol. Their guidance and support helped me to produce several published manuscripts, receive a number of grants and fellowships, and develop as a scientist.

I am grateful to S. Rogers and B. Isaac (Carnegie Museum of Natural History), C. Guyer (Auburn University Natural History Museum), C. Franklin (Amphibian and Reptile Diversity Research Center, University of Texas, Arlington), R. Brown (University of Kansas Natural History Museum), C. Austin (Louisiana State University Museum of Natural Science), and H. Dundee (Tulane University Museum of Natural History) for providing specimens. Research was supported by a SICB Grant-in-Aid-of-Research, an ASIH Gaige Fund Award, and an AMNH Roosevelt Memorial Award.

Of course, no student makes it through graduate school without the support of friends and family. I thank the Biological Sciences graduate students for their camaraderie over the past six years. In particular, I thank Dr. S. J. Hankison, T. Maie, M. Chernick, and S. M. Kawano. I also extend special thanks to R. D. Rivera, R. D. Vogel, and C. M. Vogel for their encouragement and support. Finally, I'd like to thank my best friend and wife, Angie Rivera, for getting me through the rough spots, and helping me to enjoy the rest.

TABLE OF CONTENTS

Table of Contents (Continued)

Page

LIST OF TABLES

LIST OF FIGURES

List of Figures (Continued)

Figure Page

CHAPTER ONE

INTRODUCTION

Organisms exhibit tremendous diversity in body design and modes of propulsion. Understanding how differences in body and propulsor morphology affect locomotor performance is a major focus of research in integrative organismal biology. For aquatic organisms, swimming is an important function in which performance can be strongly influenced by morphological design (Fish, 2002). Numerous studies of aquatic and semi-aquatic taxa have examined the effects of morphology on both unsteady (e.g., aquatic turning) and steady (e.g., rectilinear swimming) locomotor performance. Studies of unsteady maneuvers often evaluate performance through measures such as the space required to turn (i.e., maneuverability) and the rate of turning (i.e., agility) (Norberg and Rayner, 1987; Walker, 2000). In contrast, steady swimming performance is typically measured using parameters such as maximum swimming speed (Sepulveda and Dickson, 2000; Fisher et al., 2005), endurance (Blake et al., 2005), hydrodynamic stability (Wassersug and von Seckendorf Hoff, 1985; Webb, 1992; Fish et al., 2003), and hydrodynamic drag (Kerfoot Jr. and Schaefer, 2006).

Several morphological features that influence locomotor performance have been identified, including body depth and the shape and position of propulsors and control surfaces (Fish, 2002). However, the ability to bend the body is possibly the most influential, and most fundamental feature of morphology affecting locomotor performance. Body flexibility varies substantially

among different aquatic animals, ranging from animals that are highly flexible to those that are unable to bend their body axis. Along this continuum, three broad categories of body design can be recognized: flexible, stiff, and rigid. The degree of body flexibility varies substantially among non-rigid taxa, including considerable variation within taxonomic groups such as fishes and cetaceans (Fish, 2002). For this reason, studies comparing the effects of shape on locomotor performance are often complicated by differing levels of body flexibility. In contrast, rigid-bodied taxa, which represent the only discrete category along the continuum, all have the same level of flexibility (i.e., no capacity to bend the body axis), and as such, simplify the evaluation of specific morphological effects. For this reason, rigid-bodied taxa represent an optimal group in which to study the effects of morphology on aquatic locomotor performance. However, to date such studies have focused primarily on one taxonomic group: tetraodontiform fishes (Gordon et al., 1996; Gordon et al., 2000; Walker, 2000; Hove et al., 2001; Bartol et al., 2002; Bartol et al., 2003; Plaut and Chen, 2003; Bartol et al., 2005; Bartol et al., 2008).

One group of rigid-bodied vertebrates that provides an ideal system in which to evaluate the effects of morphology on locomotor performance is the turtles. Turtles represent the oldest extant group of rigid-bodied vertebrates and the only such group of tetrapods (Rieppel and Reisz, 1999; Santini and Tyler, 2003). In turtles, the vertebrae are fused dorsally with a bony carapace, precluding movement of the axial skeleton between the base of the neck and the

tail. As a result of their immobilized axial skeleton and reduced tail, thrust in swimming turtles is generated exclusively by the movements of fore- and hind-limbs (Pace et al., 2001). Despite the potential constraints of a rigid body on locomotion in turtles, over 100 extant species inhabit freshwater and marine environments. However, while a number of studies have examined aspects of swimming in aquatic turtles, including kinematics (Zug, 1971; Davenport et al., 1984; Pace et al., 2001; Renous et al., 2007) and motor control (Gillis and Blob, 2001; Blob et al., 2007), relatively little is known about maneuverability or stability in this lineage.

In addition to inhabiting different environments, marine and freshwater turtles have evolved two very different modes of propulsion that use differently shaped propulsors (Daniel, 1984). Marine turtles generate thrust via synchronous dorsoventral movements of their foreflippers (i.e., modified forelimbs), whereas freshwater turtles propel themselves via synchronous rowing (anteroposterior) movements of contralateral fore- and hind-limbs (Daniel, 1984; Rivera et al., 2006; Renous et al., 2007). While studies have commented on differences in swimming between these two groups (Zug, 1971; Davenport et al., 1984; Pace et al., 2001; Renous et al., 2007), no quantitative data exist on how different modes of propulsion affect hydrodynamic stability.

In addition to interspecific variation, intraspecific differences in morphology can also influence locomotor performance. Studies examining effects of intraspecific morphological variation on aquatic locomotor performance have

typically focused on differences related to ontogeny (Wakeling et al., 1999; McHenry and Jed, 2003; Seebacher et al., 2003; Pitcher et al., 2005), size (Webb, 1976; Nikora et al., 2003; Ojanguren and Brana, 2003), or sex (Kokita and Mizota, 2002). However, organisms also frequently display morphological variations that correlate with differences in environmental conditions (Langerhans and DeWitt, 2004). Patterns of morphological variation have been identified in several species of fishes inhabiting different flow regimes, suggesting that water velocity can impose selection for efficient (i.e., drag-reducing) morphologies (Brinsmead and Fox, 2002; McGuigan et al., 2003). Because fishes live exclusively in water, selection on their body shape for hydrodynamic efficiency is expected to be maximized. In contrast, many tetrapods utilize both aquatic and terrestrial environments.

Freshwater turtles in particular have adapted to life in a diverse array of aquatic flow regimes, ranging from ponds and lakes to fast flowing rivers, while also maintaining the ability to move efficiently on land (Ernst et al., 1994). Freshwater turtles perform several vital functions on land (e.g., nesting and basking) and in water (e.g., feeding and copulation) (Ernst et al., 1994). In addition, these turtles often inhabit both lentic (i.e., slow flowing) and lotic (i.e., fast flowing) habitats (Ernst et al., 1994). Although morphological data suggest that the shells of freshwater turtles are adapted for movement through aquatic habitats (Aresco and Dobie, 2000; Claude et al., 2003; Lubcke and Wilson, 2007), examinations of swimming performance in freshwater turtles have been

limited. Knowledge of aquatic locomotion in freshwater turtles consists mainly of studies of limb kinematics during rectilinear swimming or underwater walking (Zug, 1971; Davenport et al., 1984; Pace et al., 2001; Willey and Blob, 2004). Although turtles exhibit considerable intraspecific variation in shell shape, no study has yet to evaluate the extent to which these morphological differences correlate with differences in locomotor performance or hydrodynamic habitat.

In addition to their considerable variation in morphology, locomotor style, and habitat, there are many reasons why turtles provide a good system in which to study how such features interact to affect locomotor performance. First, several lines of evidence suggest that body flexibility can have considerable effects on locomotor performance, particularly affecting stability and turning performance (Walker, 2000; Fish, 2002; Fish and Nicastro, 2003). Because turtles all have rigid bodies, intraspecific comparisons of locomotor performance among turtles avoid the added complexity associated with separating the effects of body shape and body flexibility. In addition, as a result of their rigid shell, turtles provide a unique opportunity to accurately quantify the hydrodynamic properties associated with different morphologies; specifically, the rigid shell of turtles allows hydrodynamic analyses using fixed models to accurately measure forces incurred by living specimens (Bartol et al., 2003; Bartol et al., 2005). In contrast, organisms capable of bending their bodies have an infinite number of body postures during locomotion, making the use of physical models inadequate for describing the hydrodynamic forces encountered during locomotion (Schultz

and Webb, 2002; Weihs, 2002). Furthermore, two additional factors make freshwater turtles an excellent group in which to evaluate morphological variation associated with different flow regimes: (1) individual species inhabit a variety of aquatic habitats, encompassing a wide range of flow velocities within a relatively small geographic area (Ernst et al., 1994), and (2) the turtle carapace is covered by keratinized scutes, whose intersections form easily identifiable landmarks that can be used to assess morphological variation using landmark-based geometric morphometric analyses (Claude et al., 2003; Valenzuela et al., 2004).

I conducted a series of studies that examined the interaction between morphology and hydrodynamic performance in freshwater turtles. Chapter 2 describes the patterns of limb movements used to produce turns and quantifies turning performance. Chapter 3 quantifies hydrodynamic stability of the body and head in swimming freshwater turtles, tests the effects of different modes of propulsion on stability among turtles, and compares the stability of freshwater turtles to the current model for rigid-bodied stability, the tetraodontiform fishes. Chapter 4 evaluates the relationship between flow velocity and shell morphology in a semi-aquatic freshwater turtle, the river cooter (*Pseudemys concinna*). Specifically, I tested for three-dimensional differences in shell morphology between turtles from lentic and lotic flow regimes, while concomitantly testing whether the carapace and plastron demonstrated the same propensity for environmentally correlated differences. I also used physical models to test whether morphological differences of the shell confer reductions in drag. Finally,

I provide preliminary data regarding the potential role of phenotypic plasticity in generating the morphological variation observed in turtles between the two flow regimes.

Literature Cited

Aresco, M. J. and Dobie, J. L. (2000). Variation in shell arching and sexual size dimorphism of river cooters, *Pseudemys concinna*, from two river systems in Alabama. *Journal of Herpetology* **34**, 313-317.

Bartol, I. K., Gharib, M., Webb, P. W., Weihs, D. and Gordon, M. S. (2005). Body-induced vortical flows: a common mechanism for self-corrective trimming control in boxfishes. *J. Exp. Biol.* **208**, 327-344.

Bartol, I. K., Gharib, M., Weihs, D., Webb, P. W., Hove, J. R. and Gordon, M. S. (2003). Hydrodynamic stability of swimming in ostraciid fishes: role of the carapace in the smooth trunkfish *Lactophrys triqueter* (Teleostei: Ostraciidae). *J Exp Biol* **206**, 725-744.

Bartol, I. K., Gordon, M. S., Gharib, M., Hove, J. R., Webb, P. W. and Weihs, D. (2002). Flow patterns around the carapaces of rigid-bodied, multi-propulsor boxfishes (Teleostei: Ostraciidae). *Integr. Comp. Biol.* **42**, 971-980.

Bartol, I. K., Gordon, M. S., Webb, P. W., Weihs, D. and Gharib, M. (2008). Evidence of self-correcting spiral flows in swimming boxfishes. *Bioinspiration & Biomimetics* **3**.

Blake, R. W., Law, T. C., Chan, K. H. S. and Li, J. F. Z. (2005). Comparison of the prolonged swimming performances of closely related, morphologically distinct three-spined sticklebacks Gasterosteus spp. *Journal of Fish Biology* **67**, 834-848.

Blob, R. W., Rivera, A. R. V. and Westneat, M. W. (2007). Hindlimb Function in Turtle Locomotion: Limb Movements and Muscular Activation Across Taxa, Environment, and Ontogeny. In *Biology of Turtles*, eds. J. Wyneken M. H. Godfrey and V. Bels), pp. 139-162. Boca Raton: CRC Press.

Brinsmead, J. and Fox, M. G. (2002). Morphological variation between lake- and stream-dwelling rock bass and pumpkinseed populations. *Journal of Fish Biology* **61**, 1619-1638.

Claude, J., Paradis, E., Tong, H. and Auffray, J. C. (2003). A geometric morphometric assessment of the effects of environment and cladogenesis on the evolution of the turtle shell. *Biological Journal of the Linnean Society* **79**, 485-501.

Daniel, T. L. (1984). Unsteady aspects of aquatic locomotion. *American Zoologist* **24**, 121-134.

Davenport, J., Munks, S. A. and Oxford, P. J. (1984). A comparison of the swimming of marine and freshwater turtles. *Proc. R. Soc. Lond. B* **220**, 447-475.

Ernst, C. E., Lovich, J. E. and Barbour, R. W. (1994). Turtles of the United States and Canada. Washington, D. C.: Smithsonian Institution Press.

Fish, F. E. (2002). Balancing requirements for stability and maneuverability in cetaceans. *Integr. Comp. Biol.* **42**, 85-93.

Fish, F. E. and Nicastro, A. J. (2003). Aquatic turning performance by the whirligig beetle: constraints on maneurerability by a rigid biological system. *J. Exp. Biol.* **206**, 1649-1656.

Fish, F. E., Peacock, J. E. and Rohr, J. J. (2003). Stabilization mechanism in swimming odontocete cetaceans by phased movements. *Marine Mammal Science* **19**, 515-528.

Fisher, R., Leis, J. M., Clark, D. L. and Wilson, S. K. (2005). Critical swimming speeds of late-stage coral reef fish larvae: variation within species, among species and between locations. *Marine Biology (Berlin)* **147**, 1201-1212.

Gillis, G. B. and Blob, R. W. (2001). How muscles accommodate movement in different physical environments: aquatic vs. terrestrial locomotion in vertebrates. *Comparative Biochemistry and Physiology Part A* **131**, 61-75.

Gordon, M. S., Hove, J. R., Webb, P. W. and Weihs, D. (2000). Boxfishes as unusually well-controlled autonomous underwater vehicles. *Physiological and Biochemical Zoology* **73**, 663-671.

Gordon, M. S., Plaut, I. and Kim, D. (1996). How puffers (Teleostei: Tetraodontidae) swim. *Journal of Fish Biology* **49**, 319-328.

Hove, J. R., O'Bryan, L. M., Gordon, M. S., Webb, P. W. and Weihs, D. (2001). Boxfishes (Teleostei: Ostraciidae) as a model system for fishes swimming with many fins: kinematics. *J. Exp. Biol.* **204**, 1459-1471.

Kerfoot Jr., J. R. and Schaefer, J. R. (2006). Ecomorphology and habitat utilization of *Cottus* species. *Environ Biol Fish* **76**, 1-13.

Kokita, T. and Mizota, T. (2002). Male secondary sexual traits are hydrodynamic devices for enhancing swimming performance in a monogamous filefish *Paramonacanthus japonicus*. *Journal of Ethology* **20**, 35-42.

Langerhans, R. B. and DeWitt, T. J. (2004). Shared and unique features of evolutionary diversification. *The American Naturalist* **164**.

Lubcke, G. M. and Wilson, D. S. (2007). Variation in shell morphology of the western pond turtle (*Actinemys marmorata* Baird and Girard) from three aquatic habitats in northern California. *Journal of Herpetology* **41**, 107-114.

McGuigan, K., Franklin, C. E., Moritz, C. and Blows, M. W. (2003). Adaptation of rainbow fish to lake and stream habitats. *Evolution* **57**, 104-118.

McHenry, M. J. and Jed, J. (2003). The ontogenetic scaling of hydrodynamics and swimming performance in jellyfish (*Aurelia aurita*). *J Exp Biol* **206**, 4125-4137.

Nikora, V. I., Aberle, J., Biggs, B. J. F., Jowett, I. G. and Sykes, J. R. E. (2003). Effects of fish size, time-to-fatigue and turbulence on swimming performance: a case study of *Galaxias maculatus*. *Journal of Fish Biology* **63**, 1365-1382.

Norberg, U. M. and Rayner, J. M. V. (1987). Ecological morphology and flight in bats (Mammalia: Chiroptera): wing adaptations, flight performance, foraging strategy and echolocation. *Philosophical Transactions of the Royal Society of London, Series B* **316**, 335-427.

Ojanguren, A. F. and Brana, F. (2003). Effects of size and morphology on swimming performance in juvenile brown trout (*Salmo trutta* L.). *Ecology of Freshwater Fish* **12**, 241-246.

Pace, C. M., Blob, R. W. and Westneat, M. W. (2001). Comparative kinematics of the forelimb during swimming in red-eared slider (*Trachemys scripta*) and spiny softshell (*Apalone spinifera*) turtles. *J Exp Biol* **204**, 3261-3271.

Pitcher, K. W., Rehberg, M. J., Pendleton, G. W., Raum-Suryan, K. L., Gelatt, T. S., Swain, U. G. and Sigler, M. F. (2005). Ontogeny of dive performance in pup and juvenile Stellar sea lions in Alaska. *Canadian Joural of Zoology* **83**, 1214-1231.

Plaut, I. and Chen, T. (2003). How small puffers (Teleostei: Tetraodontidae) swim. *Ichthyological Research* **50**, 149-153.

Renous, S., de Lapparent de Broin, F., Depecker, M., Davenport, J. and Bels, V. (2007). Hindlimb Function in Turtle Locomotion: Limb Movements and Muscular Activation Across Taxa, Environment, and Ontogeny. In *Biology of Turtles*, eds. J. Wyneken M. H. Godfrey and V. Bels), pp. 97-138. Boca Raton: CRC Press.

Rieppel, O. and Reisz, R. R. (1999). The origin and early evolution of turtles. *Annual Review of Ecology and Systematics* **30**, 1-22.

Rivera, G., Rivera, A. R. V., Dougherty, E. E. and Blob, R. W. (2006). Aquatic turning performance of painted turtles (*Chrysemys picta*) and functional consequences of a rigid body design. *J. Exp. Biol.* **209**, 4203-4213.

Santini, F. and Tyler, J. C. (2003). A phylogeny of the families of fossil and extant tetraodontiform fishes (Acanthomorpha, Tetraodontiformes), Upper Cretaceous to Recent. *Zoological Journal of the Linnean Society* **139**, 565-617.

Schultz, W. W. and Webb, P. W. (2002). Power requirements of swimming: do new methods resolve old questions? *Integr. Comp. Biol.* **42**, 1018-1025.

Seebacher, F., Elsworth, P. G. and Franklin, C. E. (2003). Ontogenetic changes of swimming kinematics in a semi-aquatic reptile (*Crocodylus porosus*). *Australian Journal of Zoology* **51**, 15-24.

Sepulveda, C. and Dickson, K. A. (2000). Maximum sustainable speeds and cost of swimming in juvenile kawakawa tuna (*Euthynnus affinis*) and chub mackerel (*Scomber japonicus*). *J. Exp. Biol.* **203**, 3089-3101.

Valenzuela, N., Adams, D. C., Bowden, R. M. and Gauger, A. C. (2004). Geometric morphometric sex estimation for hatchling turtles: a powerful alternative for detecting subtle sexual shape dimorphism. *Copeia* **2004**, 735-742.

Wakeling, J. M., Kemp, K. M. and Johnston, I. A. (1999). The biomechanics of fast-starts during ontogeny in the common carp *Cyprinus carpio*. *J. Exp. Biol.* **202**, 3057-3067.

Walker, J. A. (2000). Does a rigid body limit maneuverability? *J. Exp. Biol.* **203**, 3391-3396.

Wassersug, R. J. and von Seckendorf Hoff, K. (1985). The kinematics of swimming in anuran larvae. *J. Exp. Biol.* **119**, 1-30.

Webb, P. W. (1976). The effect of size on the fast-start performance of rainbow troat *Salmo gairdneri*, and a consideration of piscivorous predator-prey interactions. *J. Exp. Biol.* **65**, 157-177.

Webb, P. W. (1992). Is the high cost of body/caudal fin undulatory swimming due to increased friction drag or inertial recoil? *J. Exp. Biol.* **162**, 157-166.

Weihs, D. (2002). Stability versus maneuverability in aquatic locomotion. *Integr. Comp. Biol.* **42**, 127-134.

Willey, J. S. and Blob, R. W. (2004). Tail kinematics of juvenile common snapping turtles during aquatic walking. *Journal of Herpetology* **38**, 360-369.

Zug, G. R. (1971). Buoyancy, locomotion, morphology of the pelvic girdle and hind limb and systematics of cryptodiran turtles. *Misc. Publ. Mus. Zool. Univ. Michigan* **142**, 1-98.

CHAPTER TWO

AQUATIC TURNING PERFORMANCE OF PAINTED TURTLES (*CHRYSEMYS PICTA*) AND FUNCTIONAL CONSEQUENCES OF A RIGID BODY DESIGN

Abstract

The ability to capture prey and avoid predation in aquatic habitats depends strongly on the ability to perform unsteady maneuvers (e.g., turns), which itself depends strongly on body flexibility. Two previous studies of turning performance in rigid-bodied taxa have found either high maneuverability or high agility, but not both. However, examinations of aquatic turning performance in rigid-bodied animals have had limited taxonomic scope and, as such, the effects of many body shapes and designs on aquatic maneuverability and agility have yet to be examined. Turtles represent the oldest extant lineage of rigid-bodied vertebrates and the only aquatic rigid-bodied tetrapods. I evaluated the aquatic turning performance of painted turtles, *Chrysemys picta* (Schneider, 1783) using the minimum length-specific radius of the turning path (*R/L*) and the average turning rate (ω_{avg}) as measures of maneuverability and agility, respectively. I filmed turtles conducting forward and backward turns in an aquatic arena. Each type of turn was executed using a different pattern of limb movements. During forward turns, turtles consistently protracted the inboard forelimb and held it stationary into the flow, while continuing to move the outboard forelimb and both hindlimbs as in rectilinear swimming. The limb movements of backward turns were more complex than those of forward turns, but involved near simultaneous

retraction and protraction of contralateral fore- and hindlimbs, respectively. Forward turns had a minimum *R/L* of 0.0018 (the second single lowest value reported from any animal) and a maximum ω_{avg} of 247.1°. Values of *R/L* for backward turns (0.0091-0.0950 *L*) were much less variable than that of forward turns (0.0018-1.0442 *L*). The maneuverability of turtles is similar to that recorded previously for rigid-bodied boxfish. However, several morphological features of turtles (e.g., shell morphology and limb position) appear to increase agility relative to the body design of boxfish.

Introduction

Locomotor performance is important to the survival of nearly all vertebrates. While the importance of some components of locomotor performance, such as rectilinear sprint speed and endurance, is widely appreciated, many other aspects of locomotion also can be critical to an animal's survival (Biewener and Gillis, 1999; Blob et al., 2006). For example, animals rarely move in a straight line for prolonged durations. Animals that live in complex habitats or engage in predator-prey interactions may need to change direction frequently as they negotiate obstacles or attempt to evade predators or capture food. Thus, turning performance may be a critical aspect of locomotion for many animals (Howland, 1974; Gerstner, 1999; Domenici, 2001; Hedenström and Rosén, 2001).

Turns generally incorporate two types of motion: (1) rotation about a vertical axis through the center of an organism (reorientation), and (2) translation of this axis (i.e., the center-of-rotation) across a horizontal plane (Howland, 1974; Norberg and Rayner, 1987; Webb, 1994). Turning performance can be measured with respect to both of these types of motion. The speed of reorientation is generally measured as agility, which can be defined as the angular velocity about a center-of-rotation on the animal (i.e., ω, the turning rate), with higher values indicating superior performance (Webb, 1994). Performance with respect to translational movement is generally termed maneuverability, which is defined as the ability to turn in a limited space (Norberg and Rayner, 1987). Maneuverability is most commonly measured as the minimum radius of the turning path (denoted as *R*: Howland, 1974). For *R*, performance is considered to increase as turning radii decrease. Thus, maximal turning performance is attained through superior values of both agility and maneuverability (i.e., high values of ω and low values of *R*).

Over the past few decades, several studies have investigated the effects of particular morphologies on turning performance (Norberg and Rayner, 1987; Carrier et al., 2001; Fish, 2002; Walter and Carrier, 2002). Among aquatic animals, studies of turning performance have focused primarily on actinopterygian fishes (Webb and Keyes, 1981; Webb, 1983; Blake et al., 1995; Schrank and Webb, 1998; Gerstner, 1999; Walker, 2000; Webb and Fairchild, 2001), though a few studies have also examined turning performance in

chondrichthyans (Kajiura et al., 2003; Domenici et al., 2004), cetaceans (Fish, 2002), pinnipeds (Fish et al., 2003), penguins (Hui, 1985), squid (Foyle and O'Dor, 1988), and beetles (Fish and Nicastro, 2003). For aquatic taxa, morphological attributes that are correlated with turning performance include: body shape, the position and mobility of propulsors and control surfaces (e.g., fins, flippers, and limbs), and body flexibility (Blake et al., 1995; Fish, 1999, 2002; Walker, 2000; Fish and Nicastro, 2003). Body flexibility varies substantially among different aquatic animals, ranging along a continuum from animals that are highly flexible to those that are unable to bend their body axis. Along this continuum, three broad categories of body design can be recognized: flexible, stiff, and rigid. Animals with flexible bodies can bend their body axis easily; examples include many ray-finned fishes, especially those inhabiting complex environments (Domenici and Blake, 1997). Animals with stiff bodies have a more limited capacity to bend the body axis and include many pelagic swimmers, such as thick-skinned tuna and many cetaceans (Blake et al., 1995; Fish, 2002). Finally, animals with rigid bodies are completely inflexible and have no capacity to bend the body axis. Rigid body designs can be found in many animals with exoskeletons, shells, or other forms of body armor (Walker, 2000; Fish and Nicastro, 2003).

Flexibility of the body is thought to enhance turning performance for several reasons (Fish, 1999; Walker, 2000; Fish, 2002). First, having a flexible body allows an organism to turn in a circular space with a radius of less than 0.5

body lengths (*L*), the theoretical minimum for a rigid structure turning with no translation (Walker, 2000). Second, flexibility of the body allows animals to reduce their second moment of area about the rotational axis, thereby decreasing rotational inertia (Walker, 2000; Walter and Carrier, 2002). Conversely, a rigid body should impair both of these advantages of body flexibility. Although turning performance has been studied in a large number of diverse flexible- and stiff-bodied species, explicit evaluations of turning performance among rigid-bodied animals have been limited to one invertebrate and one vertebrate: whirligig beetles (Fish and Nicastro, 2003) and boxfish (Walker, 2000). The results of these studies have led to differing conclusions as to whether rigid body designs actually constrain turning performance. In particular, boxfish can turn with a very small radius (i.e., are highly maneuverable), but turn fairly slowly (i.e., have low agility; Walker, 2000). In contrast, whirligig beetles display high angular velocities (i.e., high agility) during turns, but also have large turning radii (i.e., low maneuverability; Fish and Nicastro, 2003).

Because examinations of aquatic turning performance in rigid-bodied animals have had a limited taxonomic scope, the effects of many body shapes and designs on aquatic maneuverability and agility have yet to be evaluated. One group of vertebrates that provides an ideal system in which to evaluate the effects of rigid bodies on aquatic turning performance are the turtles. Turtles represent the oldest extant group of rigid-bodied vertebrates and the only such

group of tetrapods (Rieppel and Reisz, 1999; Santini and Tyler, 2003). The chelonian bauplan represents an evolutionary novelty that has remained relatively unchanged for over 200 million years (Burke, 1989; Gaffney, 1990). In turtles, the vertebrae are fused dorsally with a bony carapace, precluding movement of the axial skeleton between the base of the neck and the tail. As a result of their immobilized axial skeleton and reduced tail, thrust in swimming turtles is generated exclusively by the movements of fore- and hindlimbs (Pace et al., 2001). Despite the potential constraints of a rigid body on locomotion in turtles, over 100 species currently live in freshwater and marine habitats. Freshwater species in particular have adapted to life in a diverse array of aquatic flow regimes, ranging from ponds and lakes to fast flowing rivers, while also maintaining the ability to move efficiently on land (Ernst et al., 1994). Although morphological data suggest that the shells of freshwater turtles are highly suited for movement through aquatic habitats (Aresco and Dobie, 2000; Claude et al., 2003), examinations of swimming performance in freshwater turtles have been limited. Knowledge of aquatic locomotion in freshwater turtles consists mainly of studies of limb kinematics during rectilinear swimming or underwater walking (Zug, 1971; Davenport et al., 1984; Pace et al., 2001; Willey and Blob, 2004). No study has yet to evaluate how turtles generate turns, or quantify any aspect of turning performance for species in this lineage. Because they possess a very different body design than that of boxfish (with a dorsoventrally flattened body shape and jointed limbs, rather than flexible fins, as propulsors) turtles provide an

important comparison for evaluating the effects of morphological design on hydrodynamic performance in vertebrates.

To gain insight into the effects of body design on aquatic turning performance, I measured the performance of aquatic turns by painted turtles (*Chrysemys picta*), a freshwater species that exhibits a generalized morphology typical of the emydid turtle clade (Ernst et al., 1994). The specific objectives of this paper were two-fold. First, I measured limb kinematics in turning turtles in order to evaluate the mechanisms used by turtles to produce turns. Second, I compared the turning performance of painted turtles with that previously measured from other taxa in order to further evaluate the effects of different body designs on aquatic locomotor performance.

Materials and Methods

Experimental animals

Turns were performed by six yearling painted turtles, *Chrysemys picta*. Carapace lengths ranged from 3.80 to 6.16 cm (mean, 4.76 cm) and weights from 10.7 to 40.4 g (mean, 21.8 g). Turtles were obtained from a commercial turtle farm (Concordia Turtle Farm, Wildsville, LA, USA) and housed together in a large, water filled plastic tub (91 x 61 x 20 cm), located in a climate controlled greenhouse at Clemson University (Clemson, SC, USA). This housing arrangement exposed turtles to ambient light patterns and temperatures during the course of the experiments, which were conducted June-July 2005. The tank

was fitted with a water filter and a dry platform for basking, and turtles were fed commercial pellets four times a week. All animal care and experimental procedures followed Clemson University IACUC guidelines (protocol 50025).

Turning data collection

Aquatic turns were elicited from turtles by stimulating predatory behavior. Each turtle was placed individually into a 75.7 L glass aquarium filled with water to a depth of 10 cm. A Plexiglas divider was used to create a 30 x 30 cm test arena, and a submerged 100-watt heater (located inside the aquarium, but outside of the test arena) maintained water temperature between 24 and 28°C. For each trial, one (or, in some cases, two) small goldfish (*Carassius auratus*) were added to the test arena as prey for the turtle. After introduction of the prey, turtles attempted to catch the fish by chasing them around the tank, often executing turns in the process. Occasionally, turtles could not be incited to chase the fish, either at the beginning of a test day or following pursuits. These trials were halted after 30 min of inactivity and turtles were returned to their holding tank to be tested again the following day.

Turns that each turtle executed as it chased fish were filmed (150 Hz) simultaneously in ventral and lateral views using two digitally synchronized high-speed video cameras (Phantom V4.1,Vision Research, Inc.; Wayne, NJ, USA). The ventral view was captured using a mirror placed at 45° to the tank bottom, which allowed a camera to be focused on a central 25 x 25 cm area that was

delineated on the transparent bottom of the test arena. As a result, turns that occurred within 2.5 cm of the sides of the arena (~0.5 *L*) were not entirely within the field of view and were excluded from analysis; this allowed us to ensure that turtles conducted turns without contacting the sides of the arena. A 1-cm square grid filmed in the ventral view for each trial provided a distance calibration for video analyses (see below). Lateral view videos for each trial were reviewed to ensure that turtles were not in contact with the bottom of the tank, and that they remained level (less than ±15°) and in a horizontal plane throughout the turn. Any turn that did not conform to these criteria also was excluded from analysis. Acceptable trials were downloaded to a computer as proprietary format CINE (.cin) files and converted to AVI format for analysis.

Turning data analysis

To begin quantifying aquatic turning kinematics and performance in turtles, the positions of landmarks on their bodies were first digitized from ventral-view AVI video files using a modification of the public domain NIH Image program for Macintosh, developed at the U.S. National Institutes of Health and available on the internet at http://rsb.info.nih.gov/nih-image/ (the modification, QuickImage, was developed by J. Walker and is available online at http://www.usm.maine.edu/~walker/software.html). Nineteen points were digitized on every other video frame, yielding effective framing rates of 75 Hz. These points were located on the head (tip of snout), plastron (six points along

the midline: anterior edge, humeral-pectoral suture, pectoral-abdominal suture, abdominal-femoral suture, femoral-anal suture, and posterior edge), forelimbs (shoulder, elbow, and distal tip of manus), and hindlimbs (hip, knee, and distal tip of pes) (Fig. 2.1).

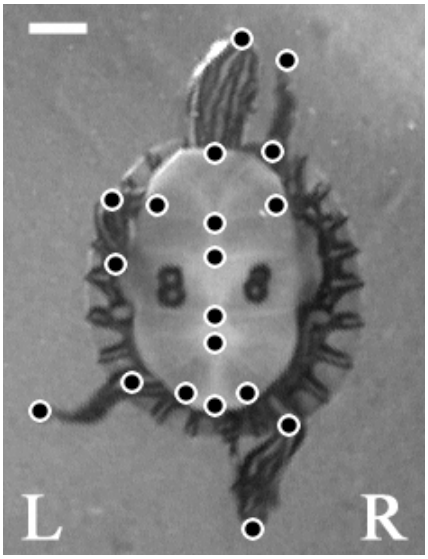

Figure 2.1: Ventral view of a painted turtle with 19 digitized landmarks. The number "8" visible on the plastron was used for identification purposes. Capital "R" and "L" in the image refer to the right and left sides of the turtle, respectively. Note that because the ventral view is reflected by a mirror, the left side of the animal appears on the left side of the image. Scale bar = 1 cm.

To evaluate the kinematic patterns that turtles used to produce aquatic turns, coordinate data were input into a custom Matlab (Ver. 7, Mathworks, Inc.; Natick, MA, USA) routine that calculated the movements of each of the four limbs throughout the course of each trial. Each limb was defined as a vector marked by the endpoints of its proximal segment (forelimb: shoulder and elbow; hindlimb: hip and knee). The position of each limb was calculated using standard

equations for the angle between two vectors, with the proximal limb segment (humerus or femur) forming the first vector, and the midline axis of the body forming the second. Angles were calculated from the ventral-view videos as two-dimensional projections onto the horizontal plane. A limb segment parallel to the midline axis and oriented cranially was assigned an angle of 0°, whereas one parallel to the midline and oriented caudally was assigned an angle of 180°.

To evaluate maneuverability for each turn, the software QuicKurve (Walker, 1998a) was used to interpolate 100 equidistant points along the line of best fit through the six midline landmarks of the plastron for each digitized frame of every trial. For each turn, these coordinate data (100 midline points per frame) were input into a custom Matlab routine, which calculated the position of the turtle's center-of-rotation (COR) as it moved along the curved turning path. The COR was calculated as the point along the turtle's midline that traveled the smallest cumulative distance throughout the turn (sensu Walker, 2000) and is used to define the turning path. I then used QuicKurve (Walker, 1998a) to fit a quintic spline to the *x*-*y* coordinates of the COR along the turning path (Woltring, 1986; Walker, 1998b), smoothing the data and allowing computation of the local (i.e., instantaneous) curvature, κ, along the path using the parametric function:

$$\kappa = |x'y'' - y'x''| / [(x')^2 + (y')^2]^{3/2},$$

where $'$ and $''$ reflect the first and second derivative of *x* and *y*. Finally, the instantaneous radius of the curved turning path is obtained by calculating the reciprocal of κ; the smallest of these values is the minimum instantaneous radius,

R. For each turn, *R* was used as an index of maneuverability. Length-specific turning radii (*R*/*L*; *L* = body length) were calculated to adjust for differences in size among individual turtles, and between turtles and other taxa. In addition, the average and maximum tangential velocity of the COR (U_{avg} and U_{max}, respectively) were calculated for each trial to examine the relationship between tangential velocity (i.e., velocity along the curved turning path) and the length-specific minimum radius of the turning path, *R*/*L*. Tangential velocity (*U*, in *L* s^{-1}) was calculated from differentiation of the cumulative displacement of the COR along the turning path (based on the positional data). Differentiation was performed using QuickSAND software (available online at http://www.usm.maine.edu/~walker/software.html). Prior to differentiation, data were smoothed in QuickSAND using a quintic spline and the generalized cross validation smoothing option (Walker, 1998b). The largest value during a trial represented U_{max}, whereas U_{avg} represents the mean of all values during a trial.

Midline coordinate data from each turn were also input into a custom Matlab routine to calculate (1) cumulative angular rotation of the midline from its initial orientation (i.e., at the beginning of the turn), and (2) the maximum angle of the turn. Angular rotation was calculated using standard equations for the angle between two vectors, with the vectors defined by the positions of the anterior and posterior edges of the plastron in the initial frame of the turn and in each digitized frame thereafter. Using the values obtained for cumulative angular rotation, the instantaneous angular velocity (ω) (i.e., the angular velocity between each pair of

sequentially digitized frames) was calculated in QuickSAND software using the procedures described above for measures of tangential velocity (*U*). The largest value during a trial represented the maximum instantaneous turning rate, ω_{max}, whereas the mean of all values during a trial was the average turning rate, ω_{avg}.

Results

A total of 50 turns performed by six turtles were analyzed. Turtles remained level (i.e., did not bank) throughout the turns. All turns were continuously powered by movements of the fore- and hindlimbs. Two types of turns were identified: forward-moving predatory turns (*N*=43) from five individuals, and non-predatory backward turns (*N*=7) from one individual. Each type of turn was characterized by distinct patterns of limb movements and different levels of performance.

Limb kinematics

Forward and backward turns showed distinct kinematic patterns. In order to describe the movement of limbs during forward swimming I will follow the terminology used by Fish and Nicastro (2003) and use “inboard” to describe the side of the turtle facing toward the center of the turn, and “outboard” to refer to the side facing away from the center of the turn. In forward turns, turtles maintain velocity while executing turns by alternating movements of the hindlimbs, similar to the pattern of hindlimb movement employed during rectilinear swimming (Fig.

2.2A, B). However, during rectilinear swimming, synchronous movements of contralateral fore- and hindlimbs appear to help maintain a straight trajectory. In forward turns the pattern of forelimb motions is modified. During forward turns, the inboard forearm is held in a protracted position throughout the turn (Fig. 2.2B); this should increase drag on the inboard side, allowing the forelimb to function as a pivot (Fish and Nicastro, 2003). The outboard forelimb continues to move as in rectilinear swimming, producing torque (i.e., a turning moment) about the inboard pivot and effecting the turn. The outboard forelimb moves in alternation with the ipsilateral hindlimb and synchronously with the contralateral hindlimb (i.e., maintains the pattern of movement seen in rectilinear swimming; Fig. 2.2B).

Limb movements for backward turns differ substantially from those for forward turns. From a forward trajectory or stationary position, a turtle can begin moving backward by synchronously protracting both hindlimbs. Once a turtle is moving backward, a turn can be initiated by additional limb movements. Although the pattern of limb movements used to produce backward turns is less stereotyped than that of forward turns, a general sequence of movements, in which turtles retract the forelimb on one side and protract the contralateral hindlimb (these two motions overlap temporally), is still apparent for most backward turns (Fig. 2.2C). This produces a torque about the center-of rotation and initiates the turn. Following retraction of the forelimb, the ipsilateral

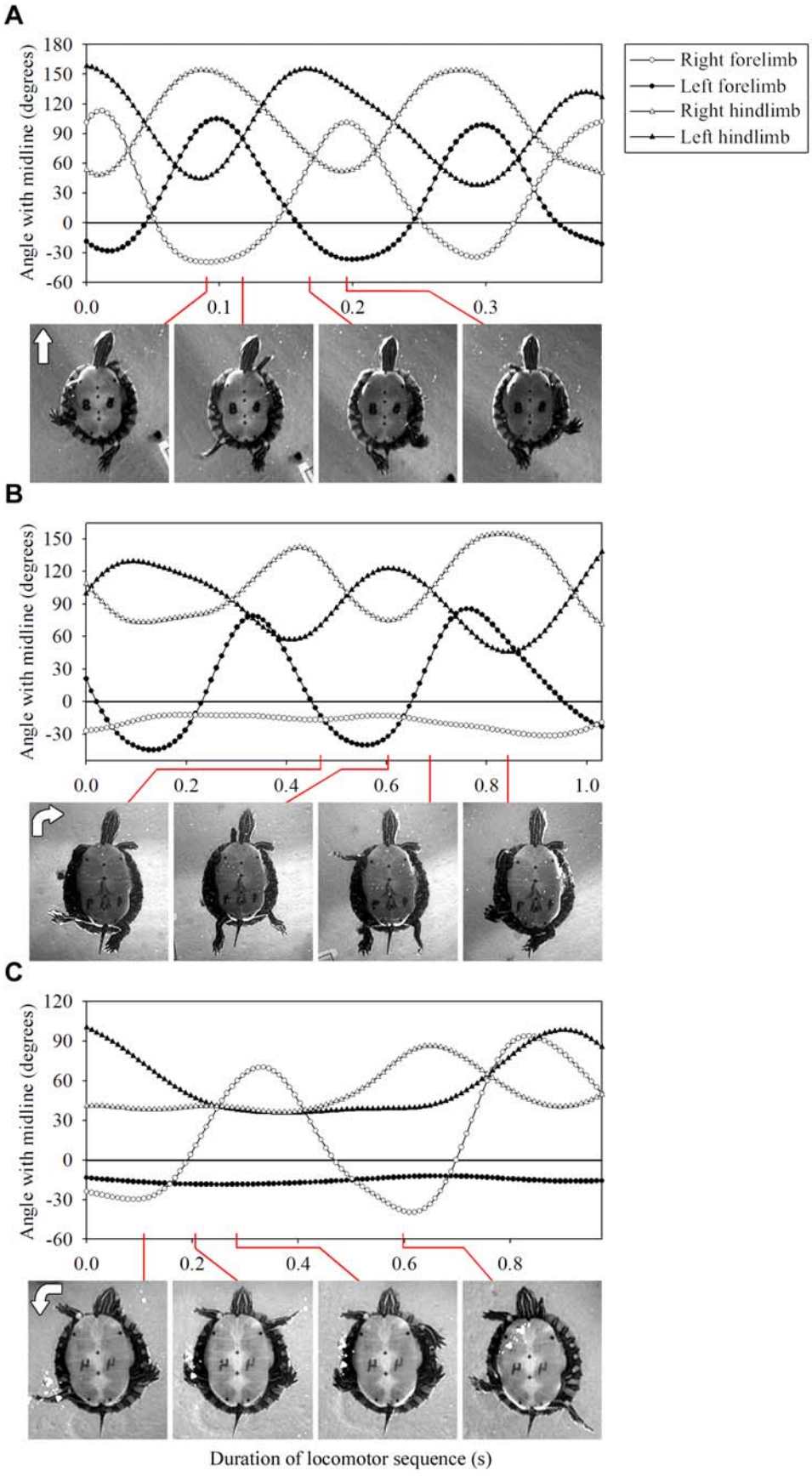
A
Angle with midline (degrees)
180
150
120
90
60
30
0
-30
-60
0.0
0.1
0.2
0.3
Right forelimb
Left forelimb
Right hindlimb
Left hindlimb
B
Angle with midline (degrees)
150
120
90
60
30
0
-30
0.0
0.2
0.4
0.6
0.8
1.0
C
Angle with midline (degrees)
120
90
60
30
0
-30
-60
0.0
0.2
0.4
0.6
0.8
Duration of locomotor sequence (s)

Figure 2.2: Representative kinematic profiles for three modes of swimming performed by painted turtles, with still images from high-speed video indicating the position of the limbs (humerus and femur) at specific times during the locomotor sequence. Circles represent forelimbs and triangles represent hindlimbs. Open symbols indicate right side of the body; closed symbols indicate left side. A decrease in the angle with midline represents limb protraction and an increase in the angle represents limb retraction. Arrows in the first still image of each sequence indicate the direction of movement during the sequence. (A) Representative kinematic profile of a painted turtle during level rectilinear swimming. Note the synchronous movements of contralateral fore- and hindlimbs and the alternating movements of the ipsilateral fore- and hindlimbs. (B) Representative kinematic profile of a turtle during a forward turn. This 82° turn had an average linear velocity (U_{avg}) of 1.83 *L*/s, resulting in an *R*/*L* of 0.24. The turtle propels itself forward using alternating movements of the hindlimbs. The inboard forelimb (open circle) is held in a protracted position for the entire turn and acts as a pivot. The outboard forelimb (closed circle) moves approximately in phase with the contralateral hindlimb, as in rectilinear swimming. (C) Kinematic profile of a backward turn. This 113° turn had an average linear velocity (U_{avg}) of 0.86 *L*/s, resulting in an *R*/*L* of 0.0091. The turtle used synchronous protraction of the hindlimbs to begin moving backward (not plotted). While moving backward, the right forelimb was retracted while the left hindlimb was protracted. During this time the other set of contralateral limbs were held motionless, after which the outboard hindlimb retracts to accelerate the turn.

hindlimb (which had been held in a relatively motionless protracted position) is retracted, providing additional thrust to the turn.

Turning performance

The smallest *R*/*L* was 0.0018 *L* (Table 2.1) and occurred during a forward turn with an average tangential velocity (U_{avg}) of 1.26 *L* s^{-1} and an average turning rate (ω_{avg}) of 134.4° s^{-1}. The second smallest *R*/*L* for a forward turn was 0.0083 *L* and had a U_{avg} of 1.40 *L* s^{-1} and a ω_{avg} of 166.9° s^{-1}. These two turns were performed by two different individuals. The smallest *R*/*L* for a backward

Table 1. *Turning Performance Data*

	R (m)	R/L (L)	U_{avg} (Ls^{-1})	U_{max} (Ls^{-1})	ω_{avg} (° s^{-1})	ω_{max} (° s^{-1})
Minimum						
Forward	0.0001	0.0018	1.26	1.89	46.2	147.7
Backward	0.0005	0.0091	0.70	1.21	81.8	135.3
Maximum						
Forward	0.0551	1.0442	4.51	6.18	247.1	501.8
Backward	0.0049	0.0950	1.59	2.44	162.1	291.6
Mean						
Forward	0.0114 (0.0017)	0.2477 (0.0365)	2.52 (0.15)	3.62 (0.19)	136.4 (6.4)	312.0 (13.5)
Backward	0.0017 (0.0006)	0.0340 (0.0116)	1.04 (0.11)	1.67 (0.15)	128.0 (9.8)	221.9 (20.7)
Forward (Extreme 20%)	0.0018 (0.0004)	0.0423 (0.0088)	3.97 (0.10)	5.47 (0.16)	198.4 (8.8)	434.0 (14.1)

Values in parentheses are standard error of the mean.
R (m) is the minimum radius of the turning path in meters.
R/L is the length-specific minimum radius of the turning path in body lengths.
U_{avg} (L s^{-1}) is the average linear velocity of the turn.
U_{max} (L s^{-1}) is the maximum instantaneous velocity of the turn.
ω_{avg} (° s^{-1}) is the average angular velocity of the turn.
ω_{max} (° s^{-1}) is the maximum instantaneous angular velocity of the turn.

turn was 0.0091 *L* with a U_{avg} of 0.86 *L* s^{-1} and a ω_{avg} of 115.1° s^{-1}. All seven backward turns had *R*/*L* less than 0.1 *L*. In contrast, only 13 of the 43 forward turns (30.2%; with each of the five turtles performing at least one) had *R*/*L* less than 0.1 *L*. The maximum ω_{avg} for all turns was 247.1° s^{-1} and was attained during a forward turn of 79.1° with an *R*/*L* of 0.2846 *L*.

In addition to showing different kinematic patterns, forward and backward turns also exhibited considerable differences in performance. Unless otherwise stated, results are reported as the mean ± S.E.M. Turn angles for forward turns ranged from 76.2° to 243.6° (mean, 118.0 ± 5.1°), and from 113.0° to 200.0° (mean, 162.0 ± 12.4°) for backward turns. The average center-of-rotation (COR) for forward turns was positioned at 30.9% (± 2.4) of the body length (*L*), whereas for backward turns it was 66.7% (± 3.6). There was a significant relationship between tangential velocity (U_{avg}) and the COR for both forward and backward turns. Least-squares regressions indicated that the COR moved farther anterior as speed increased for forward turns, whereas for backward turns the COR moved farther posterior as speed increased (r^2=0.295 and r^2=0.772, respectively; P<0.01). Forward turns showed a weak, but significant, relationship (r^2=0.420; P<0.001; Fig. 2.3) between the average tangential velocity through the turn (U_{avg}) and the length-specific minimum instantaneous radius of the turning path (*R*/*L*); this relationship for backward turns was even stronger (r^2=0.863; P<0.01; Fig. 2.3). However, no relationship was found between angular velocity (ω_{avg}) and

R/*L* for forward (r^2=0.001; *P*=0.878) or backward (r^2=0.259; *P*=0.244) turns (Fig. 2.4).

To further compare performance differences between forward and backward turns, for each of the six primary performance variables I calculated the extreme 20% (*N*=9) values for forward turns (Table 2.1). These extreme values included the minimum nine values for *R* and *R*/*L* and the maximum nine values for *U* and ω (following the precedent of Webb, 1983; Gerstner, 1999; Fish and Nicastro, 2003; Fish et al., 2003; Maresh et al., 2004). These values of *R* and *R*/*L* for forward turns were much more similar to those of backward turns; however, values of *U* and ω became substantially greater for forward turns than backward turns in this comparison.

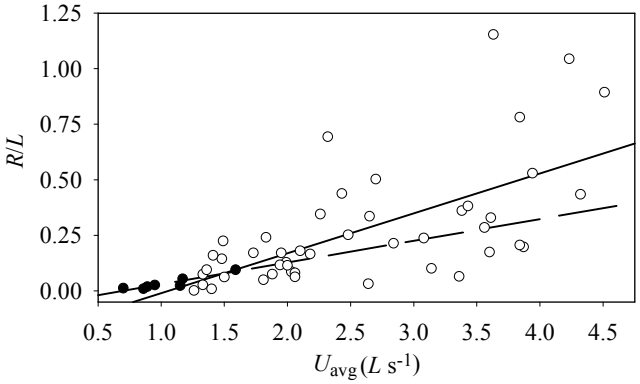

Figure 2.3: Relationship between average tangential velocity (U_{avg}) and length-specific minimum radius (*R*/*L*) for forward and backward turns. Open symbols represent forward turns (*N*=43, solid regression line); closed symbols represent backward turns (*N*=7, dashed regression line). Both relationships are significant (see text for regression statistics).

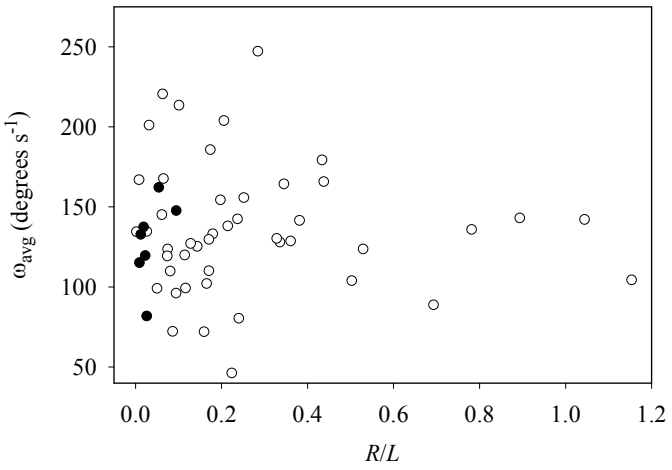

Figure 2.4: Relationship between the length-specific minimum radius of the turning path (*R*/*L*) and average angular velocity (ω_{avg}). Open symbols represent forward turns (*N*=43); closed symbols represent backward turns (*N*=7). Neither relationship is significant (see text).

Discussion

Mechanisms of aquatic turning in turtles

Because freshwater turtles have a rigid body and non-propulsory tail, which is reduced in most species, only the fore- and hindlimbs can be used to produce aquatic thrust (Pace et al., 2001). One focus of this study was to determine how painted turtles use their limbs to execute turns. Turns require an asymmetry in forces between the inboard and outboard sides of the animal, which could be produced through any of several different patterns of limb movement. Using a simplified descriptive framework, each individual limb might show one of four basic patterns of movement during a turn: (1) continue to move

as in rectilinear swimming, (2) exhibit movements modified from the pattern used during rectilinear swimming, (3) fold along the body to stop contributing to propulsion, but minimize additional drag, or (4) project out from the body to increase drag and act as a pivot. For example, either one or both inboard limbs might show pattern 3 (fold along the body) while the outboard limbs show pattern 1 or 2 (standard-rectilinear or modified rowing). Alternatively, either one or both inboard limbs might show pattern 4 (outward projection as a pivot) while the outboard limbs show patterns 1 or 2 (standard-rectilinear or modified rectilinear rowing; powered turns) or 3 (fold along the body; unpowered turns). Our data show that, during forward turns, painted turtles consistently combine patterns 4 and 1, protracting the inboard forelimb and holding it stationary into the flow, while continuing to move the outboard forelimb and both hindlimbs as in rectilinear swimming. This combination of limb movements during forward turns is a fairly basic modification of the limb movements used for rectilinear swimming, which may simplify their neural control (Macpherson, 1991; Earhart and Stein, 2000). Moreover, the functional consequence of this movement pattern is that swimming freshwater turtles execute forward turns by increasing inboard drag while still producing thrust, a combination of limb movements that should allow them to execute turns more quickly than alternative patterns (e.g., if any of the limbs were folded against the body). These patterns of turning kinematics are similar to those of another rigid-bodied species, the whirligig beetle (Fish and Nicastro, 2003), in which inboard limbs appear to function as a

pivot about which the body rotates due to both initial forward momentum and forward thrust generated by the outboard limbs. In addition, because the left and right hindlimbs of turtles show similar patterns of motion during forward turns, it is the movements of the forelimbs in particular that appear to be responsible for generating the asymmetric forces required for turtles to execute turns. These findings support the conclusion of Pace et al. (2001) that swimming freshwater turtles (except *Carettochelys* and possibly trionychid softshells) use their forelimbs primarily for balance and controlling orientation. Evaluations of the forces produced by each limb during turns (e.g. using techniques such as particle image velocimetry: Drucker and Lauder, 1999; Blob et al., 2003) could further test this hypothesis.

In addition to forward turns, I also observed backward turns by painted turtles. Although generalizations about the performance of backward turns must be made with caution because all of our observations were from a single individual, I have also observed this type of turn in two other species of freshwater turtle (the slider *Trachemys scripta* and the softshell *Apalone spinifera*; G. Rivera and R. W. Blob, unpublished), suggesting that it is not unusual for turtles to perform this behavior. The limb movements of backward turns are more complex than those of forward turns, but several distinctive characteristics can still be recognized. First, all backward turns occurred after the turtle, moving forward, approached the side of the arena and then reversed direction without rotating the body. Reversal was accomplished by synchronous

forward sweeps of both hindlimbs with the hindfoot webbing fully extended. Davenport et al. (1984) observed that sliders (Emydidae) often swept both hindlimbs forward in unison to achieve rapid braking, so it is likely that the initial protraction of the hindlimbs during backward turns by painted turtles functions to stop forward momentum (rather than contribute to the turn) and that subsequent synchronous protractions generate the forward thrust used to reverse direction. Once turtles were moving backward, turns were initiated by near simultaneous retraction of one forelimb and protraction of the contralateral hindlimb, producing a turning moment that rotated the body.

In addition to differences in kinematics, several parameters of turning performance also differed between forward and backward turns (Table 2.1). For both forward and backward turns the COR moved closer to the leading edge of the body with increasing velocity. This resulted in a cranially positioned COR for forward turns and a caudally positioned COR for backward turns. Backward swimming was slower than forward swimming and also resulted in much lower angular velocities. In addition, the *R*/*L* for backward turns generally were much smaller than those for forward turns. However, when only the minimum 20% of values for forward turns are compared to values for backward turns these differences are minimized. In fact the two smallest turning radii were from forward turns. Still, the performance of backward turns was much less variable than that of forward turns, with the range of *R*/*L* spanning only one order of magnitude (0.0091-0.0950 *L*), whereas for forward turns *R*/*L* spanned four orders

of magnitude (0.0018-1.0442 *L*). Similar comparisons of forward and backward turning performance in other aquatic taxa are available for only one other species, the angelfish (*Pterophyllum scalare*; Webb and Fairchild, 2001). In contrast to turtles, angelfish showed significantly larger length specific turning radii (*R*/*L*) during backward turning (0.71) than during forward turning (0.41), a result that may relate to the differing positions of propulsive appendages in these species.

Comparisons with other taxa

Another focus of this study was to compare the turning performance of turtles with that of other taxa, particularly those with rigid-bodies. Rigid-bodied animals that have been examined to this point have excelled in one of the two parameters of turning performance (agility or maneuverability), but not both. For example, boxfish are highly maneuverable (small *R*/*L*), but have low agility (Walker, 2000); in contrast, whirligig beetles can rotate with high agility (high angular velocities), but are not very maneuverable (i.e., they have large *R*/*L*; Fish and Nicastro, 2003). This analysis of turning performance in painted turtles shows that when compared to other rigid-bodied taxa, rather than excelling at one of the two performance parameters, painted turtles display intermediate values for both (Fig. 2.5). For each of the four measurements of *R*/*L*, the same pattern of performance was identified for the three species: boxfish < turtle < beetle. While the values for the painted turtles overlapped with both those of

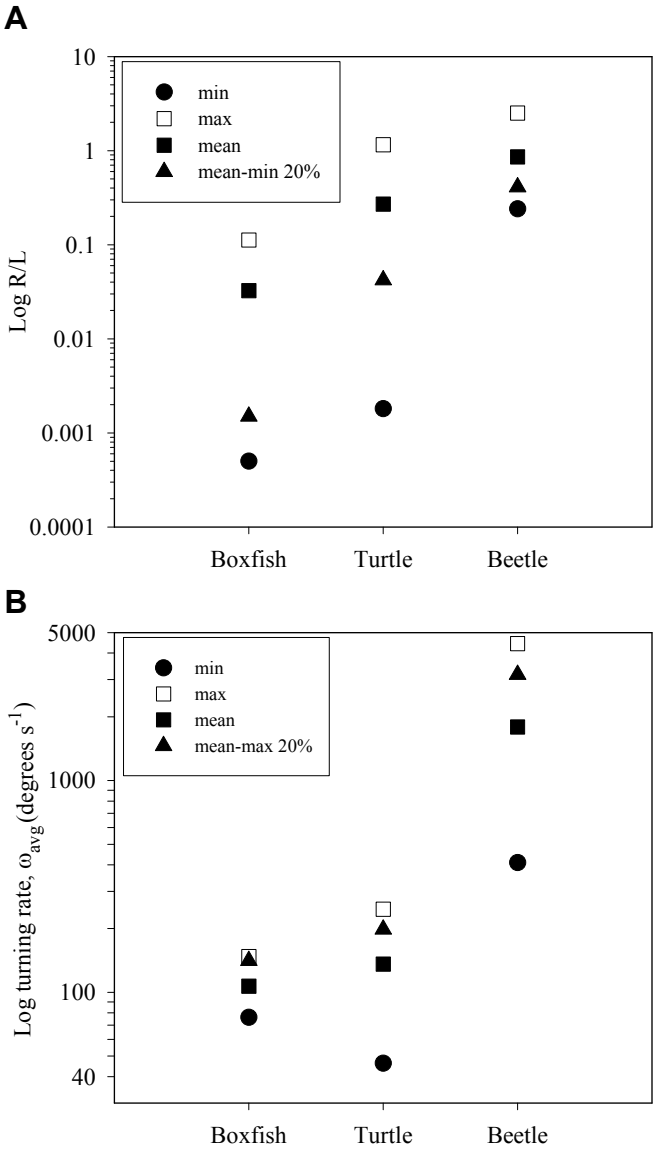

Figure 2.5: Comparison of turning performance for three rigid-bodied taxa. (A) length-specific minimum radius of the turning path (*R*/*L*). (B) Average turning rate (ω_{avg}). Closed circles indicate the single minimum value, open squares indicate the single maximum value, closed squares indicate the mean of all values, and closed triangles indicate the mean of the minimum 20% of values (A) or maximum 20% of values (B). Values for boxfish (*N*=12) are from Walker (2000); values for beetles (*N*=119) are from Fish and Nicastro (2003). Values for turtles are from this study and include only forward turns (*N*=43). Data are graphed on a log (base 10) scale.

boxfish and the whirligig beetle, the maximum *R*/*L* of boxfish (0.1121 *L*) was smaller than the minimum *R*/*L* for the beetle (0.24 *L*). The pattern is the same for ω_{avg}, with boxfish < turtle < beetle, for all but the minimum values.

If comparisons are expanded beyond rigid-bodied taxa, differences in maneuverability between painted turtles and other taxa vary considerably depending on the criteria used. Table 2.2 shows *R/L* (maneuverability) values from 18 studies that have measured turning performance in a wide range of aquatic animals. These values are most often published as an average of all trials for a given species. However, other values are also frequently reported, either as a complement to overall means or in place of them, such as the average of the minimum 20% *R*/*L* values, or single, overall minimum values (e.g., Webb, 1976; Webb, 1983; Fish, 2002; Fish et al., 2003). The most conservative comparisons rely on the average of all trials. In this case, painted turtles have an average *R*/*L* (0.25 *L*) smaller than only four previously studied taxa: whirligig beetles (0.86 *L*; Fish and Nicastro, 2003), squid (~0.5 *L*; Foyle and O'Dor, 1988), tuna (0.47 *L*; Blake et al., 1995), and angelfish, (0.41 *L*; Webb and Fairchild, 2001). However, because the goal of our study was to examine maximal turning performance in turtles (in the context of predator-prey encounters), comparisons of minimum *R*/*L* values are also justified. In these comparisons, the mean-minimum 20% *R*/*L* for painted turtles (0.0423 *L*) was smaller than the reported values for all but four previously examined species: damselfish (0.04 *L*), wrasse (0.02 *L*), surgeonfish (<0.01 *L*), and boxfish (0.0015 *L*) (Gerstner, 1999; Walker,

Table 2. *Comparison of Length-specific Turning Radii (R/L) Among Taxa*

Species	Common name	Mean	Mean-min 20%	Min	Paper
Ostracion meleagris	Spotted boxfish	0.0325	0.0015	0.0005	Walker, 2000
Acanthurus bahanius	Ocean surgeonfish	-----	<0.01	-----	Gerstner, 1999
Thalassoma bifasciatum	Bluehead wrasse	-----	0.02	-----	Gerstner, 1999
Stegastes leucostictus	Beaugregory damselfish	-----	0.04	-----	Gerstner, 1999
Chrysemys picta	Painted turtle	0.25	0.0423	0.0018	This paper
Xenomystus nigri	Knifefish	0.055†	-----	-----	Domenici and Blake, 1997
Chaetodon capistratus	Foureye butterflyfish	-----	0.06	-----	Gerstner, 1999
Pterophyllum eimekei	Angelfish	0.065	-----	-----	Domenici and Blake, 1991
Squalus acanthias	Spiny dogfish	0.067	-----	0.041	Domenici et al., 2004
Esox lucius	Pike	0.09†	-----	-----	Domenici and Blake, 1997
Zalophus californianus	Sea lion, male	-----	0.11	0.09	Fish et al., 2003
Micropterus dolomieu	Bass	-----	0.11	-----	Webb, 1983
Coryphaena hippurus	Dolphin	0.13	-----	-----	Webb and Keyes, 1981
Pseudorca crassidens	False Killer whale	-----	0.15	0.13	Fish, 2002
Cephalorhynchus commersonii	Commerson's Dolphin	-----	0.16	0.15	Fish, 2002
Inia geoffrensis	Amazon River Dolphin	-----	0.16	0.10	Fish, 2002
Salmo gairdneri	Trout	-----	0.17	-----	Webb, 1976
Delphinapterus leucas	Beluga whale	-----	0.17	0.15	Fish, 2002
Sphyrna lewini	Scalloped hammerhead shark	0.183	-----	-----	Kajiura et al., 2003
Salmo gairdneri	Trout	-----	0.18	-----	Webb, 1983
Orcinus orca	Killer whale	-----	0.18	0.11	Fish, 2002
Zalophus californianus	Sea lion, female	-----	0.19	0.16	Fish et al., 2003
Carcharhinus plumbeus	Sandbar shark	0.193	-----	-----	Kajiura et al., 2003
Tursiops truncatus	Bottlenose dolphin	-----	0.19	0.13	Fish, 2002
Tursiops truncatus	Bottlenose dolphin	0.21	0.09	0.08	Maresh et al., 2004
Metynnis hypsauchen	Silver dollar	0.22	-----	-----	Webb and Fairchild, 2001
Seriola dorsalis	Yellowtail	0.23	-----	-----	Webb and Keyes, 1981
Lagenorhynchus obliquidens	Pacific White-sided Dolphin	-----	0.23	0.20	Fish, 2002
Spheniscus humboldti	Humboldt penguin	-----	0.24‡	-----	Hui, 1985
Carassius auratus	Goldfish	0.25	-----	-----	Webb and Fairchild, 2001
Pterophyllum scalare	Angelfish	0.41	-----	-----	Webb and Fairchild, 2001
Dineutes horni	Whirligig beetle	0.86	0.41	0.24	Fish and Nicastro, 2003
Thunnus albacares	Yellowfin tuna	0.47	-----	0.20	Blake et al., 1995
Illex illecebrosus	Short-finned squid	-----	-----	~0.5	Foyle and O'Dor, 1988

Species are ranked in order of increasing mean turning radius *(R/L)*, using mean-min 20% in place of overall mean when available.
† When no information is given, values were considered to be overall means.
‡ Data represent the minimum five *R/L* out of 39 trials (minimum 13%).

2000). Moreover, when single minimum *R*/*L* values are compared, only the boxfish (0.0005 *L*) and surgeonfish (<0.01 *L*; reported as mean-min 20%) have turning radii smaller than painted turtles (0.0018 *L*). As seen with boxfish, these comparisons indicate that the rigid bodies of painted turtles do not appear to severely limit their maneuverability.

Agility (ω) also varies considerably among taxa (Fig. 2.6). The maximum ω_{avg} for turtles (247° s^{-1}) is greater than the values seen for boxfish (147° s^{-1}; Walker, 2000) and squid (90° s^{-1}; Foyle and O'Dor, 1988), but less than those seen for beetles (4438° s^{-1}; Fish and Nicastro, 2003), stiff-bodied tuna (426° s^{-1}; Blake et al., 1995), and penguins (576° s^{-1}; Hui, 1985). In addition, because body size appears to be an important underlying determinant of agility (Fish and Nicastro, 2003), the fact that much larger stiff-bodied cetaceans can turn at comparable rates suggests that they are much more agile than rigid turtles. Similarly, the fact that flexible fish of similar size are able to turn at rates much higher than turtles (Fig. 2.6) suggests that agility may be constrained by a rigid design.

Modes of turning and performance

That two of the three smallest reported *R*/*L* values are from rigid-bodied taxa (boxfish: Walker, 2000; turtles: this study) suggests that rigid-bodied taxa use modes of turning that increase maneuverability. In fact, having small turning radii may be of particular importance to rigid taxa because it is the only way to

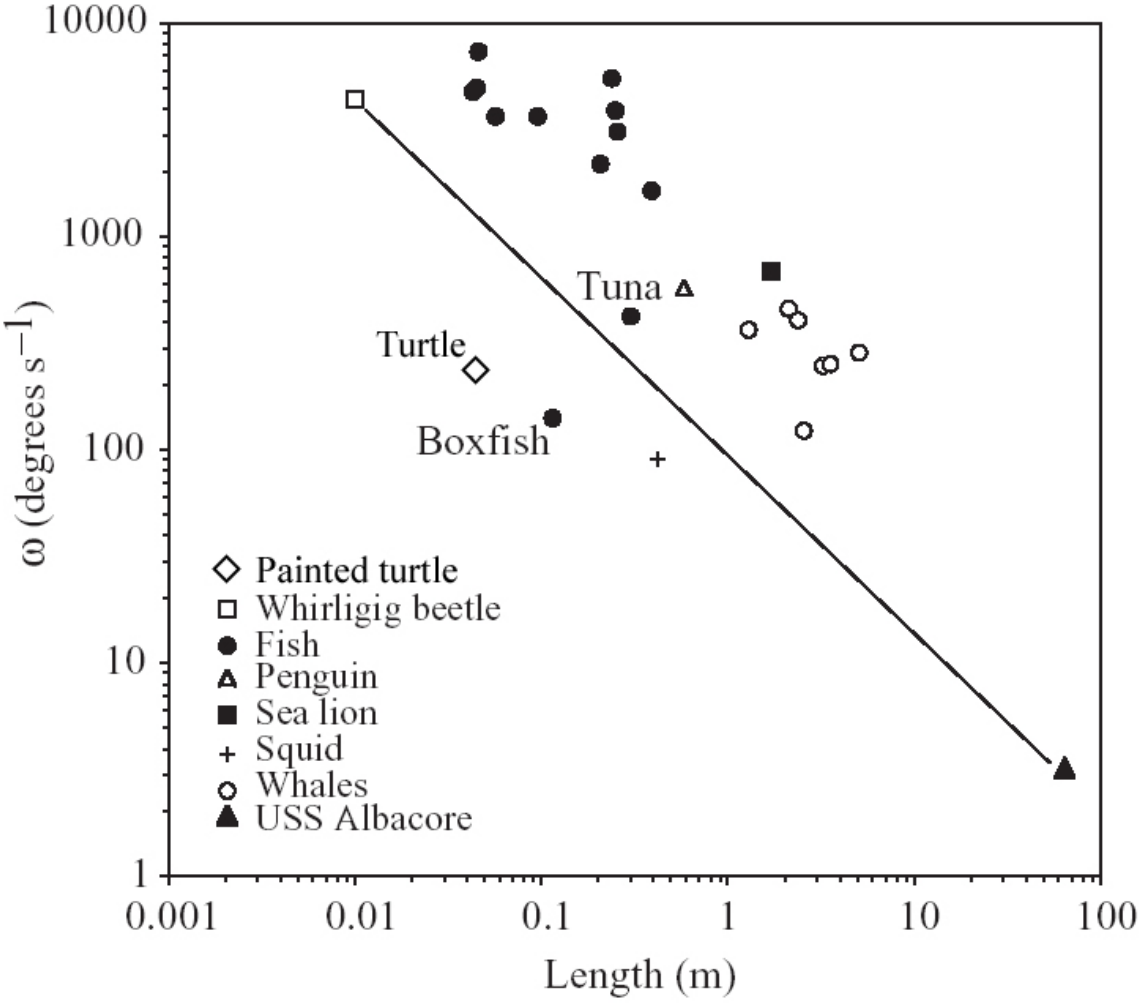

Figure 2.6: Comparison of turning rate, ω_{avg}, with respect to size among a broad range of taxa graphed on a log (base 10) scale. The line connects the beetle and submarine, both of which have rigid bodies. Other rigid-bodied taxa appear to the left of the line. Modified from Fish and Nicastro (2003) with permission. Value of ω_{avg} for turtles based on this study; position of boxfish data point moved to reflect ω_{avg} rather than ω_{max}.

decrease the space required for them to complete a turn. In contrast, flexible taxa can reduce the area required to turn simply by bending their bodies (Walker, 2000). However, rigid-bodied whirligig beetles turn with relatively large radii (Fish and Nicastro, 2003). Reasons for these differences between low- and high-*R*

among rigid-bodied taxa, as well as for the discrepancy in agility between flexible- and rigid-bodied taxa may be based on the modes of turning used by these different groups.

Aquatic organisms can generate turning forces (i.e., torque) by two mechanistically different methods: (1) actively by motion of control surfaces, or (2) passively from flows produced by movements of the body or external flow fields (Fish, 2004). Passively powered turns rely on the kinetic energy of a translating body or extended hydrofoil moving through local flow, and therefore require that turning path (R) and tangential velocity (U) be greater than 0. The effectiveness of passively powered turns should vary with speed, with torque production increasing with the square of velocity (Weihs, 1981). As a result, at low U, passive maneuvering becomes more difficult (Weihs, 1981; Fish, 2002). In contrast, actively powered turns are generated by oscillating limbs, and although R and U may be greater than 0, this is not required. Oscillating limbs have a distinct advantage over passive maneuvering when U=0, as oscillating limbs produce hydrodynamically derived drag without movement of the body (Blake, 1986). This allows turns to be composed of pure rotational movements with no body translation (Walker, 2000). As a result, it seems that oscillating limbs are a better design for maneuverability (lower R). However, there are several reasons why actively powered turns should reduce agility compared to passively powered turns regardless of whether the turn involves body translation. The first is that an object turning in place (R and U = 0) will have higher pressure

drag resisting rotation because the angle of attack between the body and the local flow is close to 90° along the entire length of the body (Walker, 2000). As long as an organism is designed to reduce drag while moving in a longitudinal direction, the angle of attack between the body and the local flow (and thus drag) will be reduced as *R* increases, being lowest while moving in a straight line. This is particularly the case for rigid-bodied taxa that cannot bend their bodies in the direction of the turn (Walker, 2000). A second reason that actively powered turns might suffer reduced agility is that for turns with translation (*R* and $U > 0$), the rate of rotation is dependent on the speed of the oscillating limbs, the latter of which is reduced overall as a result of having distinct power and recovery strokes. In addition, paddling is inefficient at high *U* because the speed differential between the body and the paddle becomes smaller with less propulsive force being generated (Blake, 1986; Fish, 1996). In contrast, passively powered turns utilize much higher tangential speeds and have the advantage that turning forces can be generated without incurring a large decelerating drag.

These ideas help to explain the patterns of maneuverability and agility that are observed for the three rigid-bodied taxa examined to date. Turtles and boxfish are able to turn with a small *R* because their use of oscillating limbs does not depend on tangential velocity. In addition, although velocity is generated by oscillating limbs in whirligig beetles, their high angular velocity is achieved by having very high tangential velocity (*U*) while traveling along a large *R*. Lastly,

while flexible-bodied organisms can have high levels of maneuverability and agility, they also have the ability to mix styles of turning, whereas most rigid-bodied taxa appear to be limited to actively powered turns using oscillating limbs.

Morphological correlates of turning performance

Differences in agility between painted turtles and boxfish may not relate exclusively to their differences in body size (Fig. 2.6). Walker (2000) gives three reasons why the rigid bodies of boxfish should limit agility: (1) an inability to bend the cranial end of the body into the turn, (2) an inability to bend and reduce the body's second moment of area about the rotational axis, resulting in high inertial resistance to rotation (Carrier et al., 2001; Walter and Carrier, 2002), and (3) high pressure drag resisting rotation because the angle of attack between the body and the local flow is close to 90° along the entire length of the body. Because turtles are also unable to bend their bodies, they must also face the same constraints on agility posed in points 1 and 2. However, painted turtles are more dorsoventrally flattened and have more rounded dorsal profiles than boxfish, both of which should reduce the pressure drag to which turtles are exposed.

Despite having rigid bodies, painted turtles may also be able to reduce second moments of area through mechanisms unavailable to boxfish. First, with very few exceptions (e.g. snapping turtles), most extant turtles have highly reduced tails (Willey and Blob, 2004). The presence of a long tail in swimming turtles would increase both the second moment of area and rotational inertia,

which would result in decreased agility (Carrier et al., 2001). Therefore, tail reduction in turtles may be a factor contributing to their greater agility in comparison to boxfish. In this context, it is perhaps not surprising that those turtles that possess long tails (Chelydrines) are primarily benthic scavengers or ambush predators that do not actively pursue evasive prey, for which high turning performance might be required (Ernst et al., 1994).

Other morphological features of turtles that may help enhance their agility compared to boxfish relate to the propulsors, or control surfaces. The fins of boxfish are supported by flexible rays, whereas the limbs of turtles are supported by more robust, stiffer limb bones that can extend farther from the body than boxfish fins. These differences in structure may help make turtle limbs a more effective brake or pivot on the inboard side, and a more powerful propulsor on the outboard side. In addition, the position of the limbs in turtles, with all four located near and approximately equidistant from the center of rotation, might also enhance maneuverability (Fish, 2002). Furthermore, because all four limbs in turtles lie within the same horizontal plane, thrust and drag forces used to generate torque are all directed within the plane of rotation. Boxfish also achieve enhanced maneuverability by using multiple control devices (i.e., five fins: Gordon et al., 2000; Walker, 2000; Hove et al., 2001), but multiple fins located outside the plane of rotation may be less effective contributors to horizontal (i.e., yawing) turns.

Directions for further study

As noted by Walker (2000), morphologies that might facilitate or limit turning have been widely discussed, but the effects of many design features on turning performance remain unresolved. Numerous studies have examined the effect of body and fin shape on turning performance among fishes and have identified morphological features correlated with turning performance (Schrank and Webb, 1998; Gerstner, 1999; Schrank et al., 1999). Similarly, it is possible that interspecific variation in the morphology of turtles could also produce substantial differences in turning performance. Although the general body plan of turtles has changed little over 200 million years (Gaffney, 1990; Rieppel and Reisz, 1999), extant freshwater turtles exhibit considerable morphological diversity. For example, softshell turtles of the genus *Apalone* are dorsoventrally flattened to an even greater degree than the painted turtles examined in this study, and possess extensive webbing on the forefeet (Webb, 1962; Pace et al., 2001). As a result, these highly aquatic species might be expected to exhibit turning performance superior to that of painted turtles. In contrast, many species of the riverine genus *Graptemys* (map turtles) have prominent mid-dorsal keels (Ernst et al., 1994). It is possible that, like the keels of boxfish (Bartol et al., 2003; Bartol et al., 2005), the keels of map turtles may aid in stabilization during rectilinear swimming, which in turn could negatively affect turning performance. Correlating parameters of turning performance (maneuverability and agility) with predator-prey interactions and habitat characteristics (e.g., flow velocity and

turbulence) could help to determine the factors that have influenced the diverse morphologies seen within turtles as well as the broad impact of rigid body designs.

Acknowledgments

I am grateful to Takashi Maie and Shala Hankison for assistance with animal care and to T. Maie, J. Long, and an anonymous referee for comments on earlier versions of this work. I am also grateful to Jeff Walker for helpful advice on data analysis, to Frank Fish for permission to reprint a figure from his previous work, and to Michael Childress for loan of the mirror frame used during filming. This work was supported by two SICB Grant-in-Aid-of-Research (GR and ARVR), an undergraduate research grant from the Howard Hughes Medical Institute through the Clemson University/South Carolina Life Program (EED), and the Clemson University Department of Biological Sciences.

Literature Cited

Aresco, M. J. and Dobie, J. L. (2000). Variation in shell arching and sexual size dimorphism of river cooters, *Pseudemys concinna*, from two river systems in Alabama. *J. Herpetol.* **34**, 313-317.

Bartol, I. K., Gharib, M., Webb, P. W., Weihs, D. and Gordon, M. S. (2005). Body-induced vortical flows: a common mechanism for self-corrective trimming control in boxfishes. *J. Exp. Biol.* **208**, 327-344.

Bartol, I. K., Gharib, M., Weihs, D., Webb, P. W., Hove, J. R. and Gordon, M. S. (2003). Hydrodynamic stability of swimming in ostraciid fishes: role of the carapace in the smooth trunkfish *Lactophrys triqueter* (Teleostei: Ostraciidae). *J. Exp. Biol.* **206**, 725-744.

Biewener, A. A. and Gillis, G. B. (1999). Dynamics of muscle function during locomotion: accommodating variable conditions. *J. Exp. Biol.* **202**, 3387-3396.

Blake, R. W. (1986). Hydrodynamics of swimming in the water boatman, *Cenocorixa bifida*. *Can. J. Zool.* **64**, 1606-1613.

Blake, R. W., Chatters, L. M. and Domenici, P. (1995). Turning radius of yellowfin tuna (*Thunnus albacares*) in unsteady swimming manoeuvres. *J. Fish Biol.* **46**, 536-538.

Blob, R. W., Rai, R., Julius, M. L. and Schoenfuss, H. L. (2006). Functional diversity in extreme environments: effects of locomotor style and substrate texture on the waterfall-climbing performance of Hawaiian gobiid fishes. *J. Zool., Lond.* **268**, 315-324.

Blob, R. W., Willey, J. S. and Lauder G. V. (2003). Swimming in painted turtles: Particle image velocimetry reveals different propulsive roles for the forelimb and hindlimb. *Integr. Comp. Biol.* **43**, 985.

Burke, A. C. (1989). Development of the turtle carapace: implications for the evolution of a novel bauplan. *J. Morphol.* **199**, 363-378.

Carrier, D. R., Walter, R. M. and Lee, D. V. (2001). Influence of rotational inertia on turning performance of theropod dinosaurs: clues from humans with increased rotational inertia. *J. Exp. Biol.* **204**, 3917-3926.

Claude, J., Paradis, E., Tong, H. and Auffray, J.-C. (2003). A geometric morphometric assessment of the effects of environment and cladogenesis on the evolution of the turtle shell. *Biol. J. Linn. Soc.* **79**, 485-501.

Davenport, J., Munks, S. A. and Oxford, P. J. (1984). A comparison of the swimming of marine and freshwater turtles. *Proc. R. Soc. Lond. B* **220**, 447-475.

Domenici, P. (2001). The scaling of locomotor performance in predator-prey encounters: from fish to killer whales. *Comp. Biochem. Physiol. A* **131**, 169-182.

Domenici, P. and Blake, R. W. (1997). The kinematics and performance of fish fast-start swimming. *J. Exp. Biol.* **200**, 1165-1178.

Domenici, P., Standen, E. M. and Levine, R. P. (2004). Escape manoeuvres in the spiny dogfish (*Squalus acanthias*). *J. Exp. Biol.* **207**, 2339-2349.

Drucker, E. G. and Lauder, G. V. (1999). Locomotor forces on a swimming fish: three-dimensional vortex wake dynamics quantified using digital particle image velocimetry. *J. Exp. Biol.* **202**, 2393-2412.

Earhart, G. M. and Stein, P. S. G. (2000). Step, swim, and scratch motor patterns in the turtle. *J. Neurophysiol.* **84**, 2181-2190.

Ernst, C. H., Lovich, J. E. and Barbour, R. W. (1994). *Turtles of the United States and Canada*. Washington: Smithsonian Institution Press.

Fish, F. E. (1996). Transitions from drag-based to lift-based propulsion in mammalian swimming. *Am. Zool.* **36**, 628-641.

Fish, F. E. (1999). Performance constraints on the maneuverability of flexible and rigid biological systems. In *Proceedings of the Eleventh International Symposium on Unmanned Untethered Submersible Technology*, pp. 394-406. Durham, New Hampshire: Autonomous Undersea Systems Institute.

Fish, F. E. (2002). Balancing requirements for stability and maneuverability in cetaceans. *Integr. Comp. Biol.* **42**, 85-93.

Fish, F. E. (2004). Structure and mechanics of nonpiscine control surfaces. *IEEE Journal of Oceanic Engineering* **28**, 605-621.

Fish, F. E., Hurley, J. and Costa, D. P. (2003). Maneuverability by the sea lion *Zalophus californianus*: turning performance of an unstable body design. *J. Exp. Biol.* **206**, 667-674.

Fish, F. E. and Nicastro, A. J. (2003). Aquatic turning performance by the whirligig beetle: constraints on maneuverability by a rigid biological system. *J. Exp. Biol.* **206**, 1649-1656.

Foyle, T. P. and O'Dor, R. K. (1988). Predatory strategies of squid (*Illex illecebrosus*) attacking small and large fish. *Mar. Behav. Physiol.* **13**, 155-168.

Gaffney, E. S. (1990). The comparative osteology of the Triassic turtle *Proganochelys*. *Bull. Am. Mus. Nat. Hist.* **194**, 1-263.

Gerstner, C. L. (1999). Maneuverability of four species of coral-reef fish that differ in body and pectoral-fin morphology. *Can. J. Zool.* **77**, 1102-1110.

Gordon, M. S., Hove, J. R., Webb, P. W. and Weihs, D. (2000). Boxfishes as unusually well-controlled autonomous underwater vehicles. *Physiol. Biochem. Zool.* **73**, 663-671.

Hedenström, A. and Rosén, M. (2001). Predator versus prey: on aerial hunting and escape strategies in birds. *Behav. Ecol.* **12**, 150-156.

Hove, J. R., O'Bryan, L. M., Gordon, M. S., Webb, P. W. and Weihs, D. (2001). Boxfishes (Teleostei: Ostraciidae) as a model system for fishes swimming with many fins: kinematics. *J. Exp. Biol.* **204**, 1459-1471.

Howland, H. C. (1974). Optimal strategies for predator avoidance: the relative importance of speed and manoeuvrability. *J. Theor. Biol.* **47**, 333-350.

Hui, C. A. (1985). Maneuverability of the Humboldt penguin (*Spheniscus humboldti*) during swimming. *Can. J. Zool.* **63**, 2165-2167.

Kajiura, S. M., Forni, J. B. and Summers, A. P. (2003). Maneuvering in juvenile carcharhinid and sphyrnid sharks: the role of the hammerhead shark cephalofoil. *Zoology* **106**, 19-28.

Maresh, J. L., Fish, F. E., Nowacek, D. P., Nowacek, S. M. and Wells, R. S. (2004). High performance turning capabilities during foraging by bottlenose dolphins (*Tursiops truncatus*). *Mar. Mamm. Sci.* **20**, 498-509.

Macpherson, J. M. (1991). How flexible are muscle synergies? In *Motor Control: Concepts and Issues*, eds. D. R. Humphrey and H. -J. Freund, pp. 33-47. Chichester: John Wiley and Sons.

Norberg, U. M. L. and Rayner, J. M. V. (1987). Ecological morphology and flight in bats (Mammalia; Chiroptera): wing adaptations, flight performance, foraging strategy and echolocation. *Phil. Trans. R. Soc. Lond. B* **316**, 335-427.

Pace, C. M., Blob, R. W. and Westneat, M. W. (2001). Comparative kinematics of the forelimb during swimming in red-eared slider (*Trachemys scripta*) and spiny softshell (*Apalone spinifera*) turtles. *J. Exp. Biol.* **204**, 3261-3271.

Rieppel, O. and Reisz, R. R. (1999). The origin and early evolution of turtles. *Ann. Rev. Ecol. Syst.* **30**, 1-22.

Santini, F. and Tyler, J. C. (2003). A phylogeny of the families of fossil and extant tetraodontiform fishes (Acanthomorpha, Tetraodontiformes), Upper Cretaceous to Recent. *Zool. J. Linn. Soc.* **139**, 565-617.

Schrank, A. J. and Webb, P. W. (1998). Do body and fin form affect the abilities of fish to stabilize swimming during maneuvers through vertical and horizontal tubes? *Environ. Biol. Fish.* **53**, 365-371.

Schrank, A. J., Webb, P. W. and Mayberry, S. (1999). How do body and paired-fin positions affect the ability of three teleost fishes to maneuver around bends? *Can. J. Zool.* **77**, 203-210.

Walker, J. A. (1998a). QuicKurve [WWW document] http://www.usm.maine.edu/~walker/software.html: Biological Sciences, University of Southern Maine.

Walker, J. A. (1998b). Estimating velocities and accelerations of animal locomotion: a simulation experiment comparing numerical differentiation algorithms. *J. Exp. Biol.* **201**, 981-995.

Walker, J. A. (2000). Does a rigid body limit maneuverability? *J. Exp. Biol.* **203**, 3391-3396.

Walter, R. M. and Carrier, D. R. (2002). Scaling of rotational inertia in murine rodents and two species of lizards. *J. Exp. Biol.* **205**, 2135-2141.

Webb, P. W. (1976). The effect of size on the fast-start performance of rainbow trout *Salmo gairdneri*, and a consideration of piscivorous predator-prey interactions. *J. Exp. Biol.* **65**, 157-177.

Webb, P. W. (1983). Speed, acceleration and manoeuvrability of two teleost fishes. *J. Exp. Biol.* **102**, 115-122.

Webb, P. W. (1994). The biology of fish swimming. In *Mechanics and Physiology of Animal Swimming*, eds. L. Maddock, Q. Bone, and J. V. Rayner, pp. 45-62. Cambridge: Cambridge University Press.

Webb, P. W. and Fairchild, A. G. (2001). Performance and maneuverability of three species of teleostean fishes. *Can. J. Zool.* **79**, 1866-1877.

Webb, P. W. and Keyes, R. S. (1981). Division of labor between median fins in swimming dolphin (Pisces: Coryphaenidae). *Copeia*, 901-904.

Webb, R. G. (1962). North American recent soft-shelled turtles (Family Trionychidae). *Univ. Kansas Publ. Mus. Nat. Hist.* **13**, 431-611.

Weihs, D. (1981). Effects of swimming path curvature on the energetics of fish motion. *Fish. Bull.* **79**, 171–179.

Willey, J. S. and Blob, R. W. (2004). Tail kinematics of juvenile common snapping turtles during aquatic walking. *J. Herpetol.* **38**, 360-369.

Woltring, H. J. (1986). A Fortran package for generalized, cross-validatory spline smoothing and differentiation. *Advances in Engineering Software* **8**, 104-107.

Zug, G. R. (1971). Buoyancy, locomotion, morphology of the pelvic girdle and hind limb and systematics of cryptodiran turtles. *Misc. Publ. Mus. Zool. Univ. Michigan* **142**, 1-98.

CHAPTER THREE

HYDRODYNAMIC STABILITY OF THE PAINTED TURTLE (*CHRYSEMYS PICTA*): THE ROLE OF MULTIPLE PROPULSORS AND KINEMATIC STRATEGIES IN A RIGID-BODIED TETRAPOD

Abstract

Hydrodynamic stability is the ability to resist recoil motions of the body produced by destabilizing forces. Previous studies have suggested that recoil motions can decrease locomotor performance, efficiency and sensory perception, and that swimming animals might utilize kinematic strategies or possess morphological adaptations that reduce recoil motions and produce more stable trajectories. I used high-speed video to assess hydrodynamic stability during rectilinear swimming in the freshwater painted turtle (*Chrysemys picta*). Parameters of vertical stability (heave and pitch) were non-cyclic and variable, while measures of lateral stability (sideslip and yaw) showed repeatable cyclic patterns. Four parameters showed significant effects of swimming velocity; heave magnitude and excursion improved with increasing velocity, while sideslip magnitude and excursion worsened. Additionally, because freshwater and marine turtles use different swimming styles, I tested the effects of propulsive mode on hydrodynamic stability during rectilinear swimming, by comparing my data from painted turtles to previously collected data from two species of marine turtle (*Caretta caretta* and *Chelonia mydas*). Painted turtles had higher levels of stability than both species of marine turtle for 6 of the 8 parameters tested, highlighting potential disadvantages associated with aquatic flight. Finally, I

compared the stability of freshwater turtles to rigid- and flexible-bodied fishes. Boxfish and pufferfish clearly outperform turtles with respect to yaw and pitch magnitude. In contrast, my results show that the heads of painted turtles exhibit similar levels of lateral displacement to many flexible-bodied fishes.

Introduction

Swimming animals are subjected to a variety of potentially destabilizing forces that can be either self-generated (e.g., propulsor movements) or external (e.g., environmental turbulence). These forces produce recoil motions, which have both rotational (pitch, yaw, and roll) and translational (heave, sideslip, and surge) components (Hove et al., 2001). Hydrodynamic stability is the ability to resist recoil motions of the body produced by destabilizing forces, thereby, allowing maintenance of a given trajectory (Webb, 2002; Weihs, 2002; Bartol et al., 2003). Previous studies have suggested that destabilizing recoil motions can decrease locomotor performance and efficiency as a result of increased drag and laterally directed thrust, and inhibit sensory perception as a result of extraneous motion of the head (Lighthill, 1975; Lighthill, 1977; Webb, 1992; Webb, 2002; Weihs, 2002). These observations suggest that swimming animals might utilize kinematic strategies (e.g., corrective fore- and hindlimb motions in sea turtles; Avens et al., 2003) or possess morphological adaptations (e.g., carapacial keels in boxfishes; Bartol et al., 2003) that dampen destabilizing forces, thereby, reducing recoil motions and producing more stable trajectories.

Because laboratory studies can establish controlled conditions that limit external destabilizing forces, studies that have been conducted in lab settings have been able to focus on understanding the effects of different modes of propulsion and corresponding morphologies on hydrodynamic stability during swimming. Based on morphology and mode of propulsion, vertebrates for which stability has been examined can be divided into two general types: (1) flexible-bodied taxa that produce thrust using undulatory (lateral or dorsoventral) motions of the body, and (2) rigid-bodied taxa that produce thrust using oscillatory motions of multiple appendages (i.e., propulsors). Stability has been studied in a broad array of undulatory taxa, including larval amphibians (Wassersug and von Seckendorf Hoff, 1985; von Seckendorf Hoff and Wassersug, 1986), fishes (Bainbridge, 1963; Videler and Hess, 1984; Webb, 1988; Webb, 1992), and odontocete cetaceans (Fish, 2002; Fish et al., 2003a). Body depth and flexibility are some of the morphological characteristics that have been shown to correlate with stability in these taxa. More recent studies of hydrodynamic stability have focused primarily on rigid-bodied taxa that swim using multiple propulsors. The model system for this area of study is the tetraodontiform fishes (e.g., boxfishes and pufferfishes), which have been found to have extremely low levels of lateral and vertical recoil (Gordon et al., 1996; Gordon et al., 2000; Hove et al., 2001; Plaut and Chen, 2003). Studies focusing on tetraodontiform fishes have identified a number of strategies that aquatic organisms can use to enhance stabilization, including keels (Bartol et al., 2002; 2003; 2005; 2008), and

propulsor position, morphology, and kinematics (Arreola and Westneat, 1996; Gordon et al., 1996; Hove et al., 2001; Plaut and Chen, 2003; Wiktorowicz et al., 2007).

Although, hydrodynamic stability has been assessed for a phylogenetically diverse array of vertebrate taxa, the effects of many different body designs and modes of propulsion remain unknown. For example, because the examination of hydrodynamic stability in rigid-bodied taxa has been limited nearly exclusively to tetraodontiform fishes, the performance of different modes of appendage-based propulsion has yet to be evaluated. In particular, very few data exist for animals propelled by jointed appendages (e.g., limbed tetrapods).

One group of rigid-bodied vertebrates that provides an ideal system in which to evaluate the effects of propulsion via oscillatory motions of jointed appendages is the turtles. Turtles are the oldest extant group of rigid-bodied vertebrates, the only such group of tetrapods (Rieppel and Reisz, 1999; Santini and Tyler, 2003), and have maintained a relatively unchanged body plan for over 200 million years (Burke, 1989; Gaffney, 1990). In turtles, the vertebrae are fused dorsally with a bony carapace, precluding movement of the axial skeleton between the base of the neck and the tail. As a result of their immobilized axial skeleton and reduced tail, thrust in swimming turtles is generated exclusively by the movements of fore- and hindlimbs (Pace et al., 2001; Blob et al., 2007). Yet, despite the potential constraints of a rigid body on locomotion in turtles, over 100 extant species inhabit marine and freshwater environments (Ernst et al., 1994).

Moreover, marine and freshwater turtles have evolved two very different modes of propulsion (Davenport et al., 1984).

Marine (sea) turtles generate thrust via synchronous dorsoventral movements of their forelimbs, a propulsive mode referred to as aquatic flight (Fig. 3.1A). This style of locomotion is rare among turtle species, only being used by the seven species of sea turtles and also (independently evolved) by a single species of freshwater turtle (*Carettochelys insculpta*) (see Rayner, 1985 for justification of aquatic flight). In contrast, the remaining species of aquatic and semi-aquatic turtles (N>100), collectively referred to as freshwater turtles, swim using a very different locomotor strategy. Freshwater turtles propel themselves via synchronous rowing (anteroposterior) movements of contralateral fore- and hindlimbs (Davenport et al., 1984; Rivera et al., 2006; Renous et al., 2007;). In this mode of locomotion, in contrast to aquatic flight, the two sets of contralateral fore- and hindlimbs move asynchronously. In addition, unlike sea turtles, freshwater turtles propel themselves using all four limbs (Fig. 3.1B). While a number of studies have examined aspects of swimming in aquatic turtles, including kinematics (Zug, 1971; Davenport et al., 1984; Pace et al., 2001; Renous et al., 2007;), motor control (Gillis and Blob, 2001; Blob et al., 2007), maneuverability (Heithaus et al., 2002; Rivera et al., 2006), and hydrodynamic implications of shell morphology (Aresco and Dobie, 2000; Claude et al., 2003; Lubcke and Wilson, 2007; Rivera, 2008; Rivera and Claude, 2008), relatively little is known about hydrodynamic stability in this lineage. Only one study has

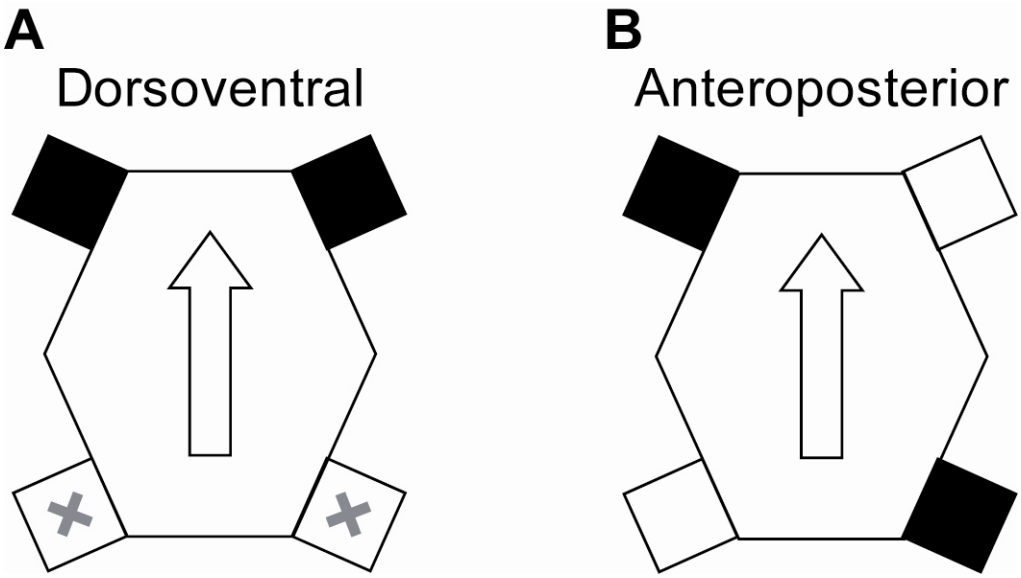

Figure 3.1: Locomotor modes used by (A) marine turtles and (B) freshwater turtles. Limbs of the same color move in-phase, while those of opposite colors move in anti-phase (sensu Long et al., 2006). "Dorsoventral" and "anteroposterior" describe the primary direction of motion for the limbs. Limbs marked by "×" have no propulsive function. Arrows point anteriorly.

quantified stability during swimming in turtles. Dougherty et al. (in press) examined stability in two species of marine turtles (*Caretta caretta* and *Chelonia mydas*), providing a quantitative description of recoil motions throughout the limb cycle during rectilinear swimming for species using flapping (i.e., dorsoventral) propulsive movements. Although the number of freshwater turtle species vastly outnumbers that of marine turtles, to date, no study has yet examined stability in freshwater turtles that use the rowing (i.e., anteroposterior) propulsive movements that are likely basal for the entire lineage (Joyce and Gauthier, 2004).

Given the differences in typical modes of propulsion utilized by freshwater and marine turtles, several testable hypotheses can be generated for how these differences might lead to differences in stability between these groups. (1) The primary direction of motion for propulsors is anteroposterior in freshwater turtles and dorsoventral in marine turtles. Because freshwater turtles move their limbs in the same plane as their direction of travel, I predict that heave will be lower in freshwater turtles. (2) Freshwater turtles produce thrust by oscillating all four limbs during swimming, while marine turtles produce thrust solely with motions of their forelimbs. Because marine turtles only oscillate limbs at one end of the body (anterior), I predict that pitch will be higher in marine turtles. (3) Motions of homologous limbs on the left and right side are asynchronous in freshwater turtles and synchronous in marine turtles. Because motions occur at the same time on both sides of the body, I predict that marine turtles will have lower levels of lateral recoil (sideslip and yaw).

As a result of the drastic differences in propulsive limb movements between freshwater and marine turtles and because freshwater turtles possess a very different body design than that of boxfish and pufferfish (with a dorsoventrally flattened body shape and jointed limbs, rather than flexible fins, as propulsors), freshwater turtles provide an important comparison for evaluating the effects of limb kinematics and morphological design on hydrodynamic stability in vertebrates. Furthermore, a comparison of measures of stability between freshwater and marine turtles may provide insights into the evolution of

the two different styles of propulsion seen in extant turtles. The goals of this study are, therefore, threefold: (1) to quantify hydrodynamic stability of the body and head in swimming freshwater turtles, (2) to test the effects of different modes of propulsion on stability among turtles, and (3) to compare the stability of freshwater turtles to the current model for rigid-bodied stability, the tetraodontiform fishes.

Materials and Methods

Experimental animals

Stability data were collected from four juvenile painted turtles (*Chrysemys picta*). Carapace lengths ranged from 9.6 to 11.6 cm (mean, 10.3 cm). Turtles were obtained from a commercial turtle dealer (Concordia Turtle Farm, Wildsville, LA, USA) and housed together in a 568 liter tank, located in a climate controlled greenhouse at Clemson University (Clemson, SC, USA). This housing arrangement exposed turtles to ambient light patterns and water temperatures between 20° and 30°C. The tank was fitted with a water filter and multiple dry platforms for basking, and turtles were fed commercial pellets and/or earthworms three to four times per week. All animal care and experimental procedures followed Clemson University IACUC guidelines (Clemson University AUP #2007-069).

Collection of video

Linear swimming trials from which stability data were obtained were elicited from turtles by stimulating predatory behavior. Each turtle was placed individually into a glass aquarium (152 cm × 61 cm × 64 cm) filled with water to a depth of 26 cm. A submerged 300-watt heater (located inside the aquarium, but outside of the central ~100 cm test area) maintained water temperature between 28° and 30°C. The tank was fitted with a manually-powered top-mounted sliding rail system that spanned its entire length, was centered between the front and back walls, and supported a vertical sting that descended into the water. Turtles were stimulated to swim in a straight line by luring with a prey stimulus (earthworm) that was attached to the base of the vertical sting, which was submerged 8 cm below the surface of the water. Use of the rail system ensured that the prey stimulus traversed the tank with no lateral or vertical displacement and, thus, minimized intentional lateral and vertical movements of the pursuing turtle. Occasionally, turtles could not be incited to chase the prey stimulus, either at the beginning of a test day or following successful pursuits. These trials were halted after 10 min of inactivity and turtles were returned to their housing tank to be tested again the following day. For each individual, all trials were collected within the span of one week.

Linear swimming trials were filmed simultaneously at 100Hz in lateral and ventral views using two digitally-synchronized high-speed video cameras (Phantom V5.1, Vision Research, Inc.; Wayne, NJ, USA). The lateral view

provided information on vertical stability and the ventral view provided information on lateral stability. The ventral view was captured using a mirror placed at a 45° angle to the tank bottom. Both cameras were focused on the central ~100 cm segment of the test tank (i.e., test area). Each filming view included a 1 cm square grid used to provide distance calibration for video analyses.

Processing of video trials

In order to calculate kinematic and stability variables from video files, each set of video files was cropped so as to include the straightest three limb cycle segment. A limb cycle was defined as the period beginning at maximum retraction of the left forelimb and ending upon the subsequent maximum retraction of the left forelimb. The positions of landmarks on the shell and limbs were then digitized in lateral view (*N*=3: tip of snout, anterior edge of carapace, posterior edge of carapace; Fig. 3.2A) and ventral view (*N*=11: tip of snout, anterior and posterior edge of plastron, left and right shoulder, left and right elbow, left and right hip, left and right knee; Fig. 3.2B) videos. Videos were digitized using the software package DLTdataviewer (Ver. 2; available online at http://www.unc.edu/~thedrick/software1.html; see Hedrick, 2008). Coordinate data were input into a custom Matlab (Ver. 7.1, Mathworks, Inc.; Natick, MA, USA) routine. This routine interpolated 98 equidistant points between the anterior and posterior points on the carapace (lateral view) and plastron (ventral

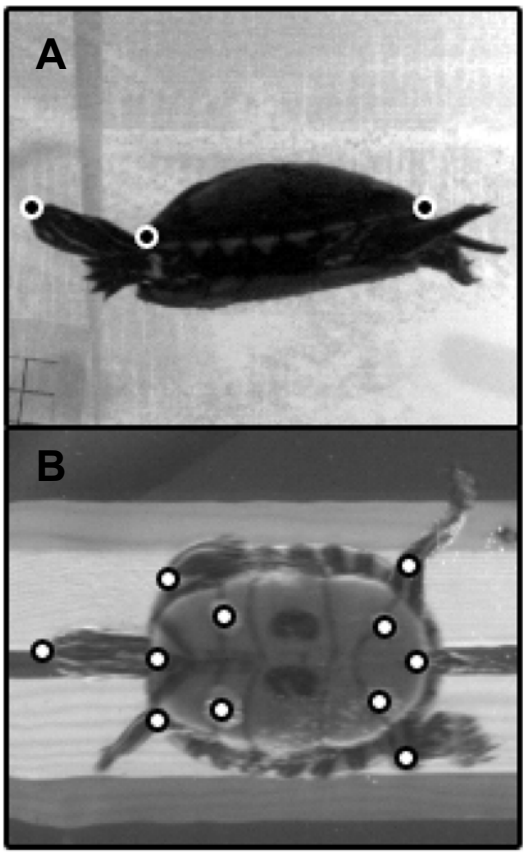

Figure 3.2: Points digitized on turtle in (A) lateral and (B) ventral views.

view), yielding 100 equidistant points along the respective body axis. For each view, the point along the body axis with the most stable trajectory throughout the trial (i.e., traveled the smallest cumulative distance) was designated as the center-of-rotation (COR; Walker, 2000; Rivera et al., 2006; Dougherty et al., in press). Linear regressions were calculated using the x and y coordinates of the COR from each frame of the trial and the resulting R^2 values provided a measure of linearity of the swimming path. In addition, the horizontal distance traveled for each swimming trial (in body lengths, BL) was calculated as the cumulative displacement of the COR in ventral view. Linear velocity (in BL s^{-1}) was

calculated from differentiation of the cumulative displacement of the COR along the swimming path (based on the x and y positional data). Data were smoothed using a quintic spline (generalized cross validation; Walker, 1998) and then differentiated using the custom Matlab software MatSAND (T. Hedrick). This procedure smoothed the data, clarifying the movement patterns of turtles by reducing variation resulting from minor errors in locating anatomical landmarks on video frames during digitizing (Blob et al., 2007). Because calculations of all stability variables (see below) were based on the linear equations of the swimming path, only trials meeting the following criteria were used: (1) R^2>0.25 for both lateral and ventral views; (2) turtles traveled a minimum horizontal distance of three body lengths; (3) turtles completed a minimum of three consecutive limb cycles during steady swimming (i.e., not starting or stopping) in the field of view of the camera. Trials that met these criteria were subdivided into individual limb cycles, for which values for distance and velocity, limb kinematics, and stability were calculated.

Acquisition of data for limb cycles

To evaluate the kinematic patterns that turtles used during limb cycles, a Matlab routine was used to calculate the movements of each of the four limbs throughout the course of each limb cycle (in ventral view). Each limb was defined as a vector marked by the endpoints of its proximal segment (forelimb: shoulder and elbow; hindlimb: hip and knee). The position of each limb was

calculated using standard equations for the angle between two vectors; the proximal limb segment (humerus or femur) formed the first vector and the midline axis of the body (i.e., segment between anterior and posterior plastron points) formed the second. A limb segment parallel to the midline axis and oriented cranially was assigned an angle of 0°, whereas, one parallel to the midline and oriented caudally was assigned an angle of 180°. Angles were calculated from the ventral view videos as two-dimensional projections onto the horizontal plane. The program MatSAND was used to fit a quintic spline to the kinematic calculations from each limb cycle, smoothing the data and allowing the limb cycles to be normalized to the same duration (101 equally-spaced increments representing 0-100% of limb cycle) prior to comparisons. These values were used to produce average profiles of limb kinematics (mean±SEM) throughout the limb cycle (Pace et al., 2001).

To evaluate stability during limb cycles, a Matlab routine was used to rotate and translate all digitized coordinates for each view so that the swimming path associated with the limb cycle (as previously calculated from trial data) was defined by a vector starting at the origin and traveling along the positive x-axis. Trials in which turtles swam from right to left required an additional reflection of coordinates. All stability variables (i.e., heave, pitch, sideslip, yaw) were then derived from the relationship between the swimming path (i.e., positive x-axis) and three additional parameters calculated from the reconfigured coordinates: (1) the position of the COR throughout the limb cycle; (2) the position and orientation

of the head throughout the limb cycle, which was calculated from the line segment formed between the tip of the snout and the anterior points of the carapace (lateral) and plastron (ventral); and (3) the position and orientation of the body axis throughout the limb cycle, which was calculated from the line segment formed between the anterior and posterior points of the carapace (lateral) and plastron (ventral). As with the kinematic data, MatSAND was used to fit a quintic spline to the stability calculations from each limb cycle, smoothing the data and allowing the limb cycles to be normalized to the same duration (101 equally-spaced increments representing 0-100% of limb cycle) prior to comparisons. These values were used to quantify stability variables (see below), produce average profiles of stability parameters (mean±SEM) throughout the limb cycle, and allowed patterns of stability to be related to the motion of the limbs throughout the limb cycle.

To quantify specific stability variables, the maximum angular and positional displacements from the smoothed and normalized data of each limb cycle were extracted. Maximum angular displacements (pitch or yaw) were defined as the maximum angle between the path of travel and the corresponding body axis and are presented in degrees. Maximum positional displacements (heave and sideslip) were defined by the orthogonal distance between the center of gravity (i.e., center of rotation) and the path of travel and are presented as proportions of carapace/body length (BL=body lengths). Excursion values were calculated as the difference between the maximum and minimum values for each

stability parameter. Due to the bilaterally symmetrical nature of the study system, in the case of yaw and sideslip, the single (left or right side) maximum value was extracted; excursion values for yaw and sideslip were calculated as the difference between the maximum left and right deviations. Because turtles are capable of swimming in a straight line while yawed at an angle from the path of travel, it is possible for excursions to be smaller than values of maximum angular displacement. In addition, because the maximum value for a given trial does not always occur at the same percent of the limb cycle, it is also possible that calculated maximum values may be different than the maximum values seen in average kinematic profiles. A list of stability variables and how they were derived is provided in Table 3.1.

As described for overall trial data, the distance traveled for each limb cycle (i.e., stride length) was calculated as the cumulative displacement of the COR during the limb cycle. Additionally, linear velocity was calculated from differentiation of the cumulative displacement of the COR along the swimming path. Distance and velocity data were calculated from ventral view data and were smoothed and normalized as previously described for the kinematic and stability data.

Table 3.1. Stability parameters collected from individual limb cycles.

Body Stability Parameters	**Definition**
Maximum heave magnitude [a, c]	Maximum distance of COR from path of travel
Maximum positive heave [a]	Maximum distance of COR above path of travel
Maximum negative heave [a]	Maximum distance of COR below path of travel
Heave excursion [a, c]	Distance between maximum positive and negative heave values
Maximum pitch magnitude [a, c]	Maximum angle of body axis from path of travel
Maximum positive pitch [a]	Maximum positive angle of body axis from path of travel
Maximum negative pitch [a]	Maximum negative angle of body axis from path of travel
Pitch excursion [a, c]	Angle between maximum positive and negative pitch values
Maximum sideslip magnitude [b, c]	Maximum distance of COR from path of travel
Sideslip excursion [b, c]	Distance between maximum left and maximum right sideslip values
Maximum yaw magnitude [b, c]	Maximum angle of body axis from path of travel
Yaw excursion [b, c]	Angle between maximum left and right yaw values
Head Stability Parameters	
Vertical head/body angle magnitude [a]	Maximum vertical angle of head axis relative to body axis
Vertical head/body angle excursion [a]	Angle between maximum and minimum vertical head/body angles
Lateral head/body angle magnitude [b]	Maximum lateral angle of head axis relative to body axis
Lateral head/body angle excursion [b]	Angle between maximum and minimum vertical head/body angles
Maximum head yaw magnitude [b]	Maximum angle of head axis from the path of travel
Maximum head yaw excursion [b]	Angle between maximum left and right head yaw values
Maximum nose displacement [b]	Maximum distance of nose from path of travel

Values for heave, sideslip, and maximum nose displacement are calculated in body lengths (BL).

Values for pitch and yaw are calculated in degrees.

All distances are measured orthogonal to the path of travel.

[a] Variables calculated from lateral view videos.

[b] Variables calculated from ventral view videos.

[c] Focal parameters used in interspecific comparisons.

Data analysis

Prior to data analysis, outliers (values greater than three standard deviations from the mean) were removed from the data set. Because ANOVA designs (see below) required three cycles from each trial, any trial containing a cycle with an outlier was excluded from the data set. Data sets were transformed as needed to meet assumptions of homoscedasticity and normality as appropriate for statistical tests. All 12 variables analyzed using ANOVAs met the assumption of homoscedasticity at $\alpha=0.01$ and 10 of 12 at $\alpha=0.05$. Moderate violations of assumptions do not generally affect analyses of variance (ANOVAs; Sokal and Rohlf, 1995), and the majority of data met homoscedasticity and normality requirements. ANOVA was used to conduct separate intraspecific and interspecific comparisons. For intraspecific comparisons, a set of nested ANOVAs (individual>trial) was used to test for individual differences between the four painted turtles for the 12 measured stability parameters. For these analyses, “individual” was analyzed as a fixed factor and “trial” (nested within individual) was treated as a random factor. For interspecific comparisons, a set of multi-level nested ANOVAs (species>individual>trial) was applied to compare data for the eight focal stability parameters (see Table 3.1) between freshwater turtles (this study) and two species of marine turtles (*Caretta caretta* and *Chelonia mydas*) from Dougherty et al. (in press). “Species” was analyzed as a fixed factor, and the remaining two levels, “individual” (nested within species) and “trial” (nested within individual×species), were treated as random factors. Pair-

wise nested ANOVAs were used to identify differences between individual species. The use of eight, rather than 12 variables reduced the number of correlated variables in the analysis and helped to minimize experiment-wise error rates. To further control for inflated error rates, sequential Bonferroni corrections (Holm, 1979; Rice, 1989) were applied to all intraspecific, interspecific, and pair-wise comparisons. Additionally, correlation and regression analyses were used to examine the relationships between path of travel linearity (i.e., R^2 values), limb motions, swimming velocity, and stability parameters. Nested ANOVAs were performed using SYSTAT 12 (Systat Software, Inc.; Chicago, IL, USA); correlations and regressions were performed using SPSS Base (v. 10; SPSS, Inc.; Chicago, IL, USA).

Results

General

Data were analyzed for 32 trials (6-11 per turtle), yielding 96 limb cycles for which stability parameters were measured. Horizontal body displacement during trials ranged from 3.23 to 5.87 BL (mean±SEM, 3.98±0.10), with average swimming velocities between 2.72 and 5.50 BL s^{-1} (mean±SEM, 3.87±0.137). The average anatomical position of the COR was 25.97±4.57% of carapace length (mean±SEM) and 38.06±2.04% of plastron length (mean±SEM) based on lateral and ventral views, respectively. The R^2 values from regressions used to determine the path of travel ranged from 0.30 to 0.97 (N=32; mean±SEM,

0.67±0.03) for lateral stability parameters (sideslip and yaw) and from 0.26 to 0.99 (*N*=32; mean±SEM, 0.75±0.03) for vertical parameters (heave and pitch). The correlation between lateral and ventral R^2 values (i.e., linearity of path of travel) was not significant (*N*=32; Pearson correlation, 0.007; *P*=0.969), indicating that lateral and ventral stability parameters are controlled independently from each other. The R^2 values of the lateral and ventral path of travel, however, were significantly correlated with several body stability parameters (Table 3.2).

Horizontal body displacement during individual cycles (i.e., stride length) ranged from 0.98 to 2.16 BL (*N*=96; mean±SEM, 1.33±0.02). Average swimming velocities for each cycle ranged between 2.63 and 5.64 BL s^{-1} (*N*=96; mean±SEM, 3.87±0.08). Swimming velocity had no significant effect on stride length across observed speeds (*N*=96; R^2=0.003; *P*=0.610).

Limb kinematics

During rectilinear swimming, painted turtles use synchronous movements of contralateral fore- and hindlimbs (Fig. 3.3). The angle between the forelimbs and body axis ranged from -23.0° to 92.3 °, while the angle between the hindlimbs and body axis ranged from 46.6° to 165.1°. By definition, maximum retraction of the left forelimb always occurs at 0% of the limb cycle. Based on how a limb cycle is defined, the switch from retraction (power stroke) to protraction (recovery stroke) occurred near the beginning or end of the limb cycle for the right hindlimb, and near the middle of the limb cycle for the right forelimb

Table 3.2. Pearson correlations between path linearity (R^2) and stability parameters.

Stability parameters	*R*
Maximum heave magnitude [a]	**-0.357***
Maximum positive heave [a]	**-0.265**
Maximum negative heave [a]	0.162
Heave excursion [a]	**-0.281**
Maximum pitch magnitude [a]	**-0.269**
Maximum positive pitch [a]	**-0.210**
Maximum negative pitch [a]	-0.177
Pitch excursion [a]	-0.053
Maximum sideslip magnitude [b]	**-0.293***
Sideslip excursion [b]	**-0.220**
Maximum yaw magnitude [b]	-0.021
Yaw excursion [b]	0.005

[a] R^2 calculated from regression of x,y coordinates of COR in lateral-view videos

[b] R^2 calculated from regression of x,y coordinates of COR in ventral-view videos

Limb cycles, N=96

Bolded values represent significant relationships (P<0.05)

* Represent significant relationships after sequential Bonferroni correction for multiple comparisons

and left hindlimb. Because of the bimodal distribution of the retraction-protraction transition for the right hindlimb, additional data on the timing of limb kinematics were calculated based on the left and right forelimbs and the left hindlimb only. Based on the timing at which each limb switched from retraction to protraction, the left and right forelimbs differed by 38% to 61% of the limb cycle (N=96;

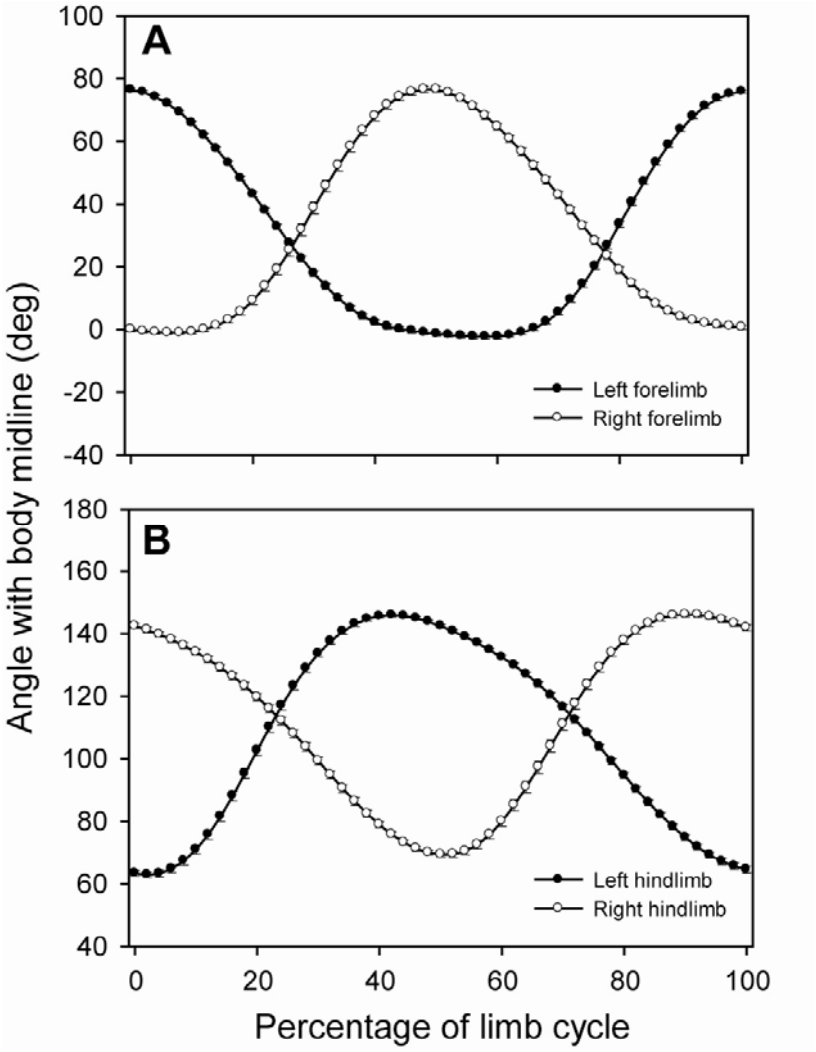

Figure 3.3: Average kinematic profiles of (A) forelimbs and (B) hindlimbs during level rectilinear swimming. Open symbols indicate right side of the body; closed symbols indicate left side. A decrease in the angle with midline represents limb protraction and an increase in the angle represents limb retraction. Note the synchronous movements of contralateral fore- and hindlimb and the alternating movements of the ipsilateral fore- and hindlimbs. Note, because the maximum value for a given trial does not always occur at the same percent of the limb cycle, it is possible that calculated maximum values may be different than the maximum values seen in average kinematic profiles.

mean±SEM, 48.4±0.5%), while the difference in timing between contralateral fore- and hindlimbs ranged from -8% to 23% of the limb cycle (*N*=96; mean±SEM, 6.78±0.57). In general, the forelimb began to protract following the initiation of protraction by the hindlimb (positive values); however, occasionally the forelimb began to protract before the hindlimb (negative values). The difference in timing between ipsilateral fore- and hindlimbs ranged from 26% to 52% (*N*=96; mean±SEM, 41.61±0.47) of the limb cycle. Correlation analyses showed that none of these relative timing variables (i.e., between limb pairs) were significantly correlated with speed ($P>0.05$). However, differences between the timing of contralateral fore- and hindlimbs are significantly correlated with maximum sideslip magnitude (*N*=96; Pearson correlation, -0.276, $P<0.05$) and sideslip excursion (*N*=96; Pearson correlation, -0.212, $P=0.038$).

Body stability

Values for body stability parameters (heave, pitch, sideslip, and yaw) were calculated for each of the individual 96 cycles and are presented along with results of an ANOVA testing for intraspecific differences in Table 3.3. Neither heave nor pitch shows a temporal pattern during the limb cycle (i.e., random and non-cyclic) and individual cycles can display a broad range of stability (Fig. 3.4A, B). Sideslip ranged from 0.05 BL to the left of the path of travel to 0.05 BL to the right of the path of travel (Fig. 3.4C). The average leftward positional displacement was 0.017 BL and the average rightward positional displacement

was 0.015 BL. Yaw ranged from 13.1° to the left of the path of travel to 12.2° to the right of the path of travel (Fig. 3.4D). The average leftward angular displacement was 6.0° and the average rightward angular displacement was 5.2°. Because of the bilaterally symmetric nature of the animal and sideslip and yaw during swimming, only the single maximum magnitude of positional and angular displacements from the path of travel, as well as the total excursion during a single limb cycle, are reported in Table 3.3.

In contrast to measures of vertical stability (heave and pitch), measures of lateral stability (sideslip and yaw) show highly repeatable cyclic patterns (Fig. 3.4C, D). At the beginning of the limb cycle, the left forelimb and right hindlimb would have just finished retracting (i.e., power stroking; Fig. 3.3), and because the right hindfoot produces more thrust than the left forefoot (Blob et al, 2003), this power stroke motion creates a torque, rotating the turtle to the left (0-20% of limb cycle, Fig. 3.4D). The body reaches its maximum leftward orientation near 20% of the limb cycle and then begins to rotate toward the right, becoming parallel with the path of travel near 40% of the limb cycle (Fig. 3.4D). The turtle is oriented to the right of the path of travel from approximately 40% to 90% of the limb cycle, and reaches a maximum rightward orientation near 60% of the limb cycle. Comparisons of temporal patterns of sideslip and yaw indicate there is a lag between changes in the direction in which the body is oriented and the

Table 3.3. Descriptive statistics for stability parameters and results of nested ANOVAs testing for differences between individuals.

Stability parameter	**Species**	**Turtle 1**	**Turtle 2**	**Turtle 3**	**Turtle 4**	$F_{3,28}$	*P*
Maximum heave magnitude	0.024±0.002 (0.005-0.078)	0.023±0.003 (0.005-0.052)	0.015±0.001 (0.006-0.026)	0.029±0.004 (0.005-0.068)	0.027±0.003 (0.006-0.078)	1.070	0.378
Maximum positive heave	0.017±0.002 (-0.015-0.078)	0.017±0.003 (0.000-0.044)	0.012±0.002 (-0.009-0.026)	0.017±0.004 (-0.013-0.058)	0.019±0.003 (-0.015-0.078)	0.434	0.730
Maximum negative heave	-0.017±0.002 (-0.068-0.012)	-0.015±0.003 (-0.052-0.012)	-0.012±0.002 (-0.026-0.002)	-0.020±0.005 (-0.068-0.010)	-0.018±0.003 (-0.058-0.011)	0.916	0.446
Heave excursion	0.033±0.002 (0.007-0.119)	0.032±0.004 (0.008-0.078)	0.023±0.003 (0.007-0.049)	0.037±0.006 (0.008-0.119)	0.037±0.004 (0.007-0.116)	0.701	0.559
Maximum pitch magnitude	4.149±0.204 (0.773-11.091)	3.363±0.301 (0.773-7.524)	4.870±0.357 (2.822-9.473)	4.022±0.511 (1.179-10.548)	4.409±0.384 (1.423-11.091)	2.210	0.109
Maximum positive pitch	2.095±0.290 (-4.185-11.091)	1.333±0.436 (-2.871-5.289)	2.839±0.796 (-2.386-9.473)	2.309±0.562 (-3.543-6.912)	2.107±0.542 (-4.185-11.091)	0.438	0.727
Maximum negative pitch	-2.287±0.276 (-10.548-5.959)	-2.581±0.362 (-7.524-0.374)	-0.553±0.794 (-6.609-4.027)	-2.806±0.591 (-10.548-2.588)	-2.690±0.452 (-9.349-5.959)	0.965	0.423
Pitch excursion	4.382±0.228 (0.591-11.073)	3.914±0.345 (1.274-7.783)	3.392±0.391 (0.793-6.693)	5.115±0.598 (0.591-11.073)	4.797±0.400 (1.683-8.981)	1.734	0.183

Table 3.3, continued

Stability parameter	Species	Turtle 1	Turtle 2	Turtle 3	Turtle 4	$F_{3,28}$	*P*
Maximum sideslip magnitude	0.022±0.001 (0.006-0.052)	0.018±0.002 (0.006-0.033)	0.024±0.002 (0.014-0.036)	0.030±0.002 (0.016-0.052)	0.019±0.001 (0.007-0.042)	5.183	**0.006**
Sideslip excursion	0.033±0.001 (0.005-0.076)	0.027±0.002 (0.005-0.052)	0.036±0.003 (0.013-0.061)	0.042±0.003 (0.015-0.076)	0.029±0.002 (0.011-0.062)	6.065	**0.003***
Maximum yaw magnitude	7.771±0.242 (3.078-13.069)	9.565±0.353 (7.065-13.069)	7.774±0.458 (4.282-11.767)	7.505±0.513 (3.078-11.198)	6.634±0.400 (3.652-11.340)	5.039	**0.006**
Yaw excursion	11.142±0.360 (4.285-20.302)	14.964±0.525 (9.339-20.302)	10.985±0.607 (6.144-16.778)	10.993±0.680 (6.098-16.397)	8.544±0.376 (4.285-12.875)	18.172	**<0.001***

Limb cycles: Total Species, *N*=96; Turtle 1, *N*=24; Turtle 2, *N*=18; Turtle 3, *N*=21; Turtle 4, *N*=33

Values are means ± standard error and ranges indicated in parentheses

Bolded values indicate a significant difference between individuals ($P<0.05$)

* Represent significant relationships after sequential Bonferroni correction for multiple comparisons

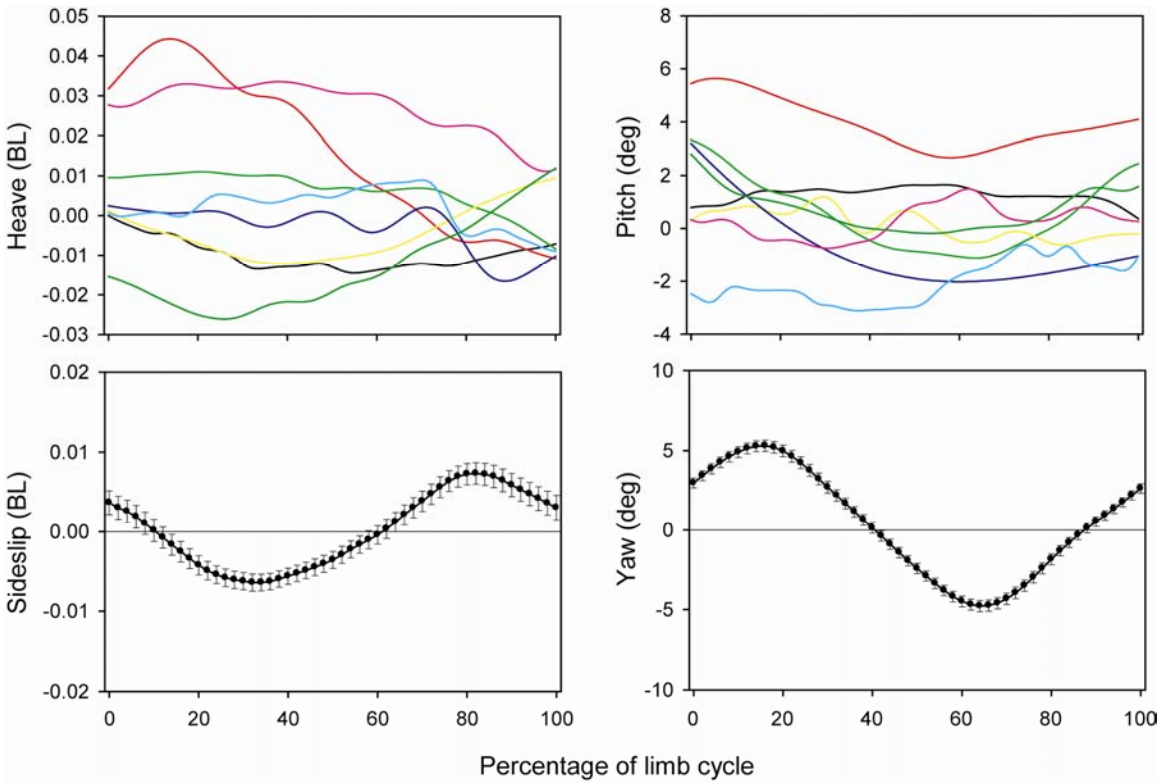

Figure 3.4: Profiles of body stability during limb cycles. (A) Heave adjusted for body length. Ten randomly-selected representative trials indicating the variable, non-cyclic behavior during the course of a limb cycle. Positive and negative values indicate that the lateral COR is above or below the path of travel, respectively. (B) Pitch. Ten randomly-selected representative trials indicating the variable, non-cyclic behavior during the course of a limb cycle. Positive and negative values indicate that the turtle is pitched upward or downward relative to the path of travel, respectively. (C) Sideslip adjusted for body length. Average profile during limb cycle showing cyclic behavior. Symbols represent means±SEM (*N*=96). Positive and negative values indicate that the ventral COR is displaced to the left or right of the path of travel, respectively. (D) Yaw. Average profile during limb cycle showing cyclic behavior. Symbols represent means±SEM (*N*=96). Positive and negative values indicate that the body is yawed to the left or right of the path of travel, respectively. Note, because the maximum value for a given trial does not always occur at the same percent of the limb cycle, it is possible that calculated maximum values may be different than the maximum values seen in average kinematic profiles.

direction in which it travels (Fig. 3.4C, D). While the turtle is oriented to the left of the path of travel (yaw), the body continues to move toward the right (sideslip). The direction of motion switches (to the left) near the time at which the body becomes parallel with the path of travel.

Correlations between the 12 body stability parameters adjusted for multiple comparisons using the sequential Bonferroni technique showed that 18 of 66 possible relationships were significant (P<0.05; Table 3.4), including two of six correlations between lateral parameters and 16 of 28 correlations between vertical parameters. However, none of the 32 correlations comparing lateral and vertical parameters were found to be significant. Additionally, four of the 12 variables of body stability displayed significant relationships with swimming velocity: maximum heave magnitude (y=-0.006x+0.05; R^2=0.086, P=0.004), heave excursion (y=-0.007+0.06; R^2=0.053, P=0.023), maximum sideslip magnitude (y=0.003x+0.01; R^2=0.055, P=0.022), and sideslip excursion (y=0.004x+0.02; R^2=0.044, P=0.040). Parameters of heave decreased (i.e., improved) with increased velocity, while parameters of sideslip increased (i.e., worsened) with increased swimming speeds.

Head stability

Values for parameters of head stability were calculated for each of the individual 96 cycles (Table 3.5). The vertical angle between the head and body did not show cyclic patterns during the cycle and instead was held fairly constant

Table 3.4. Pearson correlations between stability parameters.

	Maximum sideslip magnitude	Sideslip excursion	Maximum yaw magnitude	Yaw excursion	Maximum heave magnitude	Maximum positive heave	Maximum negative heave	Heave excursion	Maximum pitch magnitude	Maximum positive pitch	Maximum negative pitch
Sideslip excursion	**0.845***	—									
Maximum yaw magnitude	**0.244**	0.152	—								
Yaw excursion	0.099	0.001	**0.687***	—							
Maximum heave magnitude	0.147	0.122	-0.089	-0.066	—						
Maximum positive heave	0.108	0.132	-0.030	-0.059	**0.751***	—					
Maximum negative heave	**-0.223**	**-0.249**	0.021	-0.056	**-0.637***	-0.156	—				
Heave excursion	**0.217**	**0.250**	-0.034	-0.003	**0.914***	**0.766***	**-0.754***	—			
Maximum pitch magnitude	0.069	0.156	**-0.257**	**-0.211**	**0.518***	**0.476***	**-0.375***	**0.560***	—		
Maximum positive pitch	0.092	0.081	-0.061	-0.112	0.064	0.072	0.047	0.017	**0.276**	—	
Maximum negative pitch	0.048	-0.020	0.041	-0.005	**-0.274**	**-0.277**	0.164	**-0.291**	**-0.202**	**0.678***	—
Pitch excursion	0.059	0.127	-0.127	-0.137	**0.413***	**0.428***	-0.138	**0.374***	**0.597***	**0.452***	**-0.350***

Limb cycles, *N*=96

Shaded area represents correlations between lateral and vertical stability parameters

Bolded values represent significant relationships ($P<0.05$)

* Represent significant relationships after sequential Bonferroni correction for multiple comparisons

Table 3.5. Head stability data for limb cycles.

Stability parameter	Minimum	Maximum	Mean±SEM
Vertical head/body angle magnitude [a]	2.89	31.96	15.09±0.73
Vertical head/body angle excursion [a]	1.08	16.13	6.00±0.32
Lateral head/body angle magnitude [a]	5.55	28.50	14.98±0.54
Lateral head/body angle excursion [a]	9.04	34.13	18.07±0.64
Maximum head yaw magnitude [a]	3.25	21.81	9.74±0.44
Maximum head yaw excursion [a]	3.56	19.17	9.67±0.33
Maximum nose displacement [b]	0.019	0.123	0.056±0.002

[a] Angles are presented in degrees

[b] Displacements are presented in BL

Limb cycles, *N*=96

in the direction of the prey stimulus. When the body of the turtle was lower than the prey stimulus, the head was elevated. The angle between the head and body approached zero as the turtle and prey stimulus were moving at the same depth. The lateral angle (i.e., yaw) between the head and path of travel did show cyclic patterns (Fig. 3.5A, B). During the limb cycle, the head and body rotate in opposite directions of one another (Fig. 3.5A). Yawing of the head and body

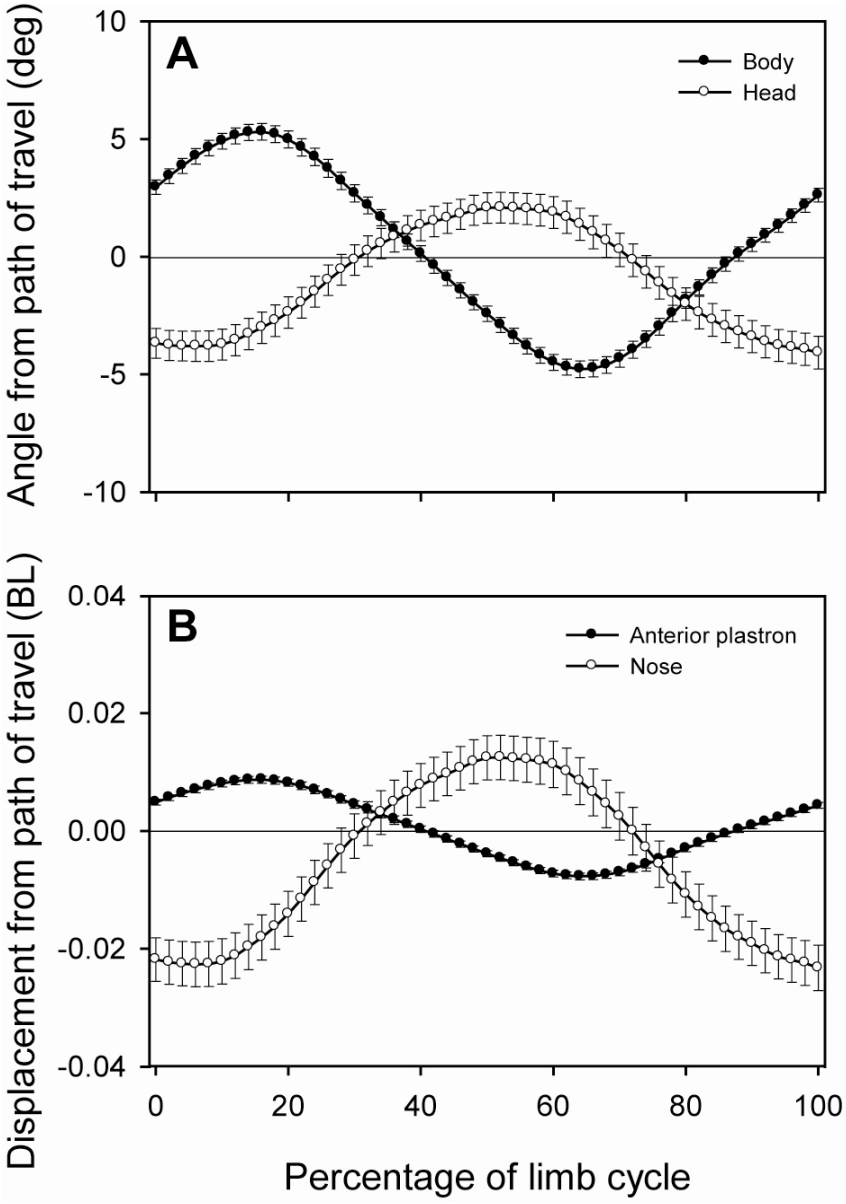

Figure 3.5. Average kinematic profiles of (A) head and body yaw and (B) sideslip of nose and anterior plastron. Symbols represent means±SEM (*N*=96). Note, because the maximum value for a given trial does not always occur at the same percent of the limb cycle, it is possible that calculated maximum values may be different than the maximum values seen in average kinematic profiles.

produces a displacement of the anterior-most point of the head (nose point) and plastron (anterior plastron point) from the path of travel (Fig. 3.5B). The displacement of these points showed the same mirrored pattern observed for the angles between the head and body and path of travel. However, while the angular deviations between the head and body and path of travel had similar magnitudes and excursions, the differences in the displacement of the nose and the anterior edge of the plastron are considerably higher, with the anterior edge of the plastron having a more stable trajectory than the nose (Fig. 3.5B).

Stability differences between freshwater and marine turtles

Nested ANOVAs were used to compare stability parameters measured in this study from the freshwater turtle *Chrysemys picta* (painted turtle) to those of the marine turtles *Caretta caretta* (loggerhead sea turtle) and *Chelonia mydas* (green sea turtle) measured in a study using similar methods (Dougherty et al., in press). Criteria for accepted trials in Dougherty et al. (in press) included that (1) the turtle swam fully submerged, (2) in a straight line, (3) for a distance of no less than three BL, and (4) completed at least three consecutive limb cycles during steady swimming in the field of view of the camera. As with the painted turtle data set, trials with path of travel R^2 values less than 0.25 were excluded from analyses. In addition, any trial containing an outlier (>3 standard deviations from the mean), for any of the variables, was removed from the data set used by Dougherty et al. (in press).

Data from Dougherty et al. (in press) included 120 cycles from 8 individual loggerheads (2-6 trials per turtle) and 72 cycles from 6 individual green turtles (3-5 trials per turtle), with animals ranging in size from 5.5 to 8.0 cm. Average swimming velocity during cycles was 5.52 BL s^{-1} for loggerheads and 5.36 BL s^{-1} for green turtles. Differences in sample size and results of statistical tests between this analysis and those presented by Dougherty et al. (in press) reflect removal of trials with outliers.

A nested ANOVA (adjusted by sequential Bonferroni) including all three species found significant species effects for 7 of 8 stability parameters tested (Table 3.6). Results of pair-wise tests are provided in Figure 3.6. Only one parameter (maximum heave magnitude) differed significantly between the two species of marine turtle (Fig. 3.6A). No significant differences were detected between the three species for maximum yaw magnitude (Fig. 3.6G). Painted turtles displayed the highest yaw excursion of the three species, although they only differed significantly from green turtles (Fig. 3.6H). For the six remaining parameters, painted turtles displayed significantly greater stability than either of the species of marine turtles (Fig. 3.6A-F).

Table 3.6. Results of mixed-model nested ANOVA testing for interspecific differences.

Stability parameter	Species			Individual			Trial		
	F	***P***	**d.f.**	***F***	***P***	**d.f.**	***F***	***P***	**d.f.**
Maximum heave magnitude	31.69	**<0.001***	2, 14.41	1.96	0.029	15, 78	3.10	<0.001	78, 192
Heave excursion	38.45	**<0.001***	2, 14.42	2.01	0.025	15, 78	1.64	0.003	78, 192
Maximum pitch magnitude	29.91	**<0.001***	2, 14.10	1.27	0.239	15, 78	1.76	<0.001	78, 192
Pitch excursion	11.90	**<0.001***	2, 14.56	2.65	0.003	15, 78	1.38	0.039	78, 192
Maximum sideslip magnitude	30.72	**<0.001***	2, 14.24	1.52	0.119	15, 78	3.79	<0.001	78, 192
Sideslip excursion	23.98	**<0.001***	2, 14.44	2.06	0.021	15, 78	1.43	0.025	78, 192
Maximum yaw magnitude	1.60	0.235	2, 14.53	2.47	0.005	15, 78	1.06	0.369	78, 192
Yaw excursion	6.48	**0.010***	2, 14.77	4.98	<0.001	15, 78	1.33	0.061	78, 192

Limb cycles: *Chrysemys picta*, *N*=96; *Caretta caretta*, *N*=120; *Chelonia mydas*, *N*=72

Bolded values indicate significant differences for main effect ($P<0.05$)

* Represent significant relationships for main effect (species) after sequential Bonferroni correction for multiple comparisons

Test of main effect corrected for unbalanced design; adjusted d.f. are indicated

See methods for detailed description of ANOVA design

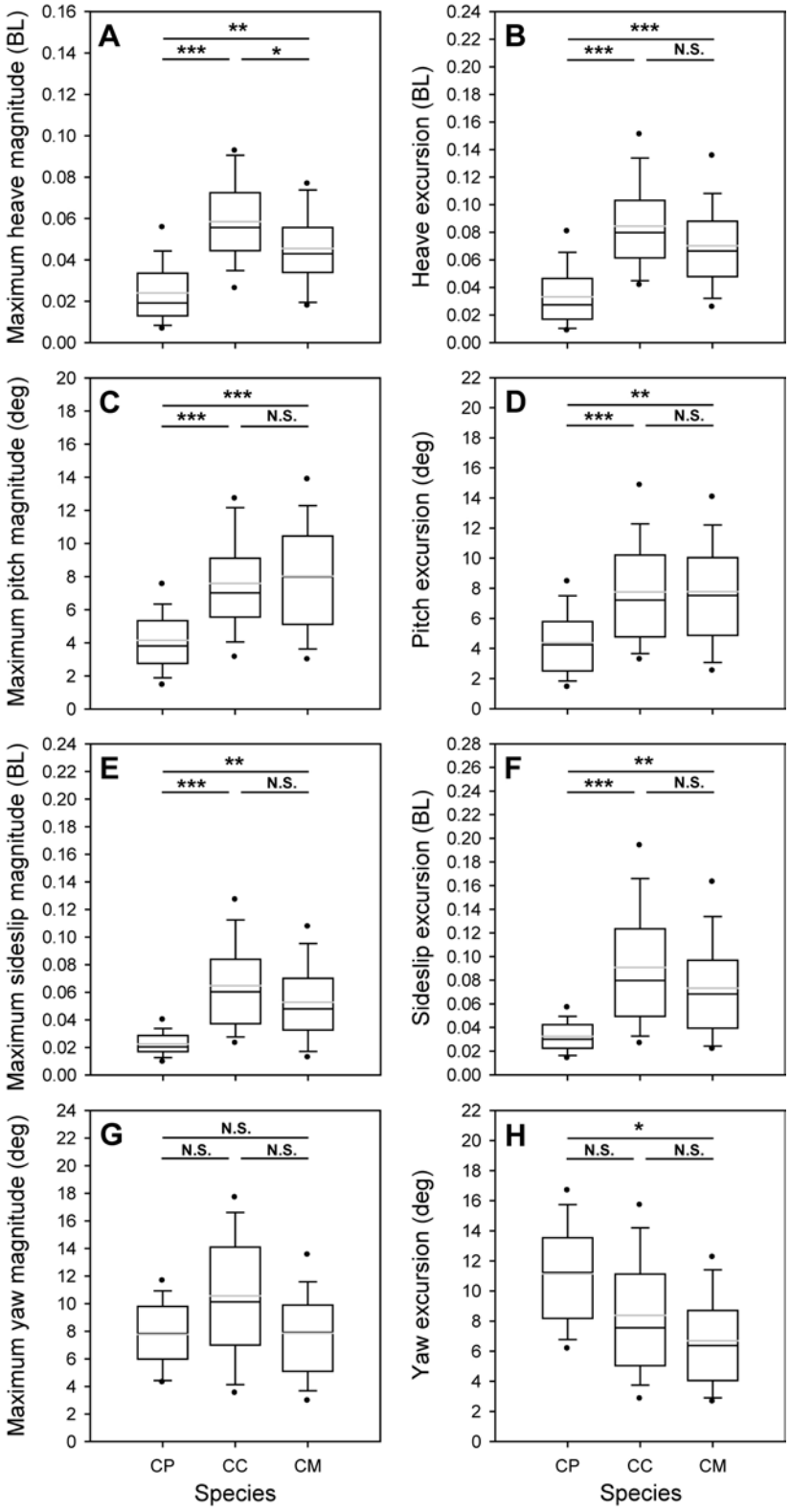
A
B
C
D
E
F
G
H
Maximum heave magnitude (BL)
Heave excursion (BL)
Maximum pitch magnitude (deg)
Pitch excursion (deg)
Maximum sideslip magnitude (BL)
Sideslip excursion (BL)
Maximum yaw magnitude (deg)
Yaw excursion (deg)
**
***
*
N.S.
CP
CC
CM
Species

Figure 3.6: Box-plots comparing values of body stability for the eight focal parameters with results of pair-wise nested ANOVAs. Painted turtles (CP; *N*=96), loggerhead turtles (CC; *N*=120) and green turtles (CM; *N*=72). Boxes enclose the median (centerline) and the 25th and 75th percentiles (bottom and top of boxes, respectively). Whiskers indicate the 10th and 90th percentiles; circles indicate the 5th and 95 percentiles. Light gray lines indicate the mean. Significance levels: *P<0.05, **P<0.01, ***P<0.001; N.S., not significant. Endpoints of horizontal lines indicate species used in each test. Sequential Bonferroni correction did not alter significance of pair-wise comparisons.

Discussion

Characteristics of aquatic stability in swimming freshwater turtles

During rectilinear swimming, painted turtles use synchronous movements of alternating pairs of contralateral fore- and hindlimbs. With this locomotor mode, maximum stability would be expected if the two contralateral limb pairs stay completely out of phase (i.e., movements differing by 50% of the limb cycle). My results showed that although there was variation in the timing of limb motions, the average difference in timing between the start of protraction for the two contralateral pairs was 48.1% of the limb cycle. The timing of protraction for the two limbs within each contralateral pair was also tightly matched, differing by an average of only 6.5% of the limb cycle. Differences in the timing of motion between contralateral fore- and hindlimbs was significantly correlated with maximum sideslip magnitude and sideslip excursion, highlighting the importance of maintaining proper phase relationships between the appendages for maintaining stability (Wiktorowicz et al., 2007)

Parameters of vertical stability (heave and pitch) are non-cyclic in painted turtles with high variability from cycle to cycle. In contrast, measures of lateral stability (sideslip and yaw) show highly repeatable cyclic patterns. Following retraction of a contralateral fore- and hindlimb pair, the body rotates (i.e., yaws) away from the side of the retracting hindlimb. This happens because the hindfeet have more webbing than the forefeet and, therefore, hindfeet act as larger paddles and are able to produce more thrust (Blob et al., 2003). The lag in timing between changes in yaw direction and changes in sideslip motion are the result of momentum that continues carrying the body in one direction for a short period even after the body has been reoriented toward the opposite direction.

The vertical angle between the head and body was related to the position of the prey stimulus relative to the turtle. If the turtle was slightly below the prey stimulus, its head would be elevated from the body toward the stimulus. The vertical angle of the head was held fairly constant during a cycle, which could be expected since there was no consistent vertical oscillation of the body. The lateral angle of the head did follow a cyclic pattern, yawing in the opposite direction of the body. The yawing motion of the head is likely due to hydrodynamic resistance as the body rotates side to side, and may help to reduce overall body yaw. An examination of the motion of the head relative to the path of travel showed that the head yawed to a similar magnitude as the body. However, the resulting lateral displacement of the anterior points of the head (nose) and the plastron show that displacement of the nose is greater than

the anterior plastron point. This discrepancy is likely related to the length of the segment that rotates away from the path of travel. The ventral COR was anteriorly positioned (mean, 38.6% of body), as a result, the segment anterior to the COR was less than half of the body length. In contrast, the head rotates at its base, meaning a longer segment is rotating away from the path of travel. For any angle from the path of travel, the longer the segment, the greater the displacement. As a result, the head is less stable than the anterior position of the shell, although, the level of head displacement was still very low and similar to that seen for the bodies of many fishes (Bainbridge, 1963; Videler and Wardle, 1978; Batty, 1981; Batty, 1984; Videler and Hess, 1984; Wassersug and von Seckendorf Hoff, 1985; von Seckendorf Hoff and Wassersug, 1986; Webb, 1988; Hove et al., 2001).

Comparison of stability between freshwater and marine turtles

A major focus of this study was to compare parameters of hydrodynamic stability between turtles using very different modes of propulsion (freshwater vs. marine turtles). In particular, I tested three hypotheses of how different modes of propulsion can produce differences in stability. My first prediction stated that because the primary direction of motion for the limbs of freshwater turtles is front-to-back, they were expected to have lower levels of heave than marine turtles. Consistent with my predictions, for heave magnitude and excursion, values were significantly smaller (approximately half) for painted turtles than the two species

of marine turtles (Fig. 3.6A, B). My second prediction stated that because marine turtles swim using limbs at only the anterior end of the body, they would encounter higher levels of pitch than freshwater turtles. Consistent with my predictions, for pitch magnitude and excursion, painted turtles had significantly lower values than the two marine turtles (Fig. 3.6C, D). My third prediction stated that because limb motions occur at the same time on both sides of the body, marine turtles would have lower levels of sideslip and yaw. Three of the four results of lateral stability were not consistent with my predictions. Of the four measured parameters of lateral stability (maximum magnitude and excursion for sideslip and yaw), painted turtles had significantly higher levels for one (Fig. 3.6E-H). Painted turtles had significantly lower values of maximum sideslip magnitude and excursion than the two marine species (Fig. 3.6E, F). Although all three species are capable of low sideslip magnitudes and excursions, marine turtles occasionally showed very large magnitudes. For parameters of yaw, marine turtles always had the smallest minimum values (Fig. 3.6G, H). For maximum yaw magnitude, the range of values for both marine turtles encompassed those of painted turtles; each displayed smaller values, but also much larger values. No significant differences were detected between the three species for maximum yaw magnitude. Painted turtles did have significantly larger values for yaw excursion, but only when compared with green turtles.

My results from the analysis of lateral stability shows that despite the perceived advantages of synchronous forelimb movement, painted turtles are

more stable than marine turtles with respect to sideslip (Fig. 3.6E, F). While theoretically marine turtles should be capable of smaller motions, this would require that both forelimbs move precisely in sync with regard to speed and orientation. In addition, although the heads of marine turtles are among the least mobile of turtles, small deviations in head orientation can also affect lateral stability. The swimming kinematics of freshwater turtles are likely critical to their lower levels of sideslip. Although the power stroke of contralateral fore- and hindlimbs produces a displacement away from the path of travel, properly phased, alternating movements of the two contralateral limb pairs pushes the COR back toward the path of travel. The same is true for the orientation of the body (i.e., yaw). Other studies have also noted the importance of phased locomotor movements in increasing stability (Fish et al., 2003b; Wiktorowicz et al., 2007). It is evident from the results that marine turtles are capable of smaller yaw recoil; however, when a sea turtle deviates from its trajectory, its limb motions will not automatically correct it, meaning that for yaw (as with sideslip) the potential for high values is very possible. It is also interesting to note that although painted turtles had a significantly larger yaw excursion compared with green turtles, there was no significant difference between the three species for maximum yaw magnitude (Fig. 3.6G). For the other three recoil motions (heave, pitch, and sideslip) patterns for parameter magnitudes mirror those for excursions. The discrepancy in this pattern for yaw occurs because while marine turtles may attain large yaw values in one direction (i.e., yaw magnitude), they

are not likely to also then rotate to the other side during the same limb cycle. In contrast, painted turtles always rotate to both sides during a limb cycle, so even if the maximum magnitude to one side is the same as that seen in a sea turtle, freshwater turtles will have larger excursion values because of their rotation to the other side. An additional point is that marine turtles can swim in a straight line even if their bodies are not pointing in the exact direction that they are traveling. Because they can maintain such a yaw angle (up to approx. 20°; Dougherty et al., in press) throughout a swimming sequence, sea turtles have the ability to produce a cycle with a yaw excursion that is smaller than the yaw magnitude.

Comparison of stability between turtles and other vertebrates

An additional goal of this study was to compare the stability of turtles with that of the model system for the study of hydrodynamic stability in rigid-bodied taxa, the tetraodontiform fishes (boxfish and pufferfish). Boxfish and pufferfish have been cited to have among the lowest levels of recoil measured from swimming animals, and they clearly outperform turtles with respect to yaw and pitch magnitude based on data available for comparison (Fig. 3.7). Boxfish and pufferfish have lower levels of pitch and yaw than turtles across the range of speeds at which they were sampled. Boxfish and pufferfish also show little effect of speed on stability. In contrast, pitch increases with increasing speed for the two sea turtle species and yaw increases with speed for two of the three turtle

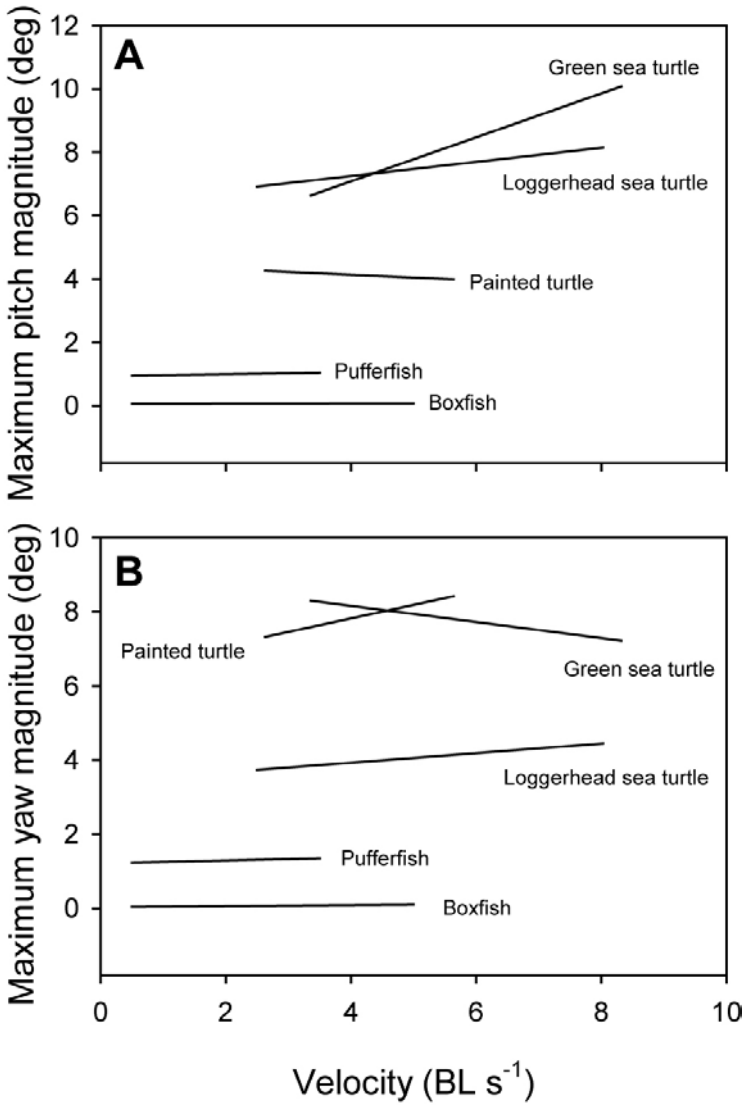

Figure 3.7. Relationship between swimming velocity and (A) pitch and (B) yaw for five species of rigid-bodied vertebrates. Lines represent regression lines; range of lines along the x-axis depict the swimming speeds at which data were sampled for the respective studies. Pitch: painted turtle, y=-0.089x+4.49 (this study); loggerhead turtle, y=0.223x+6.358 (Dougherty et al., in press); green turtle, y=0.694x+4.31 (Dougherty et al., in press); boxfish, y=0.004x+0.062 (Hove et al., 2001); pufferfish, y=0.03x+0.94 (Wiktorowicz et al., 2007). Yaw: painted turtle, y=0.365x+6.36; loggerhead turtle, y=0.130x+3.41 (Dougherty et al., in press); green turtle, y=-0.218x+9.03 (Dougherty et al., in press); boxfish, y=0.013x+0.034 (Hove et al., 2001); pufferfish, y=0.04x+1.21 (Wiktorowicz et al., 2007).

species. The coordinated movement of multiple fins, large height, and keels (Gordon et al., 2000; Hove et al., 2001; Bartol et al., 2002; 2003; 2005; 2008;) help boxfish to maintain such high levels of stability. In contrast, the dorsoventrally flattened bodies, more rounded dorsal profiles, and the position of the limbs (all four located near and approximately equidistant from the center of rotation and within the same horizontal plane), noted for increasing maneuverability in painted turtles (Rivera et al., 2006), likely contribute to their lower stability. In addition to boxfish and pufferfish, minimal stability data also exist for a number of larval amphibians (i.e., tadpoles) and flexible-bodied fish. Hove et al. (2001) calculated values of relative yaw (measured as the maximum snout excursion standardized by total body length) from a number of published sources. Values ranged from 0.02-0.09, equivalent to the values of the maximum lateral excursion of the nose in painted turtles (range, 0.020-0.12 BL; mean, 0.057 BL). These results show that the heads of painted turtles exhibit similar levels of yaw to many flexible-bodied fishes. Interestingly, if this value had been based solely on the rigid portion of the body, the lateral excursion of the anterior plastron point ranged from 0.007 to 0.037 BL, a range nearly identical to that produced for the boxfish *Ostracion meleagris* (0.007-0.038; Hove et al., 2001).

Directions for further study

This study quantified stability for the painted turtle and tested a number of hypotheses on the effects of propulsive mode. Studies similar to those of Bartol et al. (2002; 2003; 2005; 2008), that utilize a combination of flow visualization (DPIV), pressure, and force measurements would further improve our understanding of the effects of shell shape on hydrodynamic stability. Furthermore, extant freshwater turtles exhibit considerable morphological diversity, and several features of limb and shell morphology likely to affect hydrodynamics have been documented (Aresco and Dobie, 2000; Claude et al., 2003; Lubcke and Wilson, 2007; Rivera, 2008; Rivera and Claude, 2008). For example, softshell turtles of the genus *Apalone* possess similar degrees of webbing on the fore- and hindfeet, suggesting that the thrust produced during the power stroke of contralateral fore- and hindlimbs may be more similar on both sides of the body (Pace et al., 2001; Blob et al., 2007), thus reducing the torque that causes the body to yaw. Additionally, many species of the riverine genus *Graptemys* (map turtles) have prominent mid-dorsal keels (Ernst et al., 1994). It is possible that, like the keels of boxfish, the keels of map turtles may aid in lateral stabilization (yaw and sideslip) during rectilinear swimming. Furthermore, while it appears that the evolution of the sea turtle propulsive mode may have preferentially favored features that increased thrust and lowered the physiological cost of transport (Long, 2006), the keels of the highly migratory, pelagic leatherback sea turtle (*Dermochelys coriacea*) could enhance stability in this

species. Finally, although, painted turtles displayed higher levels of stability than sea turtles in this study, it is important not to generalize this finding to other size classes, as stability in juvenile and adult sea turtles may be very different. Studies addressing these topics will increase our understanding of the relationship between propulsive mode, body morphology, and hydrodynamic stability in turtles and may provide insight into the evolution of the unique morphologies of these remarkable animals.

Literature Cited

Aresco, M. J. and Dobie, J. L. (2000). Variation in shell arching and sexual size dimorphism of river cooters, *Pseudemys concinna*, from two river systems in Alabama. *J. Herpetol.* **34**, 313-317.

Arreola, V. I. and Westneat, M. W. (1996). Mechanics of propulsion by multiple fins: kinematics of aquatic locomotion in the burrfish (*Chilomycterus schoepfi*). *Proc. R. Soc. Lond. B* **263**, 1689-1696.

Avens, L., Wang, J. H., Johnsen, S., Dukes, P. and Lohmann, K. J. (2003). Responses of hatchling sea turtles to rotational displacements. *Journal of Experimental Marine Biology and Ecology* **288**, 111-124.

Bainbridge, R. (1963). Caudal fin and body movement in the propulsion of some fish. *J. Exp. Biol.* **40**, 23-56.

Bartol, I. K., Gharib, M., Webb, P. W., Weihs, D. and Gordon, M. S. (2005). Body-induced vortical flows: a common mechanism for self-corrective trimming control in boxfishes. *J. Exp. Biol.* **208**, 327-344.

Bartol, I. K., Gharib, M., Weihs, D., Webb, P. W., Hove, J. R. and Gordon, M. S. (2003). Hydrodynamic stability of swimming in ostraciid fishes: role of the carapace in the smooth trunkfish *Lactophrys triqueter* (Teleostei: Ostraciidae). *J. Exp. Biol.* **206**, 725-744.

Bartol, I. K., Gordon, M. S., Gharib, M., Hove, J. R., Webb, P. W. and Weihs, D. (2002). Flow patterns around the carapaces of rigid-bodied, multi-propulsor boxfishes (Teleostei: Ostraciidae). *Integr. Comp. Biol.* **42**, 971-980.

Bartol, I. K., Gordon, M. S., Webb, P. W., Weihs, D. and Gharib, M. (2008). Evidence of self-correcting spiral flows in swimming boxfishes. *Bioinspiration & Biomimetics* **3**.

Batty, R. S. (1981). Locomotion of plaice larvae. *Symp Zool Soc Lond* **48**, 53-69.

Batty, R. S. (1984). Development of swimming movements and musculature of larval herring (*Clupea harengus*). *J. Exp. Biol.* **110**, 217-229.

Blob, R. W., Rivera, A. R. V. and Westneat, M. W. (2007). Hindlimb Function in Turtle Locomotion: Limb Movements and Muscular Activation Across Taxa, Environment, and Ontogeny. In *Biology of Turtles*, eds. J. Wyneken M. H. Godfrey and V. Bels), pp. 139-162. Boca Raton: CRC Press.

Blob, R. W., Willey, J. S. and Lauder, G. V. (2003). Swimming in painted turtles: Particle image velocimetry reveals different propulsive roles for the forelimb and hindlimb. *Integr. Comp. Biol.* **43**, 985.

Burke, A. C. (1989). Development of the turtle carapace: implications for the evolution of a novel Bauplan. *Journal of Morphology* **199**, 363-378.

Claude, J., Paradis, E., Tong, H. and Auffray, J.-C. (2003). A geometric morphometric assessment of the effects of environment and cladogenesis on the evolution of the turtle shell. *Biol. J.Linn. Soc.* **79**, 485-501.

Davenport, J., Munks, S. A. and Oxford, P. J. (1984). A comparison of the swimming of marine and freshwater turtles. *Proc. R. Soc. Lond. B* **220**, 447-475.

Dougherty, E. E., Rivera, G., Blob, R. W. and Wyneken, J. (in press). Hydrodynamic stability in posthatchling loggerhead (*Caretta caretta*) and green (*Chelonia mydas*) sea turtles. *J. Exp. Biol.*

Ernst, C. E., Lovich, J. E. and Barbour, R. W. (1994). Turtles of the United States and Canada. Washington, D. C.: Smithsonian Institution Press.

Fish, F. E. (2002). Balancing requirements for stability and maneuverability in cetaceans. *Integr. Comp. Biol.***42**, 85-93.

Fish, F. E., Hurley, J. and Costa, D. P. (2003a). Maneuverability by the sea lion *Zalophus californianus*: turning performance of an unstable body design. *J. Exp. Biol.* **206**, 667-674.

Fish, F. E., Peacock, J. E. and Rohr, J. J. (2003b). Stabilization mechanism in swimming odontocete cetaceans by phased movements. *Marine Mammal Science* **19**, 515-528.

Gaffney, E. S. (1990). The comparative osteology of the Triassic turtle *Proganochelys*. *Bull. Am. Mus. Nat. Hist.* **194**, 1-263.

Gillis, G. B. and Blob, R. W. (2001). How muscles accommodate movement in different physical environments: aquatic vs. terrestrial locomotion in vertebrates. *Comparative Biochemistry and Physiology Part A* **131**, 61-75.

Gordon, M. S., Hove, J. R., Webb, P. W. and Weihs, D. (2000). Boxfishes as unusually well-controlled autonomous underwater vehicles. *Physiological and Biochemical Zoology* **73**, 663-671.

Gordon, M. S., Plaut, I. and Kim, D. (1996). How puffers (Teleostei: Tetraodontidae) swim. *Journal of Fish Biology* **49**, 319-328.

Hedrick, T. L. (2008). Software techniques for two- and three-dimensional kinematic measurements of biological and biomimetic systems. *Bioinspiration & Biomimetics* **3**, 034001.

Heithaus, M. R., Frid, A. and Dill, L. M. (2002). Shark-inflicted injury frequencies, escape ability, and habitat use of green and loggerhead turtles. *Marine Biology* **140**, 229-236.

Holm, S. (1979). A simple sequentially rejective multiple test procedure.*Scand. J. Stat.* **6**, 65-70.

Hove, J. R., O'Bryan, L. M., Gordon, M. S., Webb, P. W. and Weihs, D. (2001). Boxfishes (Teleostei: Ostraciidae) as a model system for fishes swimming with many fins: kinematics. *J. Exp. Biol.* **204**, 1459-1471.

Joyce, W. G. and Gauthier, J. A. (2004). Palaeoecology of Triassic stem turtles sheds new light on turtle origins. *Proc. R. Soc. Lond. B* **271**, 1-5.

Lighthill, J. (1975). Mathematical Biofluiddynamics. Philadelphia: Society for Industrial and Applied Mathematics.

Lighthill, J. (1977). Mathematical theories of fish swimming. In *Fisheries Mathematics*, (ed. J. H. Steele). London: Academic Press.

Long, J. H. (2006). Four flippers or two? Tetrapodal swimming with an aquatic robot. *Bioinspiration & Biomimetics* **1**, 20-29.

Lubcke, G. M. and Wilson, D. S. (2007). Variation in shell morphology of the western pond turtle (*Actinemys marmorata* Baird and Girard) from three aquatic habitats in northern California. *J. Herpetol.* **41**, 107-114.

Pace, C. M., Blob, R. W. and Westneat, M. W. (2001). Comparative kinematics of the forelimb during swimming in red-eared slider (*Trachemys scripta*) and spiny softshell (*Apalone spinifera*) turtles. *J. Exp. Biol.* **204**, 3261-3271.

Plaut, I. and Chen, T. (2003). How small puffers (Teleostei: Tetraodontidae) swim. *Ichthyological Research* **50**, 149-153.

Renous, S., de Lapparent de Broin, F., Depecker, M., Davenport, J. and Bels, V. (2007). Hindlimb Function in Turtle Locomotion: Limb Movements and Muscular Activation Across Taxa, Environment, and Ontogeny. In *Biology of Turtles*, eds. J. Wyneken M. H. Godfrey and V. Bels), pp. 97-138. Boca Raton: CRC Press.

Rice, W. R. (1989). Analyzing tables of statistical tests. *Evolution* **43**, 223-225.

Rieppel, O. and Reisz, R. R. (1999). The origin and early evolution of turtles. *Annual Review of Ecology and Systematics* **30**, 1-22.

Rivera, G. (2008). Ecomorphological variation in shell shape of the freshwater turtle Pseudemys concinna inhabiting different aquatic flow regimes. *Integr. Comp. Biol.* **48**, 769-787.

Rivera, G. and Claude, J. (2008). Environmental media and shape asymmetry: a case study on turtle shells. *Biol. J. Linn. Soc.* **94**, 483-489.

Rivera, G., Rivera, A. R. V., Dougherty, E. E. and Blob, R. W. (2006). Aquatic turning performance of painted turtles (*Chrysemys picta*) and functional consequences of a rigid body design. *J. Exp. Biol.* **209**, 4203-4213.

Santini, F. and Tyler, J. C. (2003). A phylogeny of the families of fossil and extant tetraodontiform fishes (Acanthomorpha, Tetraodontiformes), Upper Cretaceous to Recent. *Zoological Journal of the Linnean Society* **139**, 565-617.

Videler, J. J. and Hess, F. (1984). Fast continuous swimming of two pelagic predators, saithe (Pollachius virens) and mackerel (Scomber scombrus): a kinematic analysis. *J. Exp. Biol.* **109**, 209-228.

Videler, J. J. and Wardle, C. S. (1978). New kinematic data from high speed cine film recordings of swimming cod (*Gadus morhua*). *Neth J Zool* **28**, 465-484.

von Seckendorf Hoff, K. and Wassersug, R. J. (1986). The kinematics of swimming in the larvae of the clawed frog *Xenopus laevis*. *J. Exp. Biol.* **122**, 1-12.

Walker, J. A. (1998). Estimating velocities and accelerations of animal locomotion: a simulation experiment comparing numerical differentiation algorithms. *J. Exp. Biol.* **201**, 981-995.

Walker, J. A. (2000). Does a rigid body limit maneuverability? *J. Exp. Biol.* **203**, 3391-3396.

Wassersug, R. J. and von Seckendorf Hoff, K. (1985). The kinematics of swimming in anuran larvae. *J. Exp. Biol.* **119**, 1-30.

Webb, P. W. (1988). 'Steady' swimming kinematics of tiger musky, an esociform accelerator, and rainbow trout, a generalist cruiser. *J. Exp. Biol.* **138**, 51-69.

Webb, P. W. (1992). Is the high cost of body/caudal fin undulatory swimming due to increased friction drag or inertial recoil? *J. Exp. Biol.* **162**, 157-166.

Webb, P. W. (2002). Control of posture, depth, and swimming trajectories of fishes. *Integr. Comp. Biol.***42**, 94-101.

Weihs, D. (2002). Stability versus maneuverability in aquatic locomotion. *Integr. Comp. Biol.* **42**, 127-134.

Wiktorowicz, A. M., Lauritzen, D. V. and Gordon, M. S. (2007). Powered control mechanisms contributing to dynamically stable swimming in porcupine puffers (Teleostei: *Diodon holocanthus*). *Exp Fluids* **43**, 725-735.

Zug, G. R. (1971). Buoyancy, locomotion, morphology of the pelvic girdle and hind limb and systematics of cryptodiran turtles. *Misc. Publ. Mus. Zool. Univ. Michigan* **142**, 1-98.

CHAPTER FOUR

ECOMORPHOLOGICAL VARIATION IN SHELL SHAPE OF THE FRESHWATER TURTLE *PSEUDEMYS CONCINNA* INHABITING DIFFERENT AQUATIC FLOW REGIMES

Abstract

Populations of species that inhabit a range of environments frequently display divergent morphologies that correlate with differences in ecological parameters. The velocity of water flow (i.e., flow velocity) is a critical feature of aquatic environments that has been shown to influence morphology in a broad range of taxa. The focus of this study was to evaluate the relationship between flow velocity and shell morphology for males and females of the semi-aquatic freshwater turtle *Pseudemys concinna*. For both sexes, the carapace and plastron show significant morphological differences between habitats characterized by slow-flowing (i.e., lentic) and fast-flowing (i.e., lotic) water. In general, the most prominent pattern for both sexes is that the shells of individuals from lotic habitats are more streamlined (small height-to-length ratio) than the shells of individuals from lentic habitats. Of the two shell components (carapace and plastron), the carapace shows greater divergence between habitats, particularly for males. These results are consistent with adaptations to flow velocity, and suggest that variation in shape may be more constrained in females. I also provide empirical evidence for an adaptive benefit of the observed shape change (i.e., drag reduction) and a brief comment on the relative

roles of genetic divergence and phenotypic plasticity in generating shape differences observed in this species.

Introduction

Populations of species that inhabit a wide range of environments frequently display divergent morphologies that correlate with differences in ecological parameters. Many studies examining intraspecific morphological divergence have focused on the effects of biotic features of the environment, such as resource competition (Adams and Rohlf, 2000; Grant and Grant, 2006; Pfennig et al., 2006; Adams and Collyer, 2007) and the effects of predator-prey interactions (Bronmark and Miner, 1992; Milano et al., 2002; Langerhans and DeWitt, 2004; Eklov and Svanback, 2006; Brookes and Rochette, 2007). However, abiotic, or physical, features of the environment can also drive phenotypic divergence among intraspecific populations. The velocity of water flow, hereafter referred to as flow velocity, is a critical feature of aquatic environments that impacts numerous aspects of biology, including reproduction (Denny et al., 2002; Riffell and Zimmer, 2007), feeding (Okamura, 1984; Okamura, 1985; Marchinko, 2003; Pratt, 2008), displacement of free-swimming taxa (Gibbins et al., 2007), and dislodgement of sessile taxa (Carrington, 2002; Koehl et al., 2008; Stewart, 2008). In addition, flow velocity has been shown to influence morphology in a broad range of taxa, including plants and algae (Puijalon and Bornette, 2004; Boller and Carrington, 2006; Stewart, 2008),

invertebrates (Marchinko, 2003; Holomuzki and Biggs, 2006), and vertebrates (Pakkasmaa and Piironen, 2001; McGuigan et al., 2003; Peres-Neto and Magnan, 2004). Such patterns of morphological variation have been identified in numerous species of fishes inhabiting different flow regimes (Brinsmead and Fox, 2002; Keeley et al., 2005; Blob et al., 2008). While many of these studies are limited to the identification of a pattern of association between environment and morphology, several others have attempted to determine the adaptive benefits of divergent morphologies (Boily and Magnan, 2002; Ojanguren and Brana, 2003; Kerfoot Jr. and Schaefer, 2006). In general, these studies have observed that the shape of the body and caudal fin, as well as steady swimming performance differ in a predictable manner between lentic (i.e., slow flowing) and lotic (i.e., fast flowing) regimes (for review see Langerhans, 2008). More specifically, fishes inhabiting lentic flow regimes tend to have posteriorly deep bodies, low-aspect-ratio caudal fins, and low steady-swimming performance. In contrast, fishes from lotic environments possess streamlined bodies, high-aspect-ratio caudal fins, and increased steady-swimming performance (Langerhans, 2008). In addition, several other studies have examined the relative contribution of environmental and genetic factors on the resultant morphology (Pakkasmaa and Piironen, 2001; Imre et al., 2002; McGuigan et al., 2003; Peres-Neto and Magnan, 2004; Keeley et al., 2007; Langerhans, 2008;).

While morphological specializations to different flow regimes have been well established in fishes, the extent to which such patterns might extend to other

vertebrates is uncertain because fishes live exclusively in water and, as a result, selection on body shape for lower hydrodynamic resistance is expected to be maximized. In contrast, many tetrapods use both aquatic and terrestrial environments. For example, semi-aquatic freshwater turtles perform several vital functions on land (e.g., nesting and basking) as well as in water (e.g., feeding and copulation). Despite the potential constraints of a rigid shell, semi-aquatic freshwater turtles have adapted to life in a diverse array of aquatic flow regimes, ranging from ponds and lakes to fast flowing rivers (Ernst et al., 1994). At the most basic level, compared with terrestrial turtles, aquatic turtles possess flatter and more symmetrical shells; both of these characteristics are believed to increase swimming performance (Claude et al., 2003; Rivera and Claude, 2008). Furthermore, many species of freshwater turtles inhabit both lentic and lotic environments. Two studies examining intraspecific variation in morphology across different flow regimes have suggested that the shells of freshwater turtles are suited to the hydrodynamic environments in which they are found (Aresco and Dobie, 2000; Lubcke and Wilson, 2007). Aresco and Dobie (2000) presented the first quantitative data, by showing that the shells of river cooters (*Pseudemys concinna*) from lotic sites were flatter than those from lentic sites. More recently, Lubcke and Wilson (2007) found that western pond turtles (*Actinemys marmorata*) from lotic habitats were flatter and more narrow than those from lentic habitats. Though both of these studies identified body shapes expected to reduce drag in high-flow environments, there are several limitations

to these analyses. First, the morphological data used were based on only two (shell length and height; Aresco and Dobie, 2000) or three morphological variables (shell length, height, and width; Lubcke and Wilson, 2007); as a result, the manner in which changes in these variables occur are unknown. For example, while we may know that shell shape ranges from “flat” to “highly-domed”, we do not know what specific structural differences are responsible for these morphologies. Second, the geographic areas examined were limited to two physiographic regions within the state of Alabama (Aresco and Dobie, 2000) and three sites within a single county in California (Lubcke and Wilson, 2007). Third, it is possible that the flow environment could differentially influence shape in the two components of the shell (i.e., carapace and plastron), but these components have not yet been examined separately. Fourth, while both studies suggest that the association between flow velocity and shell morphology may be based on reducing hydrodynamic resistance, empirical effects of shell shape on hydrodynamics have yet to be tested. Lastly, as is common in studies examining correlations between environmental characteristics and morphology, an important question is whether the differences observed are the result of natural selection or of phenotypic plasticity (DeWitt et al., 1998; Langerhans, 2008; Rivera and Claude, 2008). Consequently, while these studies provide support for ecomorphological variation associated with flow velocity in turtles, many important questions remain unanswered.

Several factors make freshwater turtles an ideal group in which to evaluate morphological variation associated with different flow regimes, as well as the effects of such variation on locomotor performance. First, individual species inhabit a variety of aquatic habitats, encompassing a wide range of flow velocities within a relatively small geographic area (Ernst et al., 1994). Additionally, both components of the turtle shell are covered by keratinized scutes, the intersections of which form a large number of easily identifiable landmarks that can be used to assess morphological variation using landmark-based geometric morphometric analyses (Claude et al., 2003; Valenzuela et al., 2004; Slice, 2005; Myers et al., 2006; Rivera and Claude, 2008). The rigid shell also makes it possible to digitize these landmarks accurately and with high repeatability. Furthermore, because the shell limits axial mobility, propulsion in turtles is limited to forces generated by movements of the forelimbs and hind limbs (Pace et al., 2001; Rivera et al., 2006), which results in a decoupling between the morphology of propulsory structures and overall shape (i.e., shell morphology). In contrast, studies examining the association between flow velocity and the morphology of fishes have to interpret the complex interactions between modifications of the body and fins that reduce drag and those that increase propulsion (though see Blob et al., 2008). Turtles are also an excellent system in which to use physical models to evaluate the effects of shape on hydrodynamic forces (Koehl, 2003). Given that turtle shells are rigid, data collected from rigid models will closely approximate *in vivo* forces, as shown in

studies of other rigid-bodied taxa (Bartol et al., 2005; e.g., boxfish: Bartol et al., 2003). Finally, shell shape in turtles has been shown to possess a heritable genetic component (Myers et al., 2006), an essential requirement for divergent natural selection.

The broad goal of this study was to evaluate the relationship between flow velocity and shell morphology in a semi-aquatic freshwater turtle, the river cooter (*Pseudemys concinna*). The specific objectives of this paper are three-fold. First, I test for three-dimensional differences in shell morphology between turtles from lentic and lotic flow regimes, while concomitantly testing whether the carapace and plastron demonstrate the same propensity for environmentally correlated differences. Second, I use physical models to test whether morphological differences of the shell confer reductions in drag. Finally, I provide preliminary data regarding the potential role of phenotypic plasticity in generating the morphological variation observed in turtles between the two flow regimes.

Materials and Methods

Study system

The river cooter (*Pseudemys concinna*) is a large freshwater turtle that inhabits a broad array of aquatic environments throughout southeastern North America. Much of the species' range is divided by the Fall Line, a physiographic feature that delineates the higher-elevation Piedmont (i.e., foothills of the Appalachian Mountains) in the east and uplands in the west from the flat and

low-lying Coastal Plain. Because the populations used in this study were from either the Piedmont (sensu stricto) or the Coastal Plain, hereafter, sites located above the Fall Line are referred to as “Piedmont” and those below the Fall Line are referred to as “Coastal Plain”. Rivers above the Fall Line tend to be fast-flowing (i.e., lotic), whereas flow velocity below the Fall Line is considerably slower (i.e., lentic). The difference between the two flow regimes can be attributed to the elevation gradient between the Piedmont and Coastal Plain. While lotic environments inhabited by this species are mostly limited to rivers above the Fall Line, lentic habitats include rivers below the Fall Line, lakes, oxbows, bayous, and floodplain deltas.

Study sites

I examined carapace and plastron morphology in *Pseudemys concinna* using fluid-preserved museum specimens collected from nine sites throughout the species’ range (Fig. 4.1; Table 4.1). The list of measured specimens is given in Appendix A. Because the specific flow velocities encountered by the specimens *in vivo* are unknown, the flow regime of each site was categorized as lentic or lotic. Preliminary assessment of flow velocity was based on geography, with riverine habitats above the Fall Line classified as lotic and those below the Fall Line classified as lentic. In addition, within both of these regions (Piedmont and Coastal Plain) non-flowing bodies of water (e.g., lakes and bayous) were considered lentic flow regimes. The classification of sites was confirmed using

historical flow data from the USGS National Water Information System (NWIS; http://waterdata.usgs.gov/nwis).

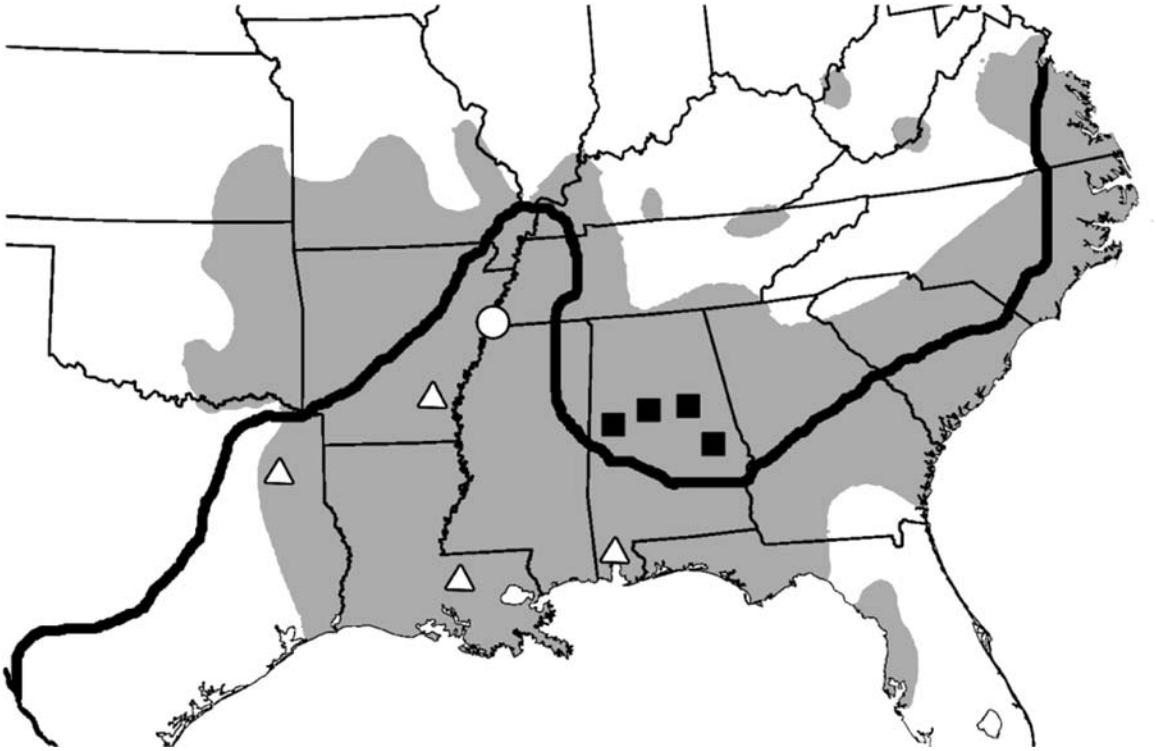

Figure 4.1: Map showing the range (shaded area) of *Pseudemys concinna* in North America. Bold line indicates the position of the Fall Line, which separates the Upland/Piedmont (above) and Coastal Plain (below). Locations of the nine populations used in this study are indicated by open triangles (lentic), filled squares (lotic), and open circle (Reelfoot Lake).

Eight of the nine sites fit clearly into one of the two flow regimes (i.e., lentic or lotic; Table 4.1). However, turtles from the remaining site (Reelfoot Lake) represent a population that inhabits a lentic environment, but whose ancestors inhabited a lotic environment less than 200 years ago. Reelfoot Lake is a natural lake located within the New Madrid Seismic Zone, the center of a series of large

Table 4.1: Sample sizes for populations.

		Male		Female	
	State	Carapace (N)	Plastron (N)	Carapace (N)	Plastron (N)
Lentic		87	84	37	38
Coon Creek Lake	Texas	27	26	5	6
Southern LA	Louisiana	14	14	11	11
Mobile River Delta	Alabama	35	32	10	9
White River	Arkansas	11	12	11	12
Lotic		41	40	16	16
Black Warrior River	Alabama	18	18	4	4
Cahaba River	Alabama	9	8	6	6
Coosa River	Alabama	8	8	2	2
Tallapoosa River	Alabama	6	6	4	4
Reelfoot Lake	Tennessee	9	9	10	9
Total		137	133	63	63

earthquakes between 1811 and 1812. These events formed the lake's basin (Mirecki, 1996), which was subsequently filled with water and colonized by turtles from the lotic Mississippi River (Fig. 4.2). This unique history provides the opportunity to examine whether turtles inhabiting the lake display morphologies associated with lentic or lotic environments. The presence of lotic morphotypes would suggest that neither selection (natural or sexual) nor phenotypic plasticity has acted on the ancestral (i.e., lotic) morphotype. However, because the lake has existed for a short period of time and because *Pseudemys concinna* has a long generation time, the presence of lentic morphotypes is more likely to suggest a role of phenotypic plasticity than of natural or sexual selection.

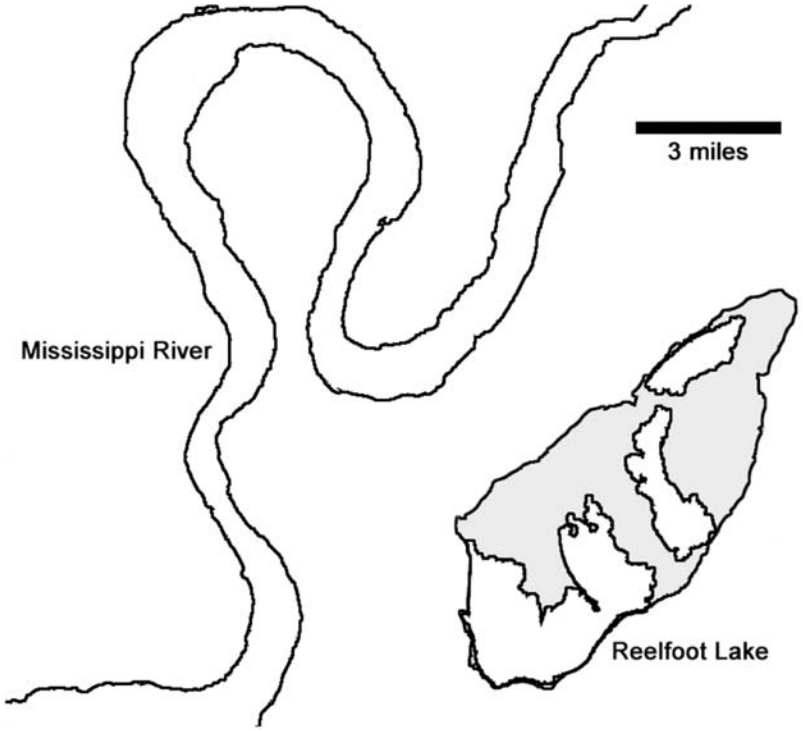

Figure 4.2: Location of Reelfoot Lake (lentic) relative to the Mississippi River (lotic). Shaded regions within Reelfoot Lake represent cypress swamps, while the unshaded regions represent basins (i.e., open areas of water).

Morphological measurements

Previous studies have noted that secondary sexual characteristics in *Pseudemys concinna* are apparent in males with carapace lengths larger than 16.0 cm (Fahey, 1987; Aresco and Dobie, 2000). Based on this information, all specimens used in this study had a carapace length of at least 16.0 cm to facilitate accurate classification of sex. Turtles were sexed based on the presence or absence of elongated foreclaws and precloacal tail length, which is considerably larger in males (Fahey, 1987; Buhlmann and Vaughan, 1991). As the position of the intersections of scutes was the basis of morphometric data,

specimens displaying developmental scute deformations were excluded from the study. Individuals with localized damage to scutes (e.g., cracks along the marginal scutes) were included as long as all landmarks on either the left or right side of the shell were intact. In some cases, when shells were damaged, only one of the two shell components (carapace or plastron) was digitized for a given specimen, producing minor differences in sample sizes between these components (Table 4.1).

To quantify the shape of the shell, three-dimensional coordinate data (x, y, z) were collected for 74 landmarks on the carapace (sensu Slice, 1993) and 17 landmarks on the plastron (Fig. 4.3) using a 3D digitizing system (Microscribe G2LX; accuracy of 0.30 mm). These landmarks were formed by the intersections of keratinized scutes covering the carapace and plastron and are type 1 (Bookstein, 1991). Two replicates of each configuration (i.e., set of landmarks) were collected for both shell components. These replicates were averaged and became the basis of the geometric morphometric (GM) analysis (Rohlf and Marcus, 1993). In order to reduce redundancy in the data and linear dependence among shape variables, only the coordinates of the right side of the shell were used for GM analyses (Bookstein, 1996; Claude et al., 2003; Valenzuela et al., 2004). For specimens in which the right side was damaged, but the left side was not, landmarks from the left side of the shell were mirrored to form a “right side”. In addition, for the carapace, there were five pairs of closely associated landmarks; one landmark from each pair was excluded

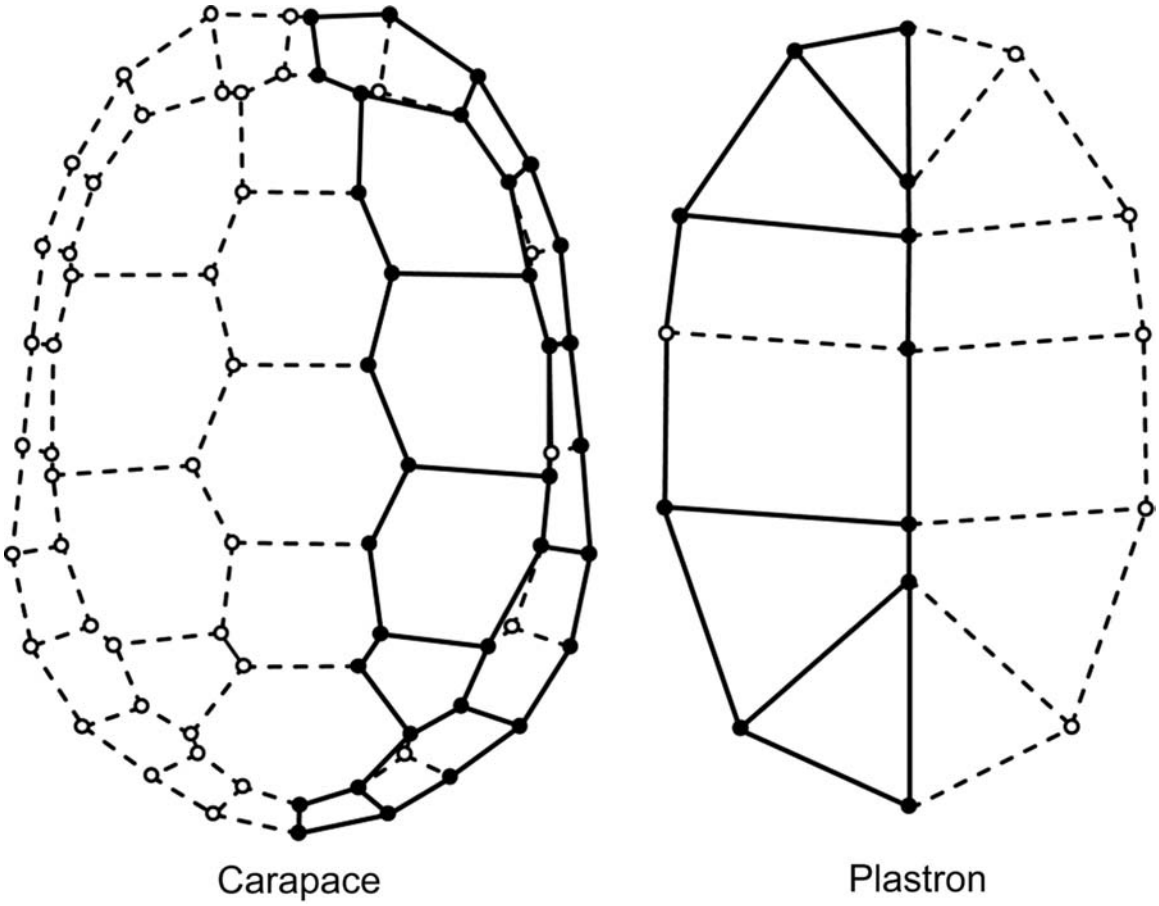

Figure 4.3: Location of landmarks (circles) digitized on the carapace (N=74) in dorsal view and on the plastron (N=17) in ventral view. Landmarks are located at the intersection of three scutes or along the edge of the shell, on the suture formed between two marginal scutes. Dashed lines indicate borders between scutes. Closed circles indicate landmarks of the right side used in GM analysis and are connected by solid lines; five landmarks were excluded from the carapace and one landmark was excluded from the plastron (see text for rationale). Anterior edges of shells oriented upward.

because (1) they provided minimal information about shape relative to the other nearby landmark, and (2) in several cases, the two landmarks within a pair appeared to occupy the same position. Similarly, a single point on the plastron was removed from the configuration. This point was along the periphery of the

plastron, and for specimens in which the plastron had been cut from the carapace, the position of this landmark was not considered accurate.

The removal of the aforementioned landmarks from each configuration produced thirty-three landmarks for the carapace and eleven landmarks for the plastron (Fig. 4.3). Many species of turtle, including *Pseudemys concinna*, display sexual dimorphism (Gibbons and Lovich, 1990; Aresco and Dobie, 2000;). For this reason, each sex was analyzed separately. Each of the four sets of configurations (male carapace, female carapace, male plastron, female plastron) was then separately superimposed (scaled, translated, and rotated) using generalized Procrustes analysis (GPA)(Rohlf and Slice, 1990). GPA removes information not related to shape (scale, position, and orientation) from configurations and allows shape to be examined independent of size (i.e., centroid size). First, GPA scales all configurations to the same centroid size. Translation occurs by moving the centroid of each configuration to the same point in three-dimensional space. Finally, configurations are rotated about all three axes to minimize the sum-of-square distances between homologous landmarks.

Following GPA, each configuration occupied a position in a curved, non-Euclidean shape space and was subsequently projected onto a tangent plane (Slice, 2001). A principle component analysis (PCA) was conducted on the coordinates of the tangent-space projected configurations to examine the major components of morphological variation. The PC scores generated from this

analysis represent the shape variables which were subsequently used in several multivariate tests (SYSTAT, v.10; nested MANOVA, discriminant function analysis, and correlation analysis) to examine the relationship between shape and flow regime. The software package *morphologika* (O'Higgins and Jones, 1998; available online at http://hyms.fme.googlepages.com/resources) was used to conduct GPA, tangent projection, and PCA of the configurations. In addition, *morphologika* provided the ability to visualize shape variation by "warping" between the extremes of the PC axes, thus allowing for a qualitative description of shapes associated with lentic and lotic flow regimes.

Drag measurements

I also examined how the observed differences in shape influence drag, a force that resists forward motion. This examination was limited to males because variation in the shape of males is less likely to be confounded by other factors (e.g., reproductive pressures). I selected two populations that conformed to the lentic and lotic morphotypes (based on DFA; see Table 4.2). *Morphologika* was used to calculate the mean configuration for each population, which was the average of the GPA superimposed configurations prior to tangent-space projection. I then selected the individual from each population that displayed the shape most similar to the mean shape of the entire population (based on minimum Procrustes distance) and used these two "average" specimens to generate plastic models. Specimens were immersed in liquid silicone (Oomoo

30, Smooth-on, Inc., Easton, PA) to generate a mold. After the mold was set, specimens were removed and the spaces into which the head and limbs had extended were filled with silicone putty. This allowed for the examination of hydrodynamic properties of the shell, without confounding effects associated with the orientation of the head and limbs (e.g., interactive effects from the head and arms can make the effective drag on the shell higher), which differed between the two specimens. Low-viscosity liquid plastic (Smooth-cast 300, Smooth-on, Inc., Easton, PA) was then poured into the silicone mold. Upon curing, remnants of the neck and limbs were sanded and smoothed-over using epoxy putty.

Each model was mounted caudally to a support rod, called a sting, in the center of a flow tank (working area, 120 cm × 333 cm × 336 cm). The horizontal sting extending posteriorly from the model was fastened to a vertical sting connected to a 1-kg bending beam load cell (EBB-1, Transducer Techniques Inc., Temecula, CA) positioned above the flow tank (Fig. 4.4). Data output from the load cell was amplified by a Vishay conditioning bridge amplifier (model 2120B; MicroMeasurements Group, Raleigh, NC, USA) and collected at a rate of 1000 Hz for 40 seconds using a customized data-acquisition program in LabVIEW (v.6.1; National Instruments). Data were collected for nine trials, including three replicates each of drag incurred by the lotic model, the lentic model, and the sting only. Each trial contained an initial five-second segment with no flow to provide a baseline value and a 30-second segment with flow velocity at 0.67 ms^{-1}, the maximum velocity at which flow remained laminar. The average force measured

from the sting apparatus was subtracted from the average overall force measurement, leaving only the drag produced by the model. Comparisons of drag were performed using the drag coefficient (C_D; an empirically derived coefficient that is fixed for a particular shape; see Vogel, 2003) for each model, which was calculated using the equation [$C_D = (2 \times D) / (\rho_w \times A_f \times u^2)$], where D is drag, ρ_w is the density of water (1 kg m^{-3}), A_f is frontal area (m^2), and u is the water velocity. Furthermore, a variant of the preceding equation ($D = 0.5 \times C_D \times \rho_w \times A_f \times u^2$) is used to calculate the drag incurred by the two morphotypes at a range of biologically relevant speeds.

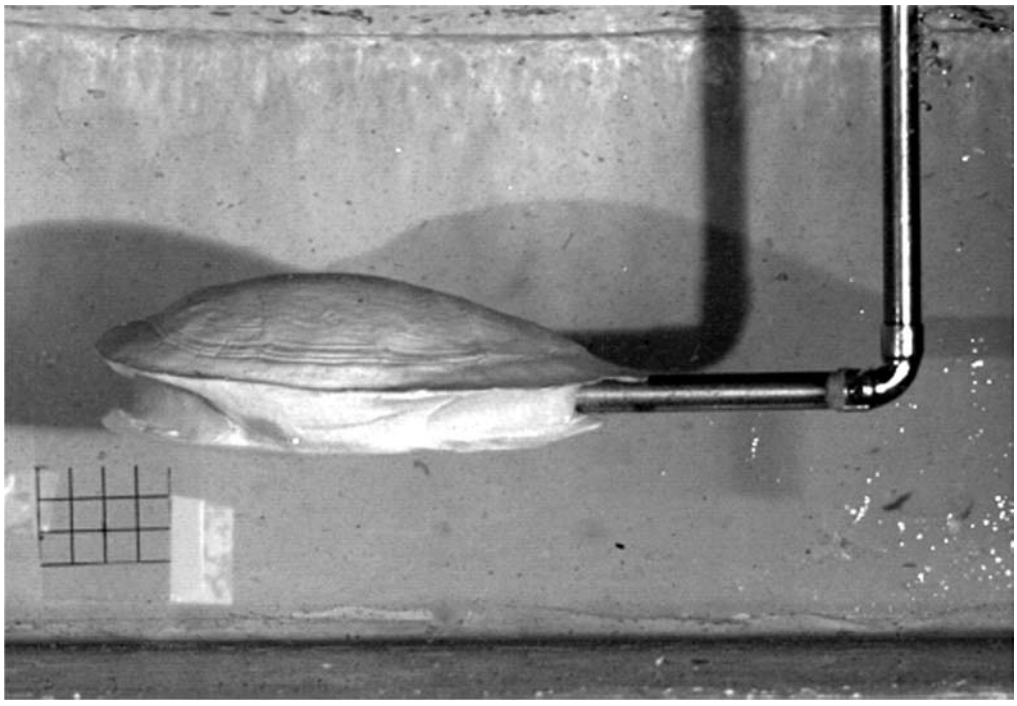

Figure 4.4: Apparatus for measuring drag. Model turtle is suspended in water column of flow tank by a horizontal sting extending posteriorly from the model and connecting to a vertical sting. The vertical sting is connected distally to a load cell located above the tank (not shown). Water flows from left to right (anterior to posterior relative to turtle). Grid=1 cm.

Table 4.2 Discriminant function analyses of lentic and lotic populations, excluding one population at a time.

	Jackknifed (Known)						Unknown	
Excluded Population	**Lentic (N)**	**Lentic (% Correct)**	**Lotic (N)**	**Lotic (% Correct)**	**Total (N)**	**Total (% Correct)**	**N**	**% Correct**
Male carapace								
Black Warrior River	87	98	23	96	110	97	18	33
Cahaba River	87	94	32	88	119	92	9	67
Coosa River	87	92	33	88	120	91	8	100
Tallapoosa River	87	91	35	89	122	90	6	100
Coon Creek Lake	60	90	41	90	101	90	27	100
Southern LA	73	92	41	90	114	91	14	93
Mobile River Delta	52	94	41	93	93	94	35	40
White River	76	88	41	95	117	91	11	73
Female carapace								
Black Warrior River	37	89	12	83	49	88	4	25
Cahaba River	37	84	10	90	47	85	6	100
Coosa River	37	81	14	71	51	78	2	100
Tallapoosa River	37	78	12	83	49	80	4	100
Coon Creek Lake	32	75	16	88	48	79	5	100
Southern LA	26	77	16	94	42	83	11	73
Mobile River Delta	27	89	16	88	43	88	10	50
White River	26	69	16	94	42	79	11	73

Table 4.2, continued

	Jackknifed (Known)						Unknown	
Excluded Population	**Lentic (N)**	**Lentic (% Correct)**	**Lotic (N)**	**Lotic (% Correct)**	**Total (N)**	**Total (% Correct)**	**N**	**% Correct**
Male plastron								
Black Warrior River	84	83	22	86	106	84	18	50
Cahaba River	84	75	32	78	116	76	8	75
Coosa River	84	77	32	81	116	78	8	88
Tallapoosa River	84	73	34	79	118	75	6	100
Coon Creek Lake	58	76	40	80	98	78	26	92
Southern LA	70	70	40	83	110	75	14	86
Mobile River Delta	52	94	40	85	92	90	32	31
White River	72	74	40	83	112	77	12	75
Female plastron								
Black Warrior River	38	84	12	92	50	86	4	25
Cahaba River	38	79	10	70	48	77	6	100
Coosa River	38	84	14	86	52	85	2	50
Tallapoosa River	38	82	12	67	50	78	4	100
Coon Creek Lake	32	81	16	81	48	81	6	100
Southern LA	27	78	16	88	43	81	11	45
Mobile River Delta	29	83	16	94	45	87	9	67
White River	26	77	16	81	42	79	12	92

N=number of actual individuals in this category; Tests used to examine influence of each population on function's overall ability to correctly classify individuals into the two flow regimes

Excluded population coded "unknown" and classified "lentic" or "lotic" based on remaining individuals

Lentic populations are Coon Creek Lake, Southern LA, Mobile River Delta, White River; Lotic populations are Black Warrior River, Cahaba River, Coosa River, Tallapoosa River

Results

I examined morphological variation of the shell, carapace and plastron, among lentic and lotic populations of the river cooter, *Pseudemys concinna*. The data were treated as four distinct units: carapaces of males, carapaces of females, plastrons of males, and plastrons of females; each of these data sets was analyzed separately. Descriptions of differences in shell morphology between turtles inhabiting lentic and lotic flow regimes, as well as the results of nested MANOVA, discriminant function analysis (DFA), and correlation analyses, are detailed in the sections below. While the population from Reelfoot Lake was used in generating the new dataset (i.e., PC axes), for all statistical tests this population was analyzed independently (see Discussion for rationale).

Morphological comparisons

Carapaces of males

PCA of the Procrustes superimposed data for all nine sites (N=137) listed in Table 4.1 produced 92 PCs. Of these, the first 31 accounted for 95.1% of the total variation, while the first 54 accounted for 99.0% of the total variation. PC 1 (22.4%) and PC 2 (15.6%) accounted for a total of 38% of the total variation (see Fig. 4.5A). Low scores for PC 1 identify individuals with strongly domed (i.e., high carapace height-to-length ratio) carapaces. The domed shell is a result of steeply oriented pleural scutes. Due to the high steepness, the carapace is narrow. The width of the carapace does not vary considerably along the length

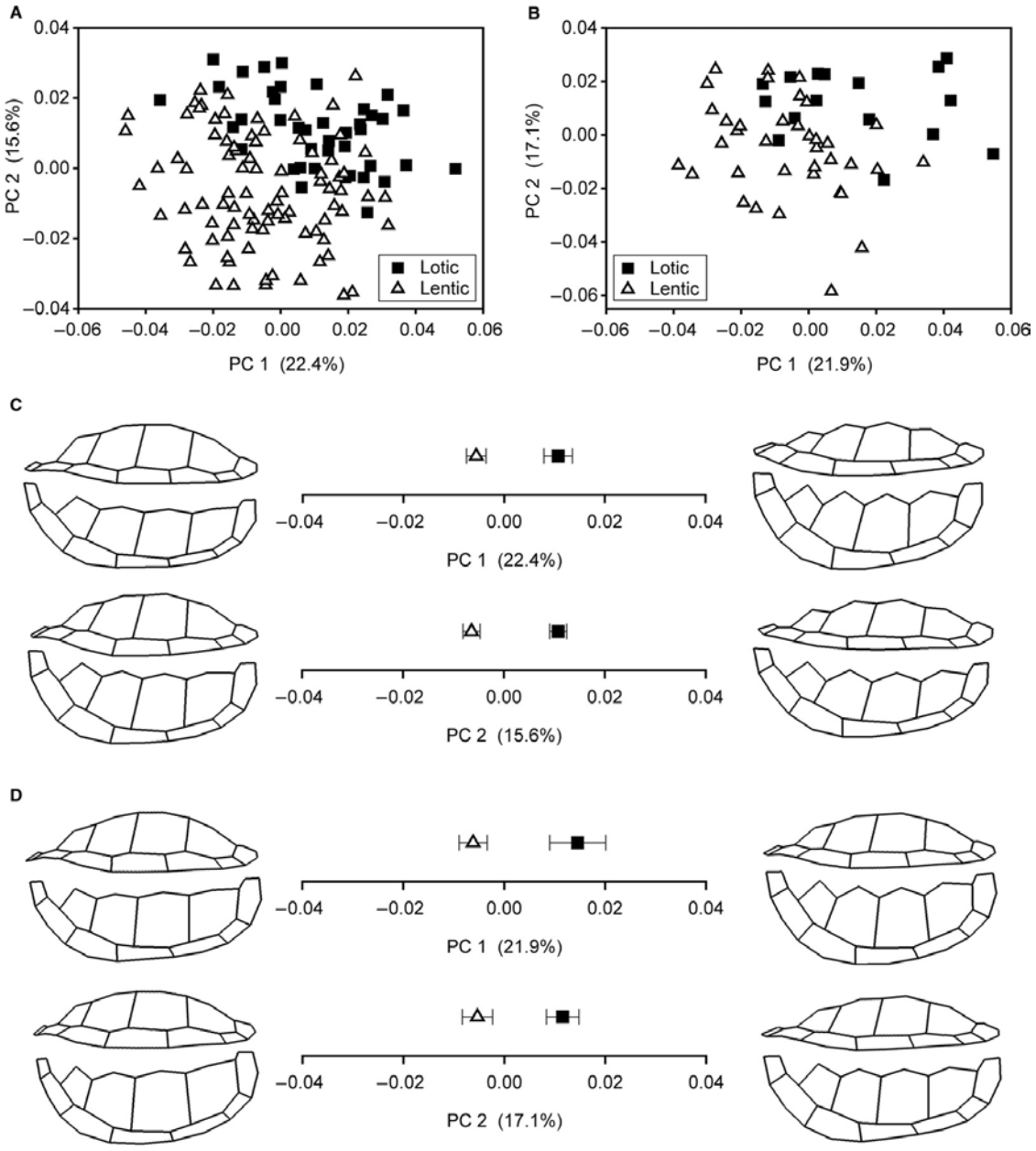
A
0.04
0.02
0.00
−0.02
−0.04
PC 2 (15.6%)
−0.06 −0.04 −0.02 0.00 0.02 0.04 0.06
PC 1 (22.4%)
Lotic
Lentic
B
0.04
0.02
0.00
−0.02
−0.04
−0.06
PC 2 (17.1%)
−0.06 −0.04 −0.02 0.00 0.02 0.04 0.06
PC 1 (21.9%)
Lotic
Lentic
C
−0.04 −0.02 0.00 0.02 0.04
PC 1 (22.4%)
−0.04 −0.02 0.00 0.02 0.04
PC 2 (15.6%)
D
−0.04 −0.02 0.00 0.02 0.04
PC 1 (21.9%)
−0.04 −0.02 0.00 0.02 0.04
PC 2 (17.1%)

Figure 4.5: Principal component analysis on the three-dimensional coordinates for the carapace. (A) First two principal components (PC 1 and PC 2) for males. (B) PC 1 and PC 2 for females. (C) Shape variation along PC 1 and PC 2 for males. (D) Shape variation along PC 1 and PC 2 for females. For C-D, turtle diagrams represent the extreme of each PC axis. Top image in each set represents the lateral (right-side) view of the carapace; bottom image represents the dorsal view of the right side of the carapace. For all diagrams of shells, anterior is to the right. Symbols on the axis represent mean ± s.e. For A-D, open triangles represent turtles from lentic habitats; filled squares represent turtles from lotic habitats. Sample sizes are given in Table 4.1.

of the body. Additionally, the marginal scutes are narrow and angled more steeply than are the pleural scutes. In contrast to low scores, high scores for PC 1 depict individuals with dorsoventrally flattened and wider carapaces. This morphology is predominantly the result of less steeply oriented pleural scutes. In addition, the angle between the pleural and marginal scutes is decreased, causing the marginal scutes to “flare out”. The posterior end of the carapace is also visibly wider than the anterior end. Low PC 1 scores correspond to morphologies displayed by “lentic” individuals, while high PC 1 scores correspond to morphologies displayed by “lotic” individuals (Fig. 4.5C). Low PC 2 scores also describe domed carapaces. The domed shape is generated by increasing the mediolateral width of the pleural scutes, rather than by changing the angle of their orientation. The possession of wide pleural scutes also increases the overall width of the carapace. Additionally, the marginal scutes are oriented downward. In contrast, high PC 2 scores are characterized by a more dorsoventrally flattened and narrower carapace. The height and width of the

carapace decreases because the width of the pleural scutes decreases. Finally, the marginal and pleural scutes are oriented at the same angle. Low PC 2 scores correspond to morphologies displayed by "lentic" individuals, while high PC 2 scores correspond to morphologies displayed by "lotic" individuals (Fig. 4.5C).

Results of a nested MANOVA on the eight focal populations (Table 4.1) using the first 31 shape variables (i.e., 95% of the variation in shape) indicated that there is a significant effect of flow regime on carapace shape (Wilks' Lambda: $F_{31,90}$=17.62, P<0.001), as well as a significant effect of site (Wilks' Lambda: $F_{186,539}$=3.909, P<0.001), which was nested within flow. Univariate F-tests identified six PCs that differed significantly between flow regimes at the 0.05-level (PCs 1-3, 9, 14, 18). These six PCs accounted for 54.8% of the total variation. I used DFA (on the first 31 variables) to determine the level of difference in shape between the two groups. Based on jackknifed results, turtles were correctly classified 91% of the time (lentic=92%, lotic=90%).

In order to examine the influence of each population on the function's overall ability to correctly classify the two groups, multiple DFA were performed on the dataset, each excluding one population at a time (Table 4.2). Concomitantly, individuals of each excluded population were coded as "unknowns" and were classified as belonging to either lentic or lotic morphotypes based on the remaining individuals (Table 4.2). Results show that the exclusion of individuals from the Black Warrior River population produced the largest

increase in the rate at which individuals were classified correctly, from 91% to 97%. Furthermore, when treated as "unknowns", individuals from this population were classified correctly 33% of the time (Table 4.2).

Carapaces of females

PCA of the Procrustes superimposed data for all nine sites (N=63) produced 62 PCs. Of these, the first 25 accounted for 95.2% of the total variation, while the first 41 accounted for 99.0% of the total variation. PC 1 (21.9%) and PC 2 (17.1%) accounted for a total of 39% of the total variation (see Fig. 4.5B). Low PC 1 scores characterize individuals with domed and narrow carapaces. In addition, marginal scutes are more steeply oriented than are pleural scutes. In contrast, high PC 1 scores characterize individuals with dorsoventrally flattened and wider carapaces. Additionally, the angle between marginal and pleural scutes is small (Fig. 4.5D). PC 2 depicts variation between short and thus more domed carapaces (low scores) and slightly elongated carapaces (high scores). Low scores for PC 1 and PC 2 correspond to morphologies displayed by "lentic" individuals, while high scores correspond to morphologies displayed by "lotic" individuals (Fig. 4.5D).

Results of a nested MANOVA using the first 25 shape variables (i.e., 95% of the variation in shape) for the eight focal populations indicated that there is a significant effect of flow (Wilks' Lambda: $F_{25,21}$=6.155, P<0.001) and site (Wilks' Lambda: $F_{150,130}$=2.032, P<0.001) on carapace shape. Univariate F-tests

identified five PCs that differed significantly between flow regimes at the 0.05-level (PCs 1-4, 11). These five PCs accounted for 60.6% of the total variation. Using the jackknifed results of a DFA (on the first 25 variables), turtles were correctly classified 83% of the time (lentic=78%, lotic=94%).

In order to examine the influence of each population on the function's overall ability to correctly classify the two groups, multiple DFA were performed on the dataset, each excluding one population at a time (Table 4.2). Concomitantly, individuals of each excluded population were coded as "unknowns" and were classified as belonging to either lentic or lotic morphotypes based on the remaining individuals (Table 4.2). Results show that the independent exclusion of two populations (Black Warrior River and Mobile River Delta) increased the rate at which individuals were classified correctly from 83% to 88% (Table 4.2). Furthermore, when treated as "unknowns", individuals from the Black Warrior River and Mobile River Delta were classified correctly 50% or less of the time (Table 4.2).

Plastrons of males

PCA of the Procrustes superimposed data for all nine sites (N=133) produced 26 PCs. Of these, the first 15 accounted for 95.4% of the total variation, while the first 21 accounted for 99.1% of the total variation. PC 1 (26.4%) and PC 2 (16.8%) accounted for a total of 43.2% of the total variation (Fig. 4.6A). In general, low scores for PC 1 describe a wide and dorsoventrally

flat plastron. In contrast, high scores for PC 1 depict a narrower plastron in which the anterior and posterior ends are angled upward, producing a more three-dimensional structure (Fig. 4.6C). Low PC 2 scores describe a wide plastron with the anterior and posterior edges slightly inclined. High scores for PC 2 indicate a narrower and dorsoventrally flattened plastron. Low scores for PC 1 and PC 2 correspond to morphologies displayed by "lentic" individuals, while high scores correspond to morphologies displayed by "lotic" individuals (Fig. 4.6C).

Results of a nested MANOVA using the first 15 shape variables (i.e., 95% of the variation in shape) indicated that there is a significant effect of flow (Wilks' Lambda: $F_{15,102}$=12.34, P<0.001) and site (Wilks' Lambda: $F_{90,580}$=4.216, P<0.001) on plastron shape. Univariate F-tests identified five PCs that differed significantly between flow regimes at the 0.05-level (PCs 1-3, 5, 9). These five PCs accounted for 63.5% of the total variation. Pearson correlation coefficients and significance values from a correlation analysis between the first three plastron PCs, which accounted for 54.4% of plastron variation, and the first five carapace PCs identified a number of significant correlations between shape variables of the carapace and plastron (Table 4.4). Using the jackknifed results of a DFA on the first 15 variables, turtles were correctly classified 78% of the time (lentic=77%, lotic=80%).

In order to examine the influence of each population on the function's overall ability to correctly classify the two groups, multiple DFA were performed

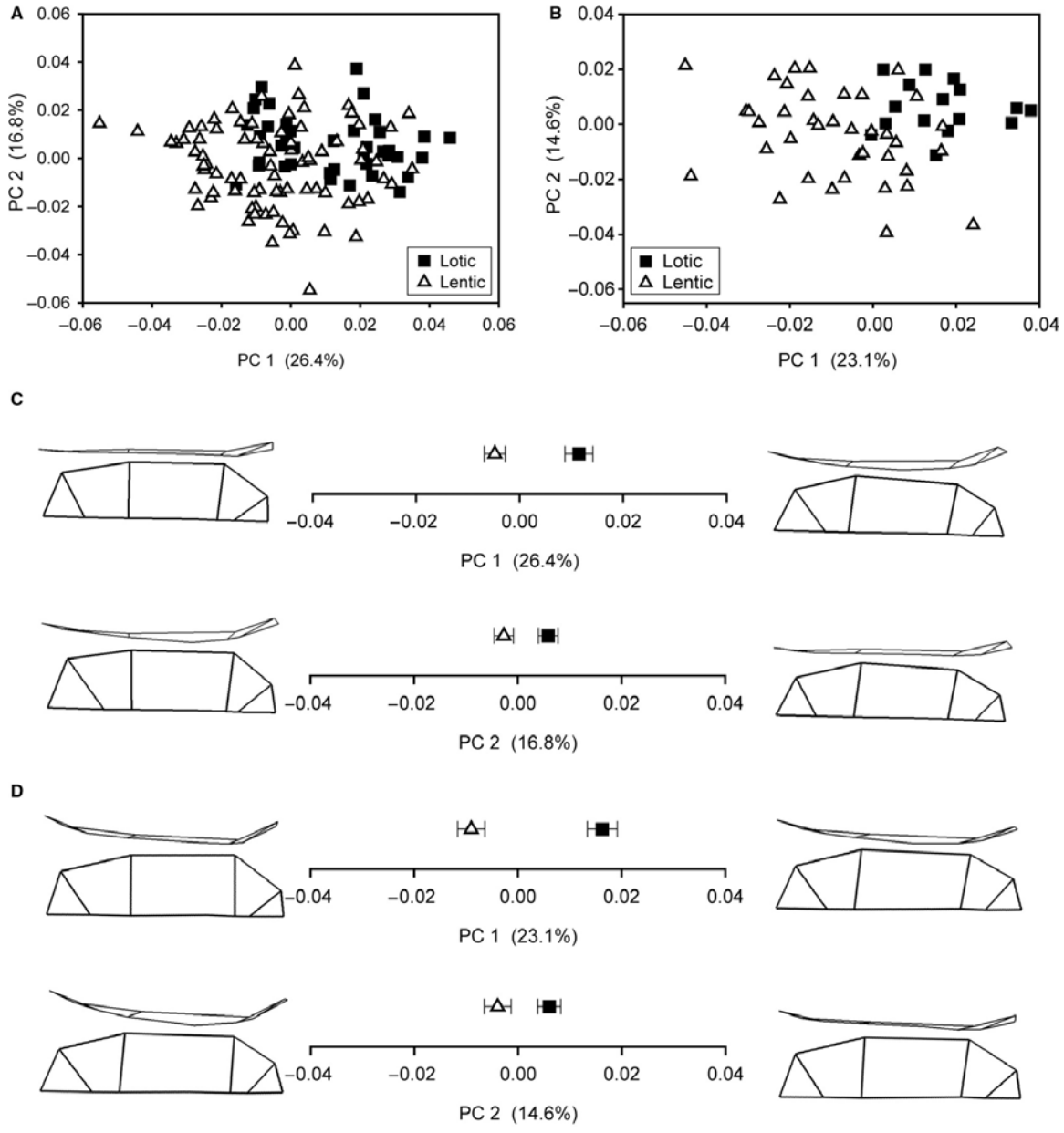
A
B
C
D
PC 2 (16.8%)
PC 1 (26.4%)
PC 2 (14.6%)
PC 1 (23.1%)
Lotic
Lentic
0.06
0.04
0.02
0.00
−0.02
−0.04
−0.06

Figure 4.6: Principal component analysis on the three-dimensional coordinates for the plastron. (A) First two principal components (PC 1 and PC 2) for males. (B) PC 1 and PC 2 for females. (C) Shape variation along PC 1 and PC 2 for males. (D) Shape variation along PC 1 and PC 2 for females. For C-D, turtle diagrams represent the extreme of each PC axis. Top image in each set represents the lateral (right-side) view of the plastron; bottom image represents the ventral view of the right side of the plastron. For all diagrams of shells, anterior is to the right. Symbols on the axis represent mean ± s.e. For A-D, open triangles represent turtles from lentic habitats; filled squares represent turtles from lotic habitats. Sample sizes are given in Table 4.1.

on the dataset, each excluding one population at a time (Table 4.2). Concomitantly, individuals of each excluded population were coded as "unknowns" and were classified as belonging to either lentic or lotic morphotypes based on the remaining individuals (Table 4.2). Results show that the exclusion of individuals from the Mobile River Delta population produced the largest increase in the rate at which individuals were classified correctly, from 78% to 90% (Table 4.2). Furthermore, when treated as "unknowns", individuals from the Mobile River Delta were correctly classified 31% of the time (Table 4.2).

Plastrons of females

PCA of the Procrustes superimposed data for all nine sites (N=63) produced 26 PCs. Of these, the first 15 accounted for 95.5% of the total variation, while the first 20 accounted for 99.0% of the total variation. PC 1 (23.1%) and PC2 (14.6%) accounted for a total of 37.7% of the total variation (Fig. 4.6B). Low PC 1 scores for the plastrons of females describe a wide

plastron with inclined anterior and posterior ends; the anterior end is inclined to a greater degree. In contrast, high PC 1 scores characterize individuals with narrower, longer, and more dorsoventrally flattened plastrons (Fig. 4.6D). PC 2 depicts variation between plastrons with a strongly inclined anterior end and a weakly inclined posterior end (low scores) and dorsoventrally flattened plastrons (high scores). Low scores for PC 1 and PC 2 correspond to morphologies displayed by "lentic" individuals, while high scores correspond to morphologies displayed by "lotic" individuals (Fig. 4.6D).

Results of a nested MANOVA using the first 15 shape variables indicated a significant effect of flow (Wilks' Lambda: $F_{15,32}$=6.453, P<0.001) and site (Wilks' Lambda: $F_{90,186}$=2.321, P<0.001) on plastron shape. Univariate F-tests identified two PCs that differed significantly between flow regimes at the 0.05-level (PCs 1-2). Pearson correlation coefficients and significance values from a correlation analysis between the first three plastron PCs, which accounted for 51.0% of plastron variation, and the first five carapace PCs identified a number of significant correlations between shape variables of the carapace and plastron (Table 4.4). Using jackknifed results of a DFA on the first 15 variables, turtles were correctly classified 83% of the time (lentic=82%, lotic=88%). In order to examine the influence of each population on the function's overall ability to correctly classify the two groups, multiple DFA were performed on the dataset, each excluding one population at a time (Table 4.2). Concomitantly, individuals of each excluded population were coded as "unknowns" and were classified

Table 4.4: Pearson correlation values for carapace and plastron PCs (cPC1-5 versus pPC1-3)

	cPC1	cPC2	cPC3	cPC4	cPC5
Male					
pPC1	0.51**	0.26**	-0.02	0.27**	0.29**
pPC2	-0.21*	0.60**	-0.01	-0.18*	-0.22*
pPC3	0.19*	0.28**	0.10	-0.13	0.28**
Female					
pPC1	0.07	0.61**	-0.38**	0.03	0.33**
pPC2	0.25	-0.06	-0.05	0.18	0.04
pPC3	0.21	-0.02	0.13	-0.11	0.44**

cPC = PC value for carapace; pPC = PC value for plastron
*Denotes P-values <0.05; **Denotes P-values <0.01
Sample size (N) = 129 for males and 61 for females

as belonging to either lentic or lotic morphotypes based on the remaining individuals (Table 4.2). Results show that the exclusion of individuals from the Mobile River Delta population produced the largest increase in the rate at which individuals were classified correctly, from 83% to 87% (Table 4.2). Furthermore, when treated as "unknowns", individuals from the Mobile River Delta were correctly classified 67% of the time (Table 4.2).

Turtles from Reelfoot Lake

In order to classify Reelfoot Lake specimens into either lentic or lotic morphotypes, multiple DFA were performed on the four datasets (Table 4.3). Specimens from Reelfoot Lake were coded as "unknowns" and were classified as belonging to either lentic or lotic morphotypes based on the populations included in the analysis. The initial analyses, which used PCs accounting for

Table 4.3: Classification of Reelfoot Lake specimens using DFA

	Jackknifed (Known)						Reelfoot Lake	
Model	Lentic (N)	Lentic (% Correct)	Lotic (N)	Lotic (% Correct)	N	Total (% Correct)	Lentic	Lotic
All populations (95% PCs)								
Male carapace	87	92	41	90	128	91	5	4
Female carapace	37	78	16	94	53	83	7	3
Male plastron	84	77	40	80	124	78	4	5
Female plastron	38	82	16	88	54	83	4	5
All populations (sig PCs)								
Male carapace	87	84	41	85	128	84	2	7
Female carapace	37	84	16	75	53	81	6	4
Male plastron	84	77	40	88	124	81	7	2
Female plastron	38	87	16	88	54	87	2	7
MRD excluded (sig PCs)								
Male carapace	52	90	41	93	93	91	0	9
Female carapace	27	89	16	88	43	88	3	7
Male plastron	52	88	40	88	92	88	5	4
Female plastron	29	86	16	88	45	87	2	7
BWR excluded (sig PCs)								
Male carapace	87	98	23	100	110	98	6	3
Female carapace	37	86	12	83	49	86	7	3
Male plastron	84	80	22	91	106	82	7	2
Female plastron	38	87	12	83	50	86	2	7

Table 4.3, continued

	Jackknifed (Known)						Reelfoot Lake	
Model	**Lentic (N)**	**Lentic (% Correct)**	**Lotic (N)**	**Lotic (% Correct)**	**N**	**Total (% Correct)**	**Lentic**	**Lotic**
MRD & BWR excluded (sig PCs)								
Male carapace	52	100	23	100	75	100	2	7
Female carapace	27	96	12	100	39	97	4	6
Male plastron	52	96	22	95	74	96	5	4
Female plastron	29	86	12	83	41	27	2	7

N=number of actual individuals in this category

Tests using “95% PCs” were conducted on the sequential set of PCs (starting with PC 1) whose cumulative total was 95% of the variation; see text for details.

Tests using “sig PCs” were conducted on the PCs that were significant based on univariate tests; see text for details

MRD=Mobile River Delta; BWR=Black Warrior River

95% of the morphological variation and included all populations, did not produce clear results. Subsequent analyses using only the PCs identified as significant in the univariate tests identified a pattern suggesting that specimens from Reelfoot Lake are more similar to turtles from lotic habitats than lentic habitats (Table 4.3).

Measurements of drag

Specimens from Coon Creek Lake (lentic) and Tallapoosa River (lotic) were selected to represent the lentic and lotic morphotype, respectively. These two sites were selected based on their DFA classification for carapace (100% correct; see Table 4.2). The specimen from Coon Creek Lake (UTA 20875; CL=22.3 cm) had a frontal area of 0.0064 m^2 and a C_D=0.56. The specimen from Tallapoosa River (AUM 34147; CL=18.1) had a frontal area of 0.0042 m^2 and a C_D=0.27. When both specimens were scaled to the same size (CL=22.3 cm), frontal area for both was 0.0064 m^2. These results indicate that the shells of turtles inhabiting lotic environments incur considerably less drag than do those of turtles inhabiting lentic environments. The difference in carapace shape and the effects of flow velocity on drag for the two specimens are given in Figure 4.7.

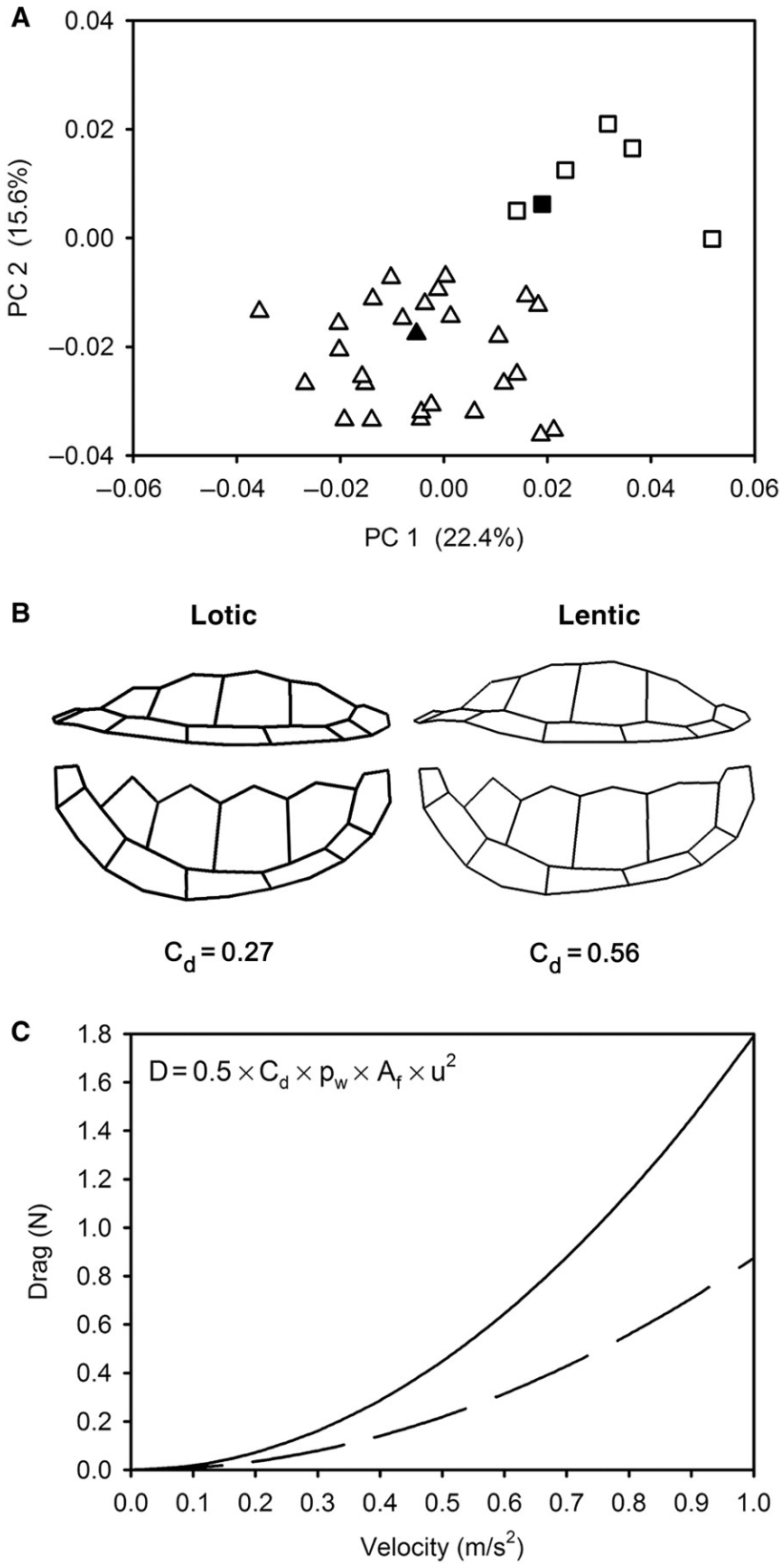
A
0.04
0.02
0.00
–0.02
–0.04
PC 2 (15.6%)
–0.06
–0.04
–0.02
0.00
0.02
0.04
0.06
PC 1 (22.4%)
B
Lotic
Lentic
$C_d = 0.27$
$C_d = 0.56$
C
$D = 0.5 \times C_d \times p_w \times A_f \times u^2$
Drag (N)
1.8
1.6
1.4
1.2
1.0
0.8
0.6
0.4
0.2
0.0
0.0 0.1 0.2 0.3 0.4 0.5 0.6 0.7 0.8 0.9 1.0
Velocity (m/s^2)

Figure 4.7: Measurements of drag. (A) PC 1 and PC 2 for male carapaces. Open triangles represent individuals from Coon Creek Lake (lentic); open squares represent individuals from Tallapoosa River (lotic). Filled triangle and square represent the individuals most similar to the mean shape of their respective population, which were therefore used to make models. (B) Diagrams of turtles indicating the shape of the carapace for the lentic and lotic models. Top image in each set represents the lateral (right-side) view of the carapace; bottom image represents the dorsal view of the right side of the carapace. (C) The relationship between flow velocity and incurred drag (*D*). Plots are generated based on turtles of the same size (CL=22.3 cm; A_f=0.0064 m^2; see text) and using the respective drag coefficients. The lentic (solid line) and lotic (dashed line) models incur similar levels of drag at low speeds, but at a speed of 1.0 m s^{-1}, drag incurred by the lentic model is approximately twice that of the lotic model.

Discussion

Morphological variation

For both sexes of *Pseudemys concinna*, the carapace and plastron show significant morphological differences between lentic and lotic flow regimes. In general, the most prominent difference between the flow regimes in both male and female carapaces is that the shells of individuals from lotic habitats are more streamlined (i.e., lower height-to-length ratio) than are those of individuals from lentic habitats. Variation in carapace shape, particularly height of the shell, was achieved in two different ways. Among males, flattened (i.e., streamlined) carapaces are achieved by either (1) decreasing the width of vertically oriented pleural scutes, or by (2) decreasing the inclination angle of wider pleural scutes. In addition, the former method generates narrower carapaces, while the latter produces wider carapaces. For females, streamlined shells are generated through a series of small changes that either flatten or lengthen the carapace.

Differences in overall shape of the plastron are more subtle. For males, individuals from lentic habitats tend to have wider plastrons, although in some cases the posterior end of plastrons of individuals from lotic habitats appeared to widen relative to the anterior end (high PC 1 scores). In addition, there is variation in the orientation of the anterior end of the plastron, although no consistent morphology is apparent among males. Among females the plastron also tends to be wider in individuals from lentic habitats. In addition, females also display variation in the orientation of the anterior end of the plastron; however, among females a consistent pattern is observed. The anterior edge of the plastron of females from lentic habitats is strongly angled upward, whereas the anterior edge of the plastron of females from lotic habitats is generally flatter.

Of the two shell components, the carapace appears to be more divergent (between the two flow regimes) than the plastron, based on the ability of DFA to correctly assign individuals to their respective flow regime (Tables 4.2 and 4.3). These results are consistent with adaptations to flow velocity, since variation in the shape of the carapace is more likely to affect hydrodynamics, particularly drag. The curved carapace encounters high pressures anteriorly and low pressures posteriorly, generating a large pressure drag; in contrast, the flat plastron has minimal influence on pressure drag. In addition, the carapace is the larger of the two structures, and thus, the larger surface area of the carapace relative to that of the plastron increases friction drag, which occurs at the interface between the shell and fluid (Vogel, 2003). Furthermore, these results

are also consistent with those of (Claude et al., 2003), who found that for two major clades of turtles, the carapace exhibits similar differences in shape between aquatic and terrestrial environments but the plastron does not. These findings suggest that for aquatic turtles, forces producing differences in shape act more strongly on carapace shape than on plastron shape.

Moreover, the results of correlation analyses suggest that the significant effect of flow regime on plastron shape might be the result of correlated changes between the carapace and plastron (Lande and Arnold, 1983). For instance, males with wider carapaces also tended to have wider plastrons (e.g., cPC 1 vs pPC 2, cPC 2 vs pPC 2, cPC 2 vs pPC 1; Table 4.4). For males, the correlation between the first three plastron PCs and the first five carapace PCs, indicated that 11 of the possible 15 correlations were significant. The same pattern may explain differences observed among females (e.g., wider carapace correlated with wider plastron: cPC 2 vs pPC 1), although fewer significant correlations exist. However, because the anterior edge of the plastron does not form contact points with the carapace, variation in the angle of the anterior edge of the plastron does not appear to be based on correlated changes.

The results also indicate that the level of morphological divergence differs between the sexes; habitat-associated differences are more distinct in carapaces of males than in those of females, while the plastrons of males and females show equivalent levels of divergence. This suggests that variation in carapace shape may be more constrained in females than in males. Factors associated with

reproductive biology (e.g., space available for eggs; Rowe, 1994; Tucker et al., 1998) and more complex modes of inheritance (Wayne et al., 2007) might limit morphological divergence in females.

Atypical populations

In addition to using DFA to examine the level of habitat-associated morphological divergence among the four structures (i.e., male carapace, female carapace, male plastron, and female plastron), a set of additional analyses examined the effects of excluding each population from the full dataset. Furthermore, I tested the ability of each model to correctly classify the excluded group to its respective flow regime. Of the 32 tests conducted (four structures and eight populations), there were nine cases in which the excluded groups were correctly classified at a rate of 50% or less (Table 4.2). Seven of these cases were from two populations, four from Black Warrior River (BWR) and three from Mobile River Delta (MRD). The ability of the model to correctly classify male carapaces increased from 91% to 97% when BWR was excluded and increased to 94% when the MRD was excluded. However, it increased to 100% when both BWR and MRD were excluded. Based on the variation in shape described by PCs 1 and 2, the BWR population is contiguous with the other lotic populations but falls within a zone of overlap between individuals from lentic and lotic habitats (Figs. 4.5 and 4.8). In contrast, individuals from MRD display both lentic and lotic morphotypes (Figs. 4.5 and 4.8). There are two possible reasons for the high

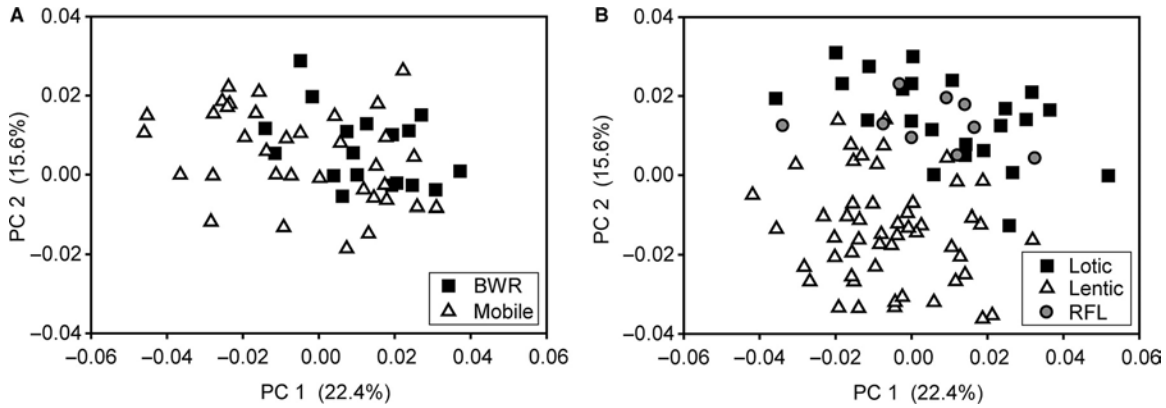

Figure 4.8: Principal component analysis on the three-dimensional coordinates for the carapace. First two principle components for males. (A) Positions of the lentic Mobile River Delta (open triangles) and lotic Black Warrior River (filled squares). Plot of PC scores indicates considerable overlap between the two populations and peculiarly high PC 2 scores for Mobile River Delta. (B) Position of Reelfoot Lake individuals relative to lentic and lotic populations. Black Warrior River and Mobile River Delta have been excluded for clarity. Symbols are open triangles (lentic), filled squares (lotic), and shaded circles (Reelfoot Lake). Sample sizes are given in Table 4.1.

morphological variance of MRD turtles. First, it is possible that selection pressure is weaker in lentic habitats, thus allowing for a broader range of morphologies. Selection for drag-reducing morphologies should be lower in lentic habitats because drag increases exponentially with water velocity. However, the other three lentic habitats do not display such a high level of morphological variation. A second possibility is that turtles from lotic habitats above the Fall Line have been displaced downstream and that gene flow from lotic to lentic habitats is responsible for the high variability in shape among turtles from MRD. The four lotic habitats examined in this study each eventually drain into the Mobile Bay through the Mobile River Delta. Each lotic site is several hundred miles from the Mobile River Delta, and while it is unlikely that turtles

from the Mobile River could reach the lotic sites due to the distance and energy required to swim against flow, the flow of water could assist in the displacement of turtles downstream. This hypothesis can be tested using genetic markers for each population (i.e., microsatellites; Hankison and Ptacek, 2008) to examine the direction (upstream vs. downstream) and intensity of gene flow between each of the four lotic sites and the Mobile River Delta.

Turtles of Reelfoot Lake

As previously noted, recent historical events have allowed turtles from the lotic Mississippi River to migrate into the lentic Reelfoot Lake. While 200 years is likely too short a time for natural selection to effect changes on shell morphology for such a long-lived animal, this habitat transition provides the opportunity to test for effects of phenotypic plasticity. The premise for such tests is that if turtles from this population display the lotic morphotype, then plasticity is not a major factor determining morphology. However, if Reelfoot Lake specimens are more similar to lentic morphotypes, this would provide support for the importance of plasticity in the determination of shape. I used several DFA models to classify the Reelfoot Lake specimens as “lentic” or “lotic” (Table 4.3). Classifications based on all populations and the full complement of shape variables (i.e., 95% variation) were inconclusive. However, subsequent DFA models using only significant variables (as determined by MANOVA; see results) provided rather consistent results. Overall, these four tests (Table 4.3) found that the rate of

classification as “lotic” for the four structures was as follows: male carapaces, 72%; female carapaces, 50%; male plastrons, 33%; and female plastrons, 78%. When the classification was based on only the significant PCs with the Mobile River Delta (MRD) and Black Warrior River (BWR) populations excluded, the overall rate of classification as “lotic” was higher, but is consistent with the aforementioned average results: male carapace, 78%; female carapace, 60%; male plastron, 44%; and female plastrons, 78%. Because the ability to correctly classify unknown specimens was highest when the MRD and BWR populations were excluded, subsequent comments are based on these results (Fig. 4.8; Table 4.3). These results indicate that specimens from Reelfoot Lake display morphologies most similar to the examined “lotic” populations, suggesting that while phenotypic plasticity may play a role in the variation in shape between the two flow regimes, it is likely less than the contribution of genetic divergence. Still, laboratory studies that simultaneously examine the influence of genetic divergence and plasticity on differences in shell shape are required (Keeley et al., 2007; Langerhans, 2008).

Effects of shape on drag

The measurement of drag from models indicates that habitat-associated morphological differences in the shells of turtles do have substantial effects on hydrodynamic characteristics. The drag coefficient (C_D=0.27) of turtles from lotic habitats is approximately half that (C_D=0.56) of turtles from lentic ones, meaning

that for turtles of the same size and a particular swimming speed, the lotic morphotype only incurs half the resistance. Moreover, these values were calculated from the individuals that represented the two population means (Coon Creek Lake and Tallapoosa River; see Fig. 4.7). Based on the variation in shape described by PCs 1 and 2 (Fig. 4.7), there are other lentic-lotic pairs that display considerably more morphological divergence, suggesting that larger differences in drag (C_D) may be observed among individuals; this is important because selection acts on the performance of individuals. Finally, because the two models had the same frontal area when scaled to the same size (CL), the results provide an even more accurate estimate of differences in drag associated with shape.

Alternative Hypotheses

Geographic variation

While I identified significant morphological differences between populations from lentic and lotic habitats, it should be noted that these results also follow a geographic pattern – all four lotic populations were from eastern sites (i.e., east of the Mississippi River), while three of the four lentic populations were from western sites (i.e., west of the Mississippi River). While this could seem to suggest that an east-to-west trend in shell shape (i.e., shells of turtles are flat in the east and become more domed in the west) is responsible for the pattern observed in this study, data from Seidel and Palmer (1991) shows that

this is not the case. Seidel and Palmer (1991) determined that *Pseudemys concinna* from central Atlantic drainages were significantly more domed (shell height/carapace length; sensu Aresco and Dobie, 2000) in the Piedmont than in the Coastal Plain. Within the Atlantic drainages, the Piedmont is located in the west and the Coastal Plain in the east. The findings of Seidel and Palmer (1991) for turtles within Atlantic drainages are consistent with results from Aresco and Dobie (2000) and those presented in this paper for turtles within Gulf drainages, in that turtles inhabiting lotic sites in the Piedmont of the Appalachian Mountains (on the eastern or western slopes) possess flattened morphologies, whereas those inhabiting lentic sites in the adjacent Coastal Plains (in the Atlantic or Gulf drainages) are more domed. This demonstrates that the pattern is not simply a longitudinal trend, and provides additional support for the assertion that differences in flow velocity, which are associated with differences in elevational gradients, are the driving force that has produced the observed morphological variation.

Predation

Aresco and Dobie (2000) proposed two hypotheses to explain morphological divergence between lentic and lotic flow regimes: (1) enhanced hydrodynamics in lotic populations and (2) stronger shells that reduce alligator predation in lentic environments. Previous studies have examined relationships between flow and predator regimes in other vertebrates and invertebrates and

found that predation can influence differences in shape (Langerhans and DeWitt, 2004; Holomuzki and Biggs, 2006). It is difficult to specifically test these hypotheses for *Pseudemys concinna* for two reasons. First, alligators do not inhabit lotic flow regimes, and second, alligators and *P. concinna* are sympatric in most lentic habitats. Nevertheless, here I propose that available evidence suggests that flow, rather than predation, is responsible for the observed morphological variation. First, lotic morphotypes are found in lentic habitats (e.g., MRD); however, lentic morphotypes are completely excluded from lotic populations. If flow had no effect, domed turtles should be observed inhabiting both flow regimes. Second, the results of the drag tests indicated a significant reduction in drag for turtles inhabiting lotic flow regimes compared to those inhabiting lentic flow regimes. These results are also likely to be conservative, with respect to maximum drag reduction, as they were calculated using "mean specimens", rather than being collected separately for each individual. As such, morphological differences between the two models were smaller than morphological differences between individuals at the extremes, suggesting that some "lotic" turtles may have even lower drag coefficients. In addition, (Lubcke and Wilson, 2007) found a similar pattern of flow-correlated shape variation for a different species of turtle (*Actinemys marmorata*) in a system without a major predator dichotomy. Moreover, it is unknown whether the observed differences in shell shape would increase the strength of the shell, or if any increase would be large enough to resist an alligator attack. Furthermore, any advantage

conferred by a change in shell shape would likely only be advantageous to larger individuals that are too big to be swallowed whole. Future studies should combine data on the forces exerted on the shells of turtles during attacks by alligators, collected from models of adult turtles subjected to alligator bites, and computational methods (e.g., finite element analysis) to examine the ability of shells of different shapes to withstand attacks.

Conclusion

This study demonstrates that *Pseudemys concinna* shows significant divergence in three-dimensional shell shape between lentic and lotic flow regimes across a wide geographic range. In addition, significant differences were detected for the carapace and plastron of both sexes, with the level of morphological divergence being greater for the carapace. Using geometric morphometrics I was able to describe the manner in which changes in shell shape have occurred. This study provides the first empirical evidence for an adaptive benefit (i.e., drag reduction) of the observed difference in shape. Finally, preliminary information collected from the Reelfoot Lake population suggests that phenotypic plasticity plays a limited role in shape variation between the flow regimes. While this study provides answers for many questions not addressed in earlier studies, it also generated several new ones. To better understand the ecomorphological divergence identified in this study, future studies should address several issues, including: (1) reproductive output

between females from lentic and lotic habitats, (2) the cause of the increased shape variation observed in the Mobile River Delta population, and (3) the relative effect of genetic and environmental factors on shape.

Acknowledgments

I am grateful to S. Rogers and B. Isaac (Carnegie Museum of Natural History), C. Guyer (Auburn University Natural History Museum), C. Franklin (Amphibian and Reptile Diversity Research Center, University of Texas, Arlington), R. Brown (University of Kansas Natural History Museum), C. Austin (Louisiana State University Museum of Natural Science), and H. Dundee (Tulane University Museum of Natural History) for providing specimens. I thank C. Guyer, H. Dundee, C. Roelke, and L. Hunt for providing accommodations during research trips. I also thank R. Blob, M. Ptacek, M. Childress, I. Bartol, and A. Rivera for helpful discussions. I am also grateful to A. Rivera for providing assistance assembling the figures. Comments by R. Blob, I. Bartol, A. Rivera, and two anonymous reviewers helped to improve upon an earlier draft of this paper. Finally, I thank R. Blob for his support and assistance with organizing this symposium. This work was supported by NSF (IOB-0517340), a SICB Grant-in-Aid-of-Research, an American Museum of Natural History Theodore Roosevelt Memorial Award, and the Clemson University Department of Biological Sciences. I am also grateful for support of this symposium provided by SICB (DCB, DEE,

DIZ and DVM), Vision Research (www.visionresearch.com), EmicroScribe (www.emicroscribe.com), and NSF (IOS-0733441).

Literature Cited

Adams, D. C. and Collyer, M. L. (2007). Analysis of character divergence along environmental gradients and other covariates. *Evolution*, 510-515.

Adams, D. C. and Rohlf, F. J. (2000). Ecological character displacement in *Plethodon*: biomechanical differences found from a geometric morphometric study. *PNAS* **97**, 4106-4111.

Aresco, M. J. and Dobie, J. L. (2000). Variation in shell arching and sexual size dimorphism of river cooters, *Pseudemys concinna*, from two river systems in Alabama. *Journal of Herpetology* **34**, 313-317.

Bartol, I. K., Gharib, M., Webb, P. W., Weihs, D. and Gordon, M. S. (2005). Body-induced vortical flows: a common mechanism for self-corrective trimming control in boxfishes. *Journal of Experimental Biology* **208**, 327-344.

Bartol, I. K., Gharib, M., Weihs, D., Webb, P. W., Hove, J. R. and Gordon, M. S. (2003). Hydrodynamic stability of swimming in ostraciid fishes: role of the carapace in the smooth trunkfish *Lactophrys triqueter* (Teleostei: Ostraciidae). *Journal of Experimental Biology* **206**, 725-744.

Blob, R. W., Bridges, W. C., Ptacek, M. B., Maie, T., Cedie, R. A., Bertolas, M. M., Julius, M. L. and Schoenfuss, H. L. (2008). Morphological selection in an extreme flow environment: body shape and waterfall-climbing success in the Hawaiian stream fish *Sicyopterus stimpsoni*. *Integrative and Comparative Biology* **48**, 734-749.

Boily, P. and Magnan, P. (2002). Relationship between individual variation in morphological characters and swimming costs in brook charr (*Salvelinus fontinalis*) and yellow perch (*Perca flavescens*). *Journal of Experimental Biology* **205**, 1031-1036.

Boller, M. L. and Carrington, E. (2006). The hydrodynamic effects of shape and size change during reconfiguration of a flexible macroalga. *Journal of Experimental Biology* **209**, 1894-1903.

Bookstein, F. L. (1996). Combining the tools of geometric morphometrics. In *Advances in Morphometrics*, eds. L. F. Marcus M. Corti A. Loy G. J. P. Naylor and D. E. Slice), pp. 131-151. New York: Plenum Press.

Brinsmead, J. and Fox, M. G. (2002). Morphological variation between lake- and stream-dwelling rock bass and pumpkinseed populations. *Journal of Fish Biology* **61**, 1619-1638.

Bronmark, C. and Miner, J. G. (1992). Predator-induced phenotypical change in body morphology in crucian carp. *Science* **258**, 1348-1350.

Brookes, J. I. and Rochette, R. (2007). Mechanism of a plastic phenotypic response: predator-induced shell thickening in the intertidal gastropod *Littorina obtusata*. *Journal of Evolutionary Biology* **20**, 1015-1027.

Buhlmann, K. A. and Vaughan, M. R. (1991). Ecology of the turtle *Pseudemys concinna* in the New River, West Virginia. *Journal of Herpetology* **25**, 72-78.

Carrington, E. (2002). Seasonal variation in the attachment strength of blue mussels: causes and consequences. *Limnology and Oceanography* **47**, 1723-1733.

Claude, J., Paradis, E., Tong, H. and Auffray, J. C. (2003). A geometric morphometric assessment of the effects of environment and cladogenesis on the evolution of the turtle shell. *Biological Journal of the Linnean Society* **79**, 485-501.

Denny, M. W., Nelson, E. K. and Mead, K. S. (2002). Revised estimates of the effects of turbulence on fertilization in the purple sea urchin, *Strongylocentrotus purpuratus*. *Biological Bulletin* **203**, 275-277.

DeWitt, T. J., Sih, A. and Wilson, D. S. (1998). Costs and limits of phenotypic plasticity. *Trends in Ecology & Evolution* **13**, 77-81.

Eklov, P. and Svanback, R. (2006). Predation risk influences adaptive morphological variation in fish populations. *American Naturalist* **167**, 440-452.

Ernst, C. E., Lovich, J. E. and Barbour, R. W. (1994). Turtles of the United States and Canada. Washington DC: Smithsonian Institution Press.

Fahey, K. M. (1987). Aspects of the life history of the river cooter, *Pseudemys concinna* (Le Conte), in the Tallapoosa River, Tallapoosa County, Alabama. *Unpubl Ph.D Dissertation, Auburn Univ, Auburn, Alabama*.

Gibbins, C., Vericat, D. and Batalla, R. J. (2007). When is stream invertebrate drift catastrophic? The role of hydraulics and sediment transport in initiating drift during flood events. *Freshwater Biology* **52**, 2369-2384.

Gibbons, J. W. and Lovich, J. E. (1990). Sexual dimorphism in turtles with emphasis on the slider turtle (*Trachemys scripta*). *Herpetological Monographs* **4**, 1-29.

Grant, P. R. and Grant, B. R. (2006). Evolution of character displacement in Darwin's finches. *Science* **313**, 224-226.

Hankison, S. J. and Ptacek, M. B. (2008). Geographical variation of genetic and phenotypic traits in the Mexican sailfin mollies, *Poecilia velifera* and *P. petenensis*. *Molecular Ecology* **17**, 2219-2233.

Holomuzki, J. R. and Biggs, B. J. F. (2006). Habitat-specific variation and performance trade-offs in shell armature of New Zealand mudsnails. *Ecology* **87**, 1038-1047.

Imre, I., McLaughlin, R. L. and Noakes, D. L. G. (2002). Phenotypic plasticity in brook charr: changes in caudal fin induced by water flow. *Journal of Fish Biology* **61**, 1171-1181.

Keeley, E. R., Parkinson, E. A. and Taylor, E. B. (2005). Ecotypic differentiation of native rainbow trout (*Oncorhynchus mykiss*) populations from British Columbia. *Canadian Journal of Fisheries and Aquatic Sciences* **62**, 1523-1539.

Keeley, E. R., Parkinson, E. A. and Taylor, E. B. (2007). The origins of ecotypic variation of rainbow trout: a test of environmental vs. genetically based differences in morphology. *Journal of Evolutionary Biology* **20**, 725-736.

Kerfoot Jr., J. R. and Schaefer, J. R. (2006). Ecomorphology and habitat utilization of *Cottus* species. *Environ Biol Fish* **76**, 1-13.

Koehl, M. (2003). Physical modeling in biomechanics. *Philosophical Transactions of the Royal Society of London B Biological Sciences* **358**, 1589-1596.

Koehl, M. A. R., Silk, W. K., Liang, H. and Mahadevan, L. (2008). How kelp produce blade shapes suited to different flow regimes: A new wrinkle. *Integrative and Comparative Biology* **48**, 834-851.

Lande, R. and Arnold, S. J. (1983). The measurement of selection on correlated characters. *Evolution* **37**, 1210-1226.

Langerhans, R. B. (2008). Predictability of phenotypic differentiation across flow regimes in fishes. *Integrative and Comparative Biology* **48**, 750-768.

Langerhans, R. B. and DeWitt, T. J. (2004). Shared and unique features of evolutionary diversification. *American Naturalist* **164**.

Lubcke, G. M. and Wilson, D. S. (2007). Variation in shell morphology of the western pond turtle (*Actinemys marmorata* Baird and Girard) from three aquatic habitats in northern California. *Journal of Herpetology* **41**, 107-114.

Marchinko, K. B. (2003). Dramatic phenotypic plasticity in barnacle legs (*Balanus glandula* Darwin): magnitude, age dependence, and speed of response. *Evolution* **57**, 1281-1290.

McGuigan, K., Franklin, C. E., Moritz, C. and Blows, M. W. (2003). Adaptation of rainbow fish to lake and stream habitats. *Evolution* **57**, 104-118.

Milano, D., Cussac, V. E., Macchi, P. J., Ruzzante, D. E., Alonso, M. F., Vigliano, P. H. and Denegri, M. A. (2002). Predator associated morphology in *Galaxias platei* in Patagonian lakes. *Journal of Fish Biology* **61**, 138-156.

Mirecki, J. E. (1996). Recognition of the 1811-1812 New Madrid earthquakes in Reelfoot Lake, Tennessee sediments using pollen data. *Journal of Paleolimnology* **15**, 183-191.

Myers, E. M., Janzen, F. J., Adams, D. C. and Tucker, J. K. (2006). Quantitative genetics of plastron shape in slider turtles (*Trachemys scripta*). *Evolution* **60**, 563-572.

Ojanguren, A. F. and Brana, F. (2003). Effects of size and morphology on swimming performance in juvenile brown trout (*Salmo trutta* L.). *Ecology of Freshwater Fish* **12**, 241-246.

Okamura, B. (1984). The effects of ambient flow velocity, colony size, and upstream colonies on the feeding success of Bryozoa.1. *Bugula stolonifera* Ryland, an arborescent species. *Journal of Experimental Marine Biology and Ecology* **83**, 179-193.

Okamura, B. (1985). The effects of ambient flow velocity, colony size, and upstream colonies on the feeding success of Bryozoa.2. *Conopeum reticulum* (Linnaeus), an encrusting species. *Journal of Experimental Marine Biology and Ecology* **89**, 69-80.

Pace, C. M., Blob, R. W. and Westneat, M. W. (2001). Comparative kinematics of the forelimb during swimming in red-eared slider (*Trachemys scripta*) and spiny softshell (*Apalone spinifera*) turtles. *The Journal of Experimental Biology* **204**, 3261-3271.

Pakkasmaa, S. and Piironen, J. (2001). Water velocity shapes juvenile salmonids. *Evolutionary Ecology* **14**, 721-730.

Peres-Neto, P. R. and Magnan, P. (2004). The influence of swimming demand on phenotypic plasticity and morphological integration: a comparison of two polymorphic charr species. *Oecologia* **140**, 36-45.

Pfennig, D. W., Rice, A. M. and Martin, R. A. (2006). Ecological opportunity and phenotypic plasticity interact to promote character displacement and species coexistence. *Ecology* **87**, 769-779.

Pratt, M. C. (2008). Living where the flow is right: How flow affects feeding in bryozoans. *Integrative and Comparative Biology* **48**, 808-822.

Puijalon, S. and Bornette, G. (2004). Morphological variation of two taxonomically distant plant species along a natural flow velocity gradient. *New Phytologist* **163**, 651-660.

Riffell, J. A. and Zimmer, R. K. (2007). Sex and flow: the consequences of fluid shear for sperm-egg interactions. *Journal of Experimental Biology* **210**, 3644-3660.

Rivera, G. and Claude, J. (2008). Environmental media and shape asymmetry: a case study on turtle shells. *Biological Journal of the Linnean Society* **94**, 483-489.

Rivera, G., Rivera, A. R. V., Dougherty, E. E. and Blob, R. W. (2006). Aquatic turning performance of painted turtles (*Chrysemys picta*) and functional consequences of a rigid body design. *Journal of Experimental Biology* **209**, 4203-4213.

Rohlf, F. J. and Marcus, L. F. (1993). A revolution in morphometrics. *Trends in Ecology & Evolution* **8**, 129-132.

Rohlf, F. J. and Slice, D. (1990). Extensions of the Procrustes method for the optimal superimposition of landmarks. *Systematic Zoology* **39**, 40-59.

Rowe, J. W. (1994). Reproductive variation and the egg size clutch size tradeoff within and among populations of painted turtles (*Chrysemys picta bellii*). *Oecologia* **99**, 35-44.

Slice, D. E. (2001). Landmark coordinates aligned by Procrustes analysis do not lie in Kendall's shape space. *Systematic Biology* **50**, 141-149.

Slice, D. E. (2005). Modern Morphometrics. In *Modern Morphometrics in Physical Antrhopology*, (ed. D. E. Slice), pp. 1-45. Vienna: Kluwer Academic.

Stewart, H. L. (2008). The role of spatial and ontogenetic morphological variation in the expansion of the geographic range of the tropical brown alga, Turbinaria ornata. *Integrative and Comparative Biology* **48**, 713-719.

Tucker, J. K., Janzen, F. J. and Paukstis, G. L. (1998). Variation in carapace morphology and reproduction in the red-eared slider *Trachemys scripta elegans*. *Journal of Herpetology* **32**, 294-298.

Valenzuela, N., Adams, D. C., Bowden, R. M. and Gauger, A. C. (2004). Geometric morphometric sex estimation for hatchling turtles: a powerful alternative for detecting subtle sexual shape dimorphism. *Copeia* **2004**, 735-742.

Vogel, S. (2003). Comparative Biomechanics: Life's Physical World. Princeton: Princeton University Press.

APPENDICES

Appendix A

List of *Pseudemys concinna* Museum Specimens

Abbreviations

AUM: Auburn University Natural History Museum
CM: Carnegie Museum of Natural History
KU: University of Kansas Natural History Museum
LSU: Louisiana State University Museum of Natural Science
UTA: Amphibian and Reptile Diversity Research Center, University of Texas, Arlington

* Specimen for which only the carapace was examined
† Specimen for which only the plastron was examined

Males

Coon Creek Lake:
UTA20847, UTA20848, UTA20860, UTA20861, UTA20863, UTA20864, UTA20866, UTA20867, UTA20868, UTA20870, UTA20871, UTA20872, UTA20873, UTA20874, UTA20875, UTA20876, UTA20878, UTA20879, UTA20880, UTA20881, UTA20882, UTA20883, UTA20884, UTA20885, UTA20886, UTA20887, UTA20888*

Southern LA:
LSU38922, LSU43389, LSU43392, LSU74814*, LSU74816, LSU74817, LSU74818, LSU74825, LSU74827†, LSU74828, LSU75195, LSU75206, LSU75212, LSU81453, LSU84132

Mobile River Delta:
AUM10145, AUM11600, AUM11604, AUM11607, AUM11610, AUM11815, AUM19359, AUM19360, AUM19361, AUM6300, AUM9958, CM95897, CM95906, CM95913, CM95914, CM95932, CM95933*, CM95934, CM95941, CM95943, CM95944, CM95945*, CM95946, CM95947, CM95948, CM95949*, CM95950, CM95951, CM95952, CM95953, CM95954, CM95955, CM95956, CM95957, CM95971

White River:
AUM27099, CM64089, CM94880, CM95179†, CM95180, CM95181, CM95182, CM95186*, CM95188†, CM95189†, KU3113, KU3353, KU3365, KU3368*

Black Warrior River:

AUM12647, AUM12648, AUM12649, AUM12653, AUM12654, AUM17810, CM95275, CM95289, CM95292, CM95293, CM95294, CM95295, CM95296, CM95297, CM95299, CM95715, CM95717, CM95718

Appendix A, continued

Cahaba River:
CM67403, CM67418*, CM95020, CM95383, CM95587, CM95596, CM95597, CM95598, CM95599

Coosa River:
CM95705, CM95735, CM95736, CM95744, CM95745, CM95774, CM95775, LSU75224

Tallapoosa River:
AUM34119, AUM34120, AUM34126, AUM34145, AUM34147, AUM8849

Reelfoot Lake:
CM95365, CM95445, CM95446, CM95449, CM95450, CM96115, CM96149, CM96150, CM96151

Females

Coon Creek Lake:
UTA20853, UTA20854, UTA20855†, UTA20857, UTA20858, UTA20865

Southern LA:
LSU18941, LSU38921, LSU41080, LSU41103, LSU57179, LSU57180, LSU74824, LSU74826, LSU74830, LSU75057, LSU75209

Mobile River Delta:
AUM10146, AUM10305, AUM6301*, AUM9589, CM67350, CM67382, CM95896, CM95958, CM95959, CM95960

White River:
CM61677, CM95187, KU3352, KU3354, KU3355, KU3357, KU3381, KU3383, KU3385, KU3445, KU3446, KU3382†

Black Warrior River:
AUM12651, AUM12656, CM94995, CM95298

Cahaba River:
CM67404, CM67419, CM95012, CM95612, CM95614, CM95698

Coosa River:
CM95737, CM95738

Appendix A, continued

Tallapoosa River:
AUM14281, AUM34141, AUM34144, AUM6203

Reelfoot Lake:
CM95513*, CM95448, CM95510, CM95511, CM95512, CM95532, CM95533, CM95534, CM95535, CM96114